ADDIS ABABA UNIVERSITY
SCHOOL OF GRADUATE STUDIES

GEOCHEMICAL EXPLORATION FOR EPITHERMAL GOLD AND ASSOCIATED BASE METALS IN THE GEDEMSA CALDERA

A THESIS
presented to
The School of Graduate studies
Addis Ababa University

In partial fulfilment
of the Requirements for the Degree
Master of Science in Geology

By

Eyoel Muluwork

August 1999
Addis Ababa

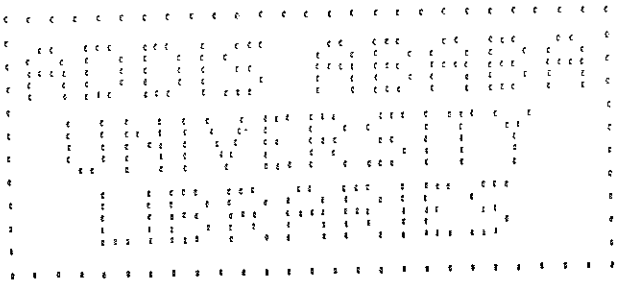

ACKNOWLEDGMENT

I am very much indebted to my adviser Dr. Solomon Tadesse for his detailed critical reading and constructive comment of the thesis as well as for the better thoughts he offered. Many of the ideas presented in the thesis owe their origin to discussions with him.

This thesis has gained much from the help of many other people to whom I express my deepest gratitude. The Ethiopian Geological Survey provided access to laboratory sample preparation and analysis. The full cooperation of Ato Tadesse Mamo in permitting access to drill core and cutting samples is gratefully acknowledged. The Cagliary University laboratory was particularly helpful in providing ICP-MS data for all samples. The AAU granted me in-country scholarship and financially assisted for the research. Last but not least are colleagues and friends whose direct or indirect help in preparing and organizing the thesis must be thanked. They were of much assistance and encouragement.

ABSTRACT

Several central volcanoes are present along the axial portion of the rift, which offered opportunities for potential geothermal resource investigations. The Gedemsa caldera, which is a Holocene volcanic complex in the central sector of the Main Ethiopian Rift (MER), is among those promoted for detailed investigation. Results of these investigations have, inturn, generated great interest in studying epithermal phenomena related to these volcanics. However, studies aimed at delineating epithermal-type mineralization of precious metals (mainly gold) within the MER is a relatively recent-phenomena. The present work deals with preliminary geological and geochemical exploration for these occurrences within the Gedemsa caldera.

Propylitic, potassic and silicification with minor argillic alteration characterize the Gedemsa Caldera. In addition to field observations, alteration is diagnosed by the presence of mineral assemblages including epidote/chlorite, calcite, quartz, k-feldspar, and oxides with some clay minerals. Ore minerals observed include pyrite, chalcopyrite with malachite/azurites, magnetite and hematite. Features indicative of epithermal activities include deposition of fine silica in the oxidized pumiceous deposits, and the thin veins of chalcedonic quartz and k-feldspar, which are intensely brecciated together with the enclosing wall rock. Occurrences of several active thermal manifestations are also known along NNE fault lines immediately outside the caldera.

A total of 79 samples (stream sediment, soil, rock/chip and drill cutting) have been assayed (ICP-MS) for Au, Ag, As, Sb, Tl, Te, Pb, Zn, Cu, Mn, U and other trace elements. Statistical parameters were computed in order to define the threshold value and to separate background from anomalous ones. Anomalous values for most elements are concentrated along the E-W running central chain of hills and at the vicinity of NNE-SSW trending faults both in the western and eastern part within the caldera. In terms of average crustal abundance, the surveyed region is of relatively higher background content for Au, Ag, Zn and Mn. Analyses of rock/chip and drill cutting samples (ICP-MS) from

Gedemsa range in value from 0.1 to 4.16 g/t Ag and from hundreds of ppb to 0.375 g/t Au, respectively. Gold values between 100-200 ppb are quite common throughout the geological profile as observed from drill hole section. The occurrence of many high gold intervals (zone) within the geologic sections reflect-different levels of mineralization. On the basis of alteration mineral assemblages and the Ag/Au ratios, a low sulphidation type of epithermal system is suggested. A preliminary reserve estimation of the gold disseminated in the upper porous pumice is discussed.

From the results obtained in this work, evidence for the presence of ore-forming phenomena is positively identified, and the study, the first of its kind, offers the preliminary results of the investigation on the occurrences of epithermal type precious(Au and Ag) metallic mineralizations in the Gedemsa caldera.

TABLE OF CONTENTS

LIST OF FIGURES

1. INTRODUCTION

1.1. GENERAL

The Ethiopian Rift valley is characterised by the presence of huge amounts of lavas and ignimbrites, which are often associated with central volcanoes containing large summit caldera. The Gedemsa volcano is one of the best-preserved recent (0.8 to 0.1 Ma) (Bigazzi et al., 1981, Elc & EIGS, 1987) volcanoes in the central sector of the Main Ethiopian Rift. It is built up of acid lavas and pyroclastics, and is characterised by a polygenic caldera resulting from large pyroclastic eruptions. In the MER, tectonic movements are still active as confirmed by numerous young faults and intense seismicity of the whole region (Di Paola, 1972).

Many authors (e.g., Franco Pirajno, 1992;Bethke et al., 1985) suggest that continental rift systems in general, including the MER, are accompanied by voluminous subaerial intracratonic volcanic activities, which would generate fossil and active geothermal systems that are among the favourable settings for "epithermal" precious type gold and associated base metal mineralizations. It is now widely recognized that these epithermal systems have originated from fossil or active geothermal systems, connected with the terminal phases of subaerial volcanic centres. These active geothermal systems are commonly found in areas of recent tectonic and igneous activities at plate boundaries, and most geothermal fields are infact associated with volcanic structures - in particular calderas - at both convergent margins (volcanic arcs) and intracontinental divergent boundaries (rift valleys).

In regards to the above facts, the Gedemsa caldera, being supported by the results of its volcanologic, tectonic and geothermal studies, has become one of

the possible target areas for investigation of epithermal gold occurrences in the MER. However, no geochemical exploration has been carried out in the area for its economic importance, which implies that the area is at all virgin as far as mineral exploration is concerned.

On this basis, a preliminary geochemical exploratory survey was carried out in the Gedemsa caldera with the aim to determine epithermal gold potential in the area.

The fieldwork, which was carried out in a period of eight weeks, covered an approximate surface area of 80 km^2 including,

- A geological mapping at a scale 1:50 000,
- Stream sediment sampling (15 samples),
- Systematic soil sampling (25 samples),
- Rock sampling of main rock formations in the surveyed area for petrographic studies (20 samples),
- Rock/chip sampling for chemical analysis (10 samples),

Samples have been analyzed in the EIGS and Cagliari University laboratories using AAS & ICP-MS methods. Petrographic analysis and sample preparation for chemical analysis were done in EIGS lab.

Geological and geochemical maps were prepared for each survey type mentioned above at a scale 1:50000, and data processing and interpretation were aided by computer programs.

1.2. LOCATION AND ACCESS OF THE STUDY AREA.

The Gedemsa caldera is situated in the central sector of the Main Ethiopian Rift (MER) (fig. 1) about 25 km south west of Nazret town close to the eastern rift margin. It lies between 39° 08'- 39° 13'E and 8°19'N - 8°24'N. The area is bounded to the north by the Awash River, to the west by the lake Koka and to the east by Wonji Sugar Plantation.

The nearest town to the study area is Wonji town, which is located about 20 km SW of Nazret with a few thousand inhabitants. Many scattered villages are found within the caldera, and local inhabitants live on a small-scale farming (mostly corn and teff) and cattle breeding as their means of subsistence.

Access to and within the area is fairly good. Two dry-weather roads lead to the are: one which starts from Wonji Sugar factory rising to the north eastern rim of the caldera and another one that runs from Wonji town to the western side of the caldera. Within the caldera access is possible only with a four-wheel drive vehicle, except the central volcanic chain. Numerous gorges especially in the eastern sector impose some difficulties. The northern part of the caldera is relatively easy to access, while in the south, the presence of gorges and fresh blocky lava out crops sharply limit accessibility.

Fig.1 Location map of Gedemsa area

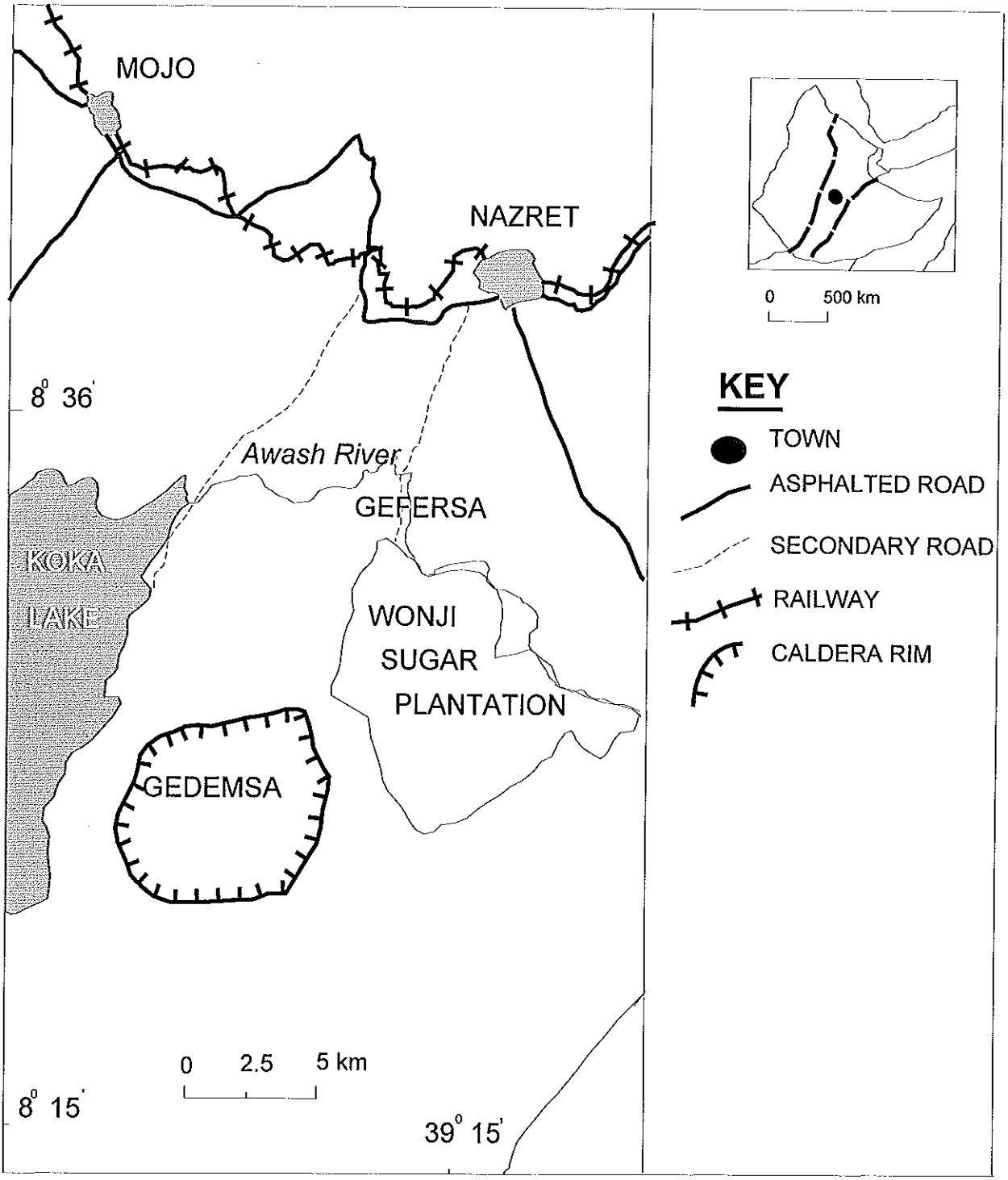

1.3. SURFICIAL ENVIRONMENT

1.3.1. Topography and Landscape

The Gedemsa caldera is a large volcanic depression about 10 kms in diameter and with the rims reaching a maximum altitude of 1950m. It has an almost flat floor, slightly tilted to the North, with elevation ranging between 1740 & 1630m above sea level. The central part is occupied by E-W running irregular chains of hills, locally named Itissa, which resulted from the coalescence of several volcanic edifices. One of these volcanoes, sited at the eastern edge of the chain, contains an explosion crater (Kore crater) being perfectly preserved with a diameter of about 1km and an average depth of 100m. The rim of the caldera is well preserved in three sides having vertical inside walls with a height of 100-200m. Only a small section of the NW rim is not recognized.

1.3.2. Drainage

The drainage system is poorly defined where watercourses have, as a rule, a temporary character and very limited extent, often disappearing in the ground (fig.2). Tectonic features, as clearly shown in the eastern sector of the caldera where streams run along faults, regardless of the topographic slopes generally control their direction. However, few streams in the central part follow topographic slopes.

1.4. CLIMATE AND VEGETATION

The area has warm, temperate climate with mean annual rainfall of 800mm and means annual temperature of 20.9°c (National meteorological service Agency, 1970).

The vegetation in the study area is sparse and mostly of thickets and wood plants, with scattered small shrubs and low acacia trees in a ground cover of annual and perennial grasses and herbs.

1.5. PREVIOUS WORK

Several authors (e.g. Mohr, 1967; Di Paola, 1972; Baker et al., 1971; Merla, 1972, etc,) have given an account of the volcanology, geology and tectonics of the area around Gedemsa caldera.

These studies demonstrated that the Gedemsa volcano is built up during various phases of explosive and effusive activities all of which are characterised by the emission of acidic lavas or, more commonly, pyroclastics.

Di Paola (1972) mentioned briefly the geology of major units of the volcanic centre and indicated the presence of dextral dislocation associated with the normal movement. He has also mentioned that weak traces of fumarolic activities are visible at the base of the western rim of the caldera, on a small pumice cone in the west.

Thrall (1973) described and classified the volcanic products on the basis of field characteristics and analytical (major element) data. He suggested a foundering of a large part of the core along a cylindrical fault, as a cause for the collapse of the caldera rather than outpourings of ignimbrites and pumice falls.

EIGS and Elc (1987) have made a geothermal reconnaissance study of selected sites of the Ethiopian rift system, one of which is the Gedemsa caldera. They suggested that the caldera was formed through ignimbritic eruptions and attributed a phreatomagmatic origin to the kore crater. Furthermore, a probable ages of the Gedemsa caldera and the Ittissa domes (the last silicic episodes) were given as 0.8 - 0.5 Ma. and 0.2 - 0.1 Ma, respectively.

The subsurface geothermal resource of the area has also been investigated (Solomon, 1988) by two exploratory wells with an average depth of 180 Mts. The stratigraphies of the two wells have been reported and consist of volcanic and volcano-sedimentary sequences (fig.12 and 13).

Dereje (1994) and Peccerillo et al. (1995) suggested plinian pumice and ignimbritic eruptions to be responsible for the collapse of the Gedemsa caldera, the former being the main cause. On the basis of geochemical data (major & trace element variations), the above authors have suggested that the rocks of Gedemsa (predominantly acidic volcanic with minor mafic occurrences) have originated from crystal or liquid fractionation starting from mafic parental liquid, possibly with some interaction with crustal wall rocks.

2. GEOLOGY

2.1. REGIONAL GEOLOGY AND TECTONICS

The Gedemsa volcano is found in extensional tectonic setting in rift where voluminous volcanism occurs. The East African Rift System is one of the most interesting continental rift areas. The Ethiopian Rift valley is an important part of this structure owing to its junction, in the Afar depression, with the Red Sea-Gulf of Aden oceanic mega structure, where sea-floor spreading is taking place (Di Paola, 1972).

The Main Ethiopian Rift (MER) is a half graben, which transects the uplifted Ethio - Somali plateau for about a length of 700 kms. It has an average width of 70-80 stretching NNE, from the Ethio- Kenyan border in the south to its junction at the Afar depression in the north (Baker et al., 1972; Merla et al., 1979). It is well exposed by a series of step faults in most parts of the margins, producing remarkable differences in altitude (~1000mts) between the plateaux and the rift floor. All these faults are normal faults which trend NNE, arranged in en-echelon patterns. The differing tectonic style existing between the eastern and western escarpments makes the MER asymmetric, i.e., the eastern escarpment of the MER is morphologically well expressed by the step faults with significant throw as compared to the western, where the boundary between the rift floor and the plateaux is rather gradual and often subdued (Di Paola, 1972).

The floor of the MER is affected by a narrow belt of active faulting and volcanism, which is referred to as the Wonji Fault-Belt (Mohr, 1967). These

faults, which have developed during the upper Pleistocene - Quaternary times (EIGS & Elc, 1987) and running parallel to each other in NNE direction, are located very close to the eastern margin (also marking the asymmetric nature of the MER). Some of these faults are antithetic, so as to determine a minor rift-in-rift structure (Di Paola, 1972).

The Ethiopian rift is associated with volcanism of Pliocene to present. The most prominent petrologic features of the MER are the abundance of silicic peralkaline volcanics, the transitional nature of the basaltic sequence, and the scarcity of rocks of intermediate composition (Mohr, 1967; Di Paola, 1972; Zanettin et al.; 1978; Merla et al., 1979). The distribution of the rock units and the alignments of the volcanic ranges are parallel to the major NNE trend.

The central sector of the MER is exclusively made up of volcanic and volcano sedimentary products that are devoid of both marine sediments and crystalline rocks. Lacustrine sediments, however, are well represented covering large part of the rift and at places with great thickness.

Older volcanic units (Pre-Pliocene) outcrop at the margins where as Pliocene to present volcanism is restricted to the rift floor (Kazmin et al., 1980; Mohr and potter, 1976; Merla et al., 1979; Zanettin et al., 1978). The latter is dominantly of acidic composition with subordinate amount of fissural basalt of both transitional and alkaline affinity.

The axial portion of the Rift is characterised by Quaternary central volcanoes that have emitted peralkaline trachytes and rhyolites sometimes with

subordinate amounts of basic and intermediate products. The Gedemsa is one of these volcanoes.

Di Paola (1972) assigns the volcanic activities with in the rift to the following succession of events: -

- fissure eruptions with emplacement of ignimbrite products followed by volcano-tectonic collapses, and successive buildings of rare silicic central volcanoes;

- basaltic fissure eruptions with subsequent alkali trachytic lava flows and domes;
- Edification of mostly pantelleritic centres.

The stratigraphic succession of products reconstructed by Di Paola (1972) is as follows:

- Ignimbrites of the rift floor (Pliocene to present)
- Alkali trachyte and subordinate basalt (Pliocene to present)
- Pantelleritic lavas and pumice flows (Pleistocene to present)
- Basalt lava flows and cinder cones (Pleistocene to present)

Tectonic movements are still active in the MER, as confirmed by young faults often affecting very recent formations and the high seismicity of the whole region.

2.2. GEOLOGY OF GEDEMSA CALDERA

2.2.1. GENERAL

The Gedemsa caldera is a Holocene volcanic complex in the central sector of the MER (fig.2), relatively closer to the eastern margin. The volcanic history of the centre has been dominated by eruptions, in the form of both lavas and pyroclasites, of silicic magmas. The lowest exposed products are represented by acidic lavas, rhyolitic in composition, which are covered by thick plinian pumice fall deposits. An ignimbrite deposit overlies these pumice deposits. Postcaldera activity has resulted in the emission of intracaldera lava flows and interbedded pyroclastic products. A separate stage of volcanic activity (basaltic volcanism) formed scoria cones and lavas both within and outside the caldera. Extensive sediment successions developed within the depression, which are typical continental sediments (fluvial, alluvial fan and lacustrine).

Petrologically, the volcanic products of the Gedemsa consists mainly of peralkaline trachytes and rhyolites, mafic rocks being represented only as minor occurrences of mingled mafic – rhyolitic magma within some of the post caldera products (Peccerillo et al., 1995).

The Caldera is a composite volcanic structure that resulted from repeated collapses following large plinian pyroclastic eruptions (Dereje, 1994; Peccerillo et al., 1995).

Fig 2. Generalized Geological Map of Gedemsa Caldera (modified after Peccerilo et al., 1995)

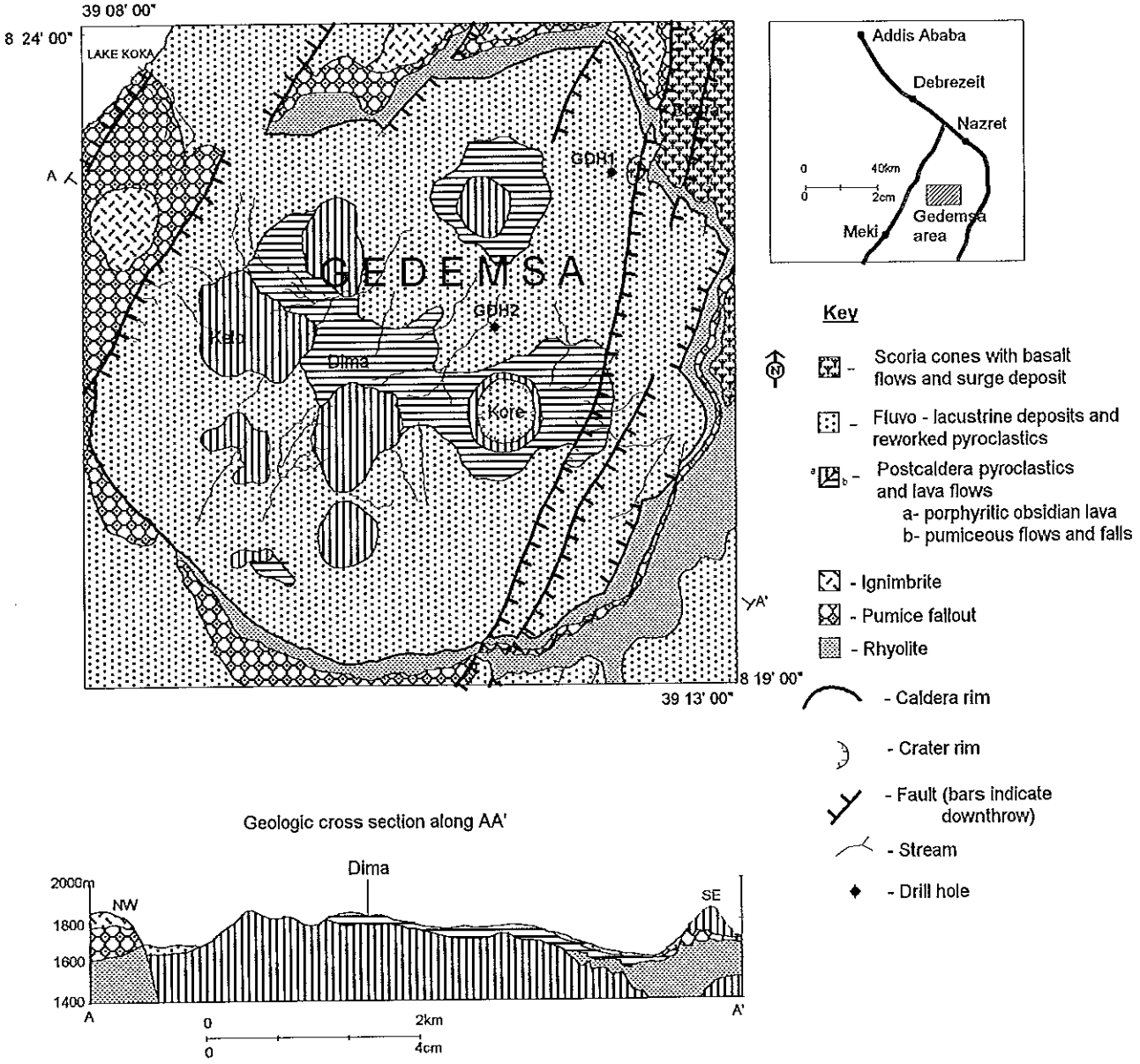

2.2.3. Pumice Fallout

This unit is the most widespread and consists of thick plinian pumice fall deposits of rhyolitic composition with lithic clasts.

It crops out very extensively in SW and western flank and minor occurrences are in the S, SE and NE flank of the caldera. In the southeastern sector a rhyolitic lava overlies the unit with dome like structure.

It is generally grey to light grey in colour, fine-grained with crude stratification commonly dipping away from the caldera rim with average dip amount of 30^0.

In most cases (NW, NE, SW, E parts) the deposits contain considerable amount of obsidian, scoria & rhyolite fragments. At places the rhyolites are altered. In the southwestern part, it dips 20^0 NW and contains large pumice clasts. These large pumice clasts are evidences for emission from a central crater. Sometimes it also consists of a black, completely welded glassy rock, which mantles the underlying topography. The thickness and size of the pumice clasts decrease to the NE edge indicating distal appearance from the vent.

2.2.4. Ignimbrite

This unit predominantly outcrops in the north and northeastern sector of the volcano, with overall geometry varying with underlying topography. It generally shows variations from ignimbrites rich in lithics and lithic breccia

to densely welded ignimbrites, which show features typical of normal ignimbrite flow. Lithics consist of mainly fresh and hydrothermally altered lavas (rhyolites).

The colour of the ignimbrite is dark - brown and green showing eutaxitic structure. It has a secondary vesiculation parallel to a stretched fiammae and contains black vesiculated materials resembling basaltic scoria.

Two Age dating (K/Ar) by previous investigations on ignimbrites from the caldera rim were given as 0.85 Ma and 0.7 Ma (Dereje, 1994).

2.2.5. Postcaldera lava, and pyroclastics (pumice fallouts and flows)

These are formed, following the caldera collapse, by an intense volcanic activity characterised by the eruption of pumices that partly (very thin) cover the caldera ring faults and by the emplacement of the Ittisa hills (a small range of domes and dome-flows of peralkaline rhyolitic composition) (EIGS-Elc, 1987), where in its eastern margin a large crater (Kore), probably of phreatomagmatic origin, is found. The rocks consist of unwelded pumice flows, falls and ashes with some obsidian flows, which are generally porphyritic in texture. The kore crater and associated pumice fall deposits probably represent the latest stage (0.2 and 0.1 Ma.) of explosive episodes accompanying the emplacement of the eastern domes (Di Paola, 1972; Elc & EIGS, 1987).

Obsidian and rhyolitic lavas overlain by pumice deposits constitute the Kore crater. These rocks are characterised by intense brecciation and fractures often

silicified and filled by fine silica or chalcedony. Its northern edge contains deposits of pumiceous breccia containing rhyolitic blocks (very similar to the lavas which form its upper part) with mingled aphyric or poorly porphyritic rhyolite and vesicular mafic lava containing abundant plagioclase and sometimes olivine phenocrysts. In the northern and northwestern parts of Kore, the rocks are greenish and silicified along fractures having yellowish spots of weathered crystals (? carbonates). Near the crater rim in the north there are thin veinlets (~1cm) of chalcedonic- quartz containing dissemination of oxidized crystals (? pyrite) with spots of reddish brown colour. These veinlets generally trend NNE with subvertical dip.

The eastern cone is made up of rhyolitic lava consisting of mingled mafic - acidic lava overlain by a pumiceous breccia containing lithic clasts. At the top there is loose ash fall and flow deposit, with rhyolitic pumice and pumiceous material containing lithic fragments. The lithic breccia is also common in the extreme east along a major fault plane and its viscinity.

The western hills consist of both pyroclastics and lava flows. The western most edge of the hill is composed of pumice and homogenous perlitic lava flows, dipping 35^0-40^0 NW. In the western ridge at Kelbo area, the black porphyritic obsidian grades to greenish, fine grained acidic rock, with flow structures. Surficially the rock shows spots of reddish yellow colour (oxidized pyrite? or Fe carbonate?).

In the northern flanks of Dima, the pumice deposit is overlain by thick welded perlitic material, which mantles the previous topography.

At Kello hill, in its northern part, mingled mafic - rhyolitic lava underlies pumice fall containing pumiceous bombs. The lava consists of white - grey rhyolite containing mafic inclusion. At places this lava contains porphyritic obsidian, probably representing the external part of the flow.

2.2.6. Alluvium & lacustrine sediments with reworked pyroclastics

Sedimentary deposits are found in several places within the caldera depression and their thickness, at places, testifies for an important role of accumulation of epiclastic materials in filling up the caldera depression. These sediments are cut by the recent faults. Generally, they consist of reworked pumiceous materials.

In the eastern edge a fault exposed a section, which comprises a soil covering a deposit of pumice clasts upto size of some tens of centimetre.

At the NW base of Kelo hill, deep cuts exposed a deposit of fine material containing loose grains of pumice ashes and lenses of rounded pebbles of elluvial-colluvial origin.

2.2.7. Phreatomagmatic tuffs (surge deposits), and Scoria cone and basaltic lava

The phreatomagmatic tuffs consist of a thick series of stratified, laminated and massive deposits representing multiple surge events (water lain deposits). These deposits outcrop close to the eastern border of the caldera (which is characterised by the closely spaced faults).

The post-caldera magmatic activity also originated two scoria cones on the caldera floor accompanied by basaltic lava flows. This phase of the volcanic activity is related to the strong tensional tectonism (Wonji Fault) affecting the caldera structure and the whole region. Moreover, outside the caldera, following these tensional faults several volcanic centres of similar origin may be observed. They often have elongated forms, which are parallel to the general trend of the Rift.

2.3. PETROGRAPHY

The studied rock samples include pyroclastics [Ignimbrite, lithic (pumiceous) tuff], rhyolite and basalt.

The ignimbrites mostly show mixed texture of porphiritic and vitrophyric, but the dominant one is porphyritic. They usually contain lithic fragments of mafic and acidic composition (rhyolite, pumice). The phenocryst includes quartz, feldspar and pyroxene in a fine groundmass. The groundmass usually consists of glass shards, which may or may not be welded, and very fine dust of various compostions.

Pumice and pumiceous tuffs are vesicular and composed of feldspars and pyroxene in a glassy matrix, and also contain rock fragments of pumice, rhyoites and trachytes, respectively.

Rhyolites are of various textures (porphyritic, vitrophyric, spherulitic). In the case of porphyritic texture, quartz, feldspar and pyroxene constitute the phencrysts in a glassy groundmass. Devitrification to pyroxene or microlitic feldspar of glassy

groundmass is common. In spherulitic texture, spherulitic feldspar covers the groundmass. Some vesicles are filled with calcite and chalcedony.

The basalts are porphyritic in texture with phenocrysts of olivine, pyroxene and plagioclase set in a fine groundmass of the same composition as the phenocryst. The basalts in some cases are vesicular where some of the vesicles are filled with calcite and silica.

The petrographic description of fifteen rock samples is given in the following table.

Table1. Petrographic description of selected samples

1. Sample No. GRS-002

Rock type	Rhyolite
Composition:	Quartz (25%), plagioclase (45%), opaque (1%), biotite (1%), Pyroxene (15%), glass (13%)
Texture:	Porphyritic
Remark :	Phenocrysts of quartz and plagioclase are seen over the groundmass. The groundmass is composed of microlitic feldspar glass.

2. Sample No. GRS - 004A

Rock type:	Pumiceous tuff
Composition:	Glass (69%) , feldspar (3%), quartz (6%), Pyroxene (aegirine) (2%), rock fragments (15%), Opaque (5%).
Texture :	Vitropyric and/or porphyritic
Remark :	Crystals (Quartz, feldspar and pyroxene) and lithic fragments (andesitic/trachyte, rhyolite and pumiceous) lie over glassy mud. Glass shards are not welded together. Devitrification to microlitic k-feldspar and fine quartz is observed. Interlocked plagioclase surrounded by dark microlitic feldspars and pyroxenes.

3. Sample No. GRS - 004B

Rock type:	Rhyolite
Composition:	Glass (58%), quartz (4%), k-feldspar (20%), hornblende (<1), aegirine (15%), opaque (<1%),

Texture :	Vitropyric
Remark :	Feldspar and quartz phenocrysts are seen over glassy groundmass. Glassy materials in the groundmass are devitrified into feldspars. Acicular or fibrous grains of pyroxene (aegirine) are also seen over glassy groundmass.

4. Sample No. GRS - 005

Rock Name :	Rhyolite
Compostion :	Quartz (20%), feldspar (50%), glass (15%) pyroxene (15 %)
Texture :	Porphyritic
Remark :	Microlitic feldspar, acicular pyroxene and quartz dominate the groundmass. Quartz phenocrysts lie over fine/ glassy groundmass.

5 Sample No. GRS - 006A

Rock Name :	Welded tuff/Ignimbrite
Composition :	Glass (95%), rock fragment (5%), opaque (<1%)
Texture :	Vesicular
Remark :	Glass shards are flattened and welded together. Some pumiceous and few rhyolite fragments lie over glassy groundmass

6. Sample No. GRS-004C

Rock type	Rhyolite
Composition:	Glass (16%), feldspar (10%), qtz (6%), biotite (1%), hornblende (1%), pyroxene (6%), opaque (<1%)
Texture:	vitrophyric
Remark :	Quartz phenocrysts lie over glassy groundmass. Fibrous (crystallites) feldspar and pyroxenes are seen over the groundmass.

7. Sample No. GRS - 006B

Rock Name :	Quartz bearing Trachytes
Composition:	Feldspar (%) , Quartz (%), pyroxene (%), opaque (%)
Texture :	Porphyritic
Remark :	Lath shaped feldspar microclites show flow texture. Quartz and feldspar phenocrysts are seen over groundmass of microlite feldspar.

8. Sample No. GRS - 006C

Rock Name:	Rhyolite
Composition:	Quartz (10%), feldspar (62%) pyroxene (25%), opaque (3%)
Texture :	porphyritic

	Remark :	Quartz, feldspar and pyroxene lie over devitrified cryptocrystalline matrix. Pyroxene phenocrysts show corona texture (rimed with iron oxide material). The glassy material devitrified into microlite feldspars, and pyroxenes are also seen over the grounmass.
9.	Sample No. GRS - 006D	
	Rock Name :	Rhyolite (altered)
	Composition :	Glass (20%), feldspar (30%), quartz (10%), aegirine (20%) epidote (20%).
	Texture :	porphyritic
	Remark :	Epidote, cryptocrystalline feldspar and quartz glass dominate the grounmass. Phenocrysts of quartz and feldspar are seen over the groundmass. Glassy material in the grounmass are devitrified and epidotized.
10.	Sample No. GRS - 007A	
	Rock Name :	Rhyolite
	Composition :	Feldspar (65%), pyroxene (15%), calcite (6%), chalcedony (2%), Glass (11%), opaque (<1%)
	Texture:	Spherulitic
	Remark :	Spherulitic feldspars cover the groundmass. Some vesicles are filled with calcite and chalcedony.
11.	Sample No. GRS-009A	vesicular olivine basalt
	Rock Name	
	Composition:	Pyroxene (25%), plagioclase (45%), olivine (10%), opaque (20%).
	Texture:	Porphyritic
	Remark :	Large vesicles are seen in the groundmass, euhedral olivine, pyroxene, and lath shaped plagioclases are seen as phenocryst over the groundmass. The groundmass in dominated by intergranular pyroxene, opaque and microlite plagioclase.
12.	Sample No. GRS - 009C	
	Rock Name :	lithic tuff
	composition:	Pyroxene (25%), glass (15%), feldspar (25%), quartz (10%) opaque (3%), biotite (1%), chlorite (10%), rock fragments (20%)
	Texture :	Porphyritic
	Remark :	Lithic (basaltic, andesitic and rhyolitic) and crystal fragments are seen over devitrified glass and pyroxene matrix. The

crystal material includes quartz, feldspar and mafic minerals.

13 Sample No. GRS - 009B

Rock Name :	Welded Tuff
Composition:	Glass (73%), pyroxene (2%), Rock fragments (5%), opaque (7%), feldspar (7%), quartz (6%).
Texture :	Porphyritic
Remark :	Lithic fragments are seen as phenocrysts over glassy (mud) matrix.

14. Sample No. GRS - 010

Rock Name :	Tuff (altered)
Composition :	Quartz (9%), feldspar (15%), opaque (3%), hornblende (4%), epidote (20%), glass (34%), pyroxene (13 %), biotite (2%).
Texture :	Porphyritic
Remark :	Phenocrysts of quartz & feldspars are seen over glassy groundmass. Devitrified glasses in the groundmass are epidotized.

2.4. STRUCTURES

Despite some uncertainties, the age of the Gedemsa volcanic structure can be placed within the range of 0.8 - 0.5 Ma (Elc & EIGS, 1987). The last silicic episodes (the Ittisa domes) are probably 0.2 - 0.1 Ma old. The fissured basaltic eruptions are also of recent age (an age of 0.6 Ma is given by Bigazzi et al., 1981).

The caldera, in general, seems to be mainly affected by a series of faults striking NNE - SSW that may have a lateral extent of over 10 km and are of tensional type. Thermal springs are sometimes located in correspondence of the faults. Together with these are different sets of fractures to be important structural elements in the area. In most cases, these fractures are confined within a 3 km.

wide graben (from previous geophysical investigations) that trends NE – SW across the central south part encompassing the Kore crater (Elc & EIGS, 1987).

2.5. EPITHERMAL ACTIVITIES

Despite the strong tensional activity, which is well visible surficially and the widespread permeability of the shallow formations, the hydrothermal manifestations in the Gedemsa are scarce. This is attributed to the shallow ground water circulation pattern and partly due to lateral flows of hydrothermal fluids away from the caldera under the impervious, compact rock units. In the first case, the pattern is such that a cold meteoric water directly infiltrates through the open fractures at the surface, which partly feeds the unconfined ground water and in part continuously cooling a shallow aquifer, thus originating the condensation of any steam which might have escaped from the deeper aquifer. Secondly, where the water table is low or the convective system was capped by rocks of low permeability the discharging fluids could have been dispersed in ground water of the area (White, 1981; Elc & EIGS, 1987). However, the buffering effect of the ground water doesn't affect the most mobile elements, such as CO_2 and Hg (Elc & EIGS, 1987), which still can leak and form soil anomalies in correspondence of the most fractured zones (e.g. a graben structure). Occurrences of several active thermal manifestations are also known (warm alkali-bicarbonate springs) to issue along NNE fault lines immediately outsides the caldera proper. Evidence for fossil hydrothermal activity is observed in the northwest caldera wall and on a small dome inside the caldera manifested as oxidized pumiceous deposits with some deposition of silica. The pronounced Hg anomaly (EIGS & Elc, 1987) recognized immediately to the west of the graben is presumed to be related partly with escape of geothermal gases along the western

margin of this structure and partly with fossil hydrothermal activity along the chain of post-caldera volcanic products, presently dying off due to self-sealing. Furthermore, this fossil activity is evident from hydrothermally related features seen in the Gedemsa including clay-altered horizon (in the northern and western part and in the central chains of hills), veins of fine quartz or chalcedony (+/- pyrite) ranging in width from microscopic to about 3cm. Crosscutting indicates that there was multiple episode of veining. these chalcedony (+/- pyrite) veins also contain angular fragments of wall rock, features which may suggest that vein formation was the result of violent, possibly explosive fracturing which could probably be caused by fluid over pressure (Reith and Muffler, 1978). At places, within the chain of post - caldera volcanic products, (e.g. around Kore crater) a number of hydrothermal breccias, composed of veined clasts of altered rock in a chaotic matrix of chalcedony $\pm$ oxidized pyrite (?) and quartz grains provide further evidence of intense hydrofracturing activity which resulted from progressive sealing of the once-permeable units by silicification and other types of alteration.

2.6. ALTERATION

The alterations observed in the Gedemsa include silicification, clay alteration, potassic alteration; propylitization (epidotization) and oxidation caused some reddish-brown and greenish-yellow stainings). As it is well known, hydrothermal alteration is a result of fluid - rock interaction with factors such as permeability, porosity and temperature controlling the intensity and rank of alteration. Fluid composition and host rock primary mineralogy can also influence alteration mineralogy (Silberman and Berger, 1985). At the surface, zones of silicification, minor argillic alteration and epidotization are exposed in different parts of the study area. Alteration is strongly

fracture controlled, and the intensity decreases away from it. This is especially true of silicification as indicated by limonitized microcrystalline to chalcedonic quartz veins (e.g. in rocks of Kore crater). Petrographic observation revealed that rocks are silicified by deposition of hydrothermal quartz with minor k-feldspar and Fe-oxides. Potassic alteration is by progressive replacement by potassic minerals and/or recrystallization of the host rock to k-feldspar, whereas propylitization is represented by assemblages of calcite-chlorite-epidote-qtz (samples R6A, R10). In all cases alteration intensity ranges from weak, where part (groundmass) of the host rock has been altered to intense, where all evidence of primary volcanic texture has been obliterated. In the former case, for instance, minerals in the vesicles of pumiceous rhyolite, at the western rim, are altered to clay. The most intense alteration forms a "scavenging" or "capping" making the distribution irregular. The mineral assemblage that is observed under thin section also includes calcite, fine quartz, feldspars (fine) by devitrification of glass and often accompanied by hematitization. Also evident under thin section are epidotes and/or chlorite, aegirene, opaque, and quartz. In some cases (sample R7A) vesicles are filled by calcite, silica (chalcedony) and fluorite (Dereje, 1994). All these are important alteration mineral assemblages of one type or another.

2.7. MINERALIZATION

The ore minerals observed in the study area are sulphides and Fe oxides.

The sulphide minerals include pyrite, chalcopyrite with malachite and azurite.

pyrite :- Occurs in hydrothermally altered rock and thin quartz or chalcedony veins as disseminated grains. In some case it

occurs as well formed crystals (evident from cubic box work structure left in the veins). The fresh euhedral mineral surfaces are interpreted as indicative of equilibrium among sulphides and the deep fluids (White,1981).

Chalcopyrite: is less abundant and only seen in a rock sample (GRS-001) from the post-caldera volcanic product. It occurs as scattered anhedral grains together with occurrences of malachite and azurite staining.

The Metallic oxides observed include magnetite and hematite. Magnetite is found in the hydrothermally altered rocks of the caldera rim as disseminated euhedral crystals. Hematite is observed as reddish-brown surface on altered wall rocks along fractures. It is also observed under thin section as an alteration product from pyroxene in a sample of rhyolite (GRS-006c) with a corona structure (pyroxene rimmed with Fe-oxide material). Moreover, at Kelbo area and also in the NW part within the caldera, the rocks show a reddish brown surface (limonite?, carbonates?), along fractures.

3. GEOCHEMICAL EXPLORATION

3.1. COLLECTION, PREPARATION & ANALYSIS OF SAMPLES

3.1.1. Sample collection

The type of sampling carried out in the area includes stream sediment, soil and rock sampling.

Stream sediment samples were collected from the active streambed of first and second order streams. Sample locations were marked on a 1: 50,000 base map.

Systematic soil samples were collected from the termite mounds, which are enormously distributed in the caldera. Similarly details of geochemical parameters were recorded and sample location points were marked on the same base map.

Chip/rock samples were collected, for chemical analysis, from the exposed fresh rocks, alteration zones and mineralized part, both for petrographic and chemical analyses.

3.1.2. Sample preparation and analysis

All sample preparations were done in the EIGS laboratory. As mentioned earlier, sample analytical work were carried out both in the EIGS and Cagliary University laboratories, by AAS and ICP-MS.

Four certified reference standard materials were analysed throughout the work to provide data quality assurance (precision and accuracy). They were: Soil GSS-$ for soils; Granite GSR-1 for chip rock samples; stream sediment GSD-11 for stream sediment samples; platinum ore SARM-7 for Au And Ag in all samples:

Instrumentation

Each sample was mineralised in a Milestone MLS 1200 system, which has a 100% full power output of 1200 watts. The unit is provided with a rotating 12-position carousel and capping device. Acid digestion were carried out in closed 120 ml Teflon PFA vessels with pressure release valves resistant to 830 kpa. 100-ml evaporating dishes in Teflon PFA. All the element determinations were made with a Perkin-Elmer SCIEXELAN model 5000 ICP-MS system.

Sample Decomposition

Multielement trace determinations

Samples were dried at 105^0c for 4h in oven and stored in dessicator.

Subsamples of 0.2g. were placed inside Teflon vessels and created with 3 ml HF, 2 ml HNO_3 and 1ml $HClO_4$. After capping the vessels, each series of 12 samples was microwaved as follows:

35% power for 15 minutes; 50% power for 5 minutes; 40% power for 10 minutes.

The containers were cooled quickly under running water to condense the vapours produced during the procedure and then uncapped. The solutions were transferred carefully and quantitatively into the evaporating dishes and taken to dryness on a hot plate at 150. Then 2 ml HNO3 plus water were added and the content heated to dryness again. The resulting residues were finally treated with 1 ml HNO3 plus water, covered and gently warmed for about 15 minutes. This solution was rinsed into 100 ml volumetric flask and diluted to volume after the addition of 100 ppb rhodium and

rhenium as internal standards to avoid errors due to instrumental fluctuations. The clear 1% HNO3 solutions were used for determinations by ICP-MS.

Rapid technique for gold and silver determinations.

Freshly prepared aqua regia (20 ml) were added to the sample powder (10g, grounded below 200 mesh) in 500 ml graduated flask. The mixture was stirred on magnetic stirring table for 40 minutes at room temperature. The aqua regia leach solution were made up to volume, after adding 100 ppb of rhenium as internal standard, then filtered in a polythene bottle. The clear solution was made ready for ICP-MS determinations.

ICP-MS operating conditions:

Plasma Rf power	1.050 kw	Sample delay	60 s
Washing time	40s	Plasma gas flow	15.0 1/min
Auxiliary gas flow	1.40 1/min	Dwell time	40 ms
Sweeps/reading	5	Nebulizer gas flow	0.8 1/min
Sample uptake flow	1.0 1/min	Numbers of replicate	5

Table 3. Data showing working condition of ICP-MS.

	Mean	'SD	'RSD	GSS-4			GSD-11			GSR-1			SARM-7		
	('n=7)		%	Cert.	Found	E%	Cert.	Found	E%	Cert.	Found	E%	Cert.	Found	E%
Be	3.08	0.11	3.6	1.8	1.63	-9.4	26	28.7	-9.4	12.4	13.1	+5.6			
Mn	972	25	2.6	1354	1362	-2.14	2478	2407	-2.86	464	450	-3.2			
Co	18.4	0.66	3.59	22.3	23.67	+6.14	8.5	8.72	+2.59	3.4	3.21	-5.58			
Cu	65.8	2.82	4.29	40.5	39.3	-2.96	78.6	76.3	-2.92	3.2	3.56	+11.5			
Zn	210	9.51	4.53	210	227	+8.1	373	391	+4.82	28	31.3	+11.8			
As	9.8	0.86	8.77	58	64.9	+12	188	200	+6.38	2.1	2.3	+9.52			
Mo	3.64	0.18	4.9	2.6	3.19	+22.7	5.9	6.4	+8.47	3.5	3.43	-2			
Sb	8.9	0.23	2.58	6.3	6.82	+8.25	14.9	16.01	+4.47	0.21	0.22	+4.76			
Te	0.12	0.01	8.33	0.15	0.18	+20	0.38	0.38	---	0.02	---	---			
Ba	976	32.8	3.37	213	226	+6.1	260	273	+5.0	343	331	-3.6			
W	3.13	0.1	3.3	6.2	6.68	+7.74	126	114	-9.5	8.4	8.58	+2.14			
Ti	1.36	0.03	2.20	0.94	0.88	-6.38	2.9	2.64	-8.7	1.93	1.78	-7.77			
Pb	41.3	1.62	3.92	58.5	56.6	-3.25	636	597	-6.1	31	35	+12.9			
Bi	0.27	0.02	7.41	1.04	1.03	-0.96	50	47.4	-5.2	0.53	0.49	-7.55			
Th	5.18	0.09	1.74	6.7	6.9	+2.98	9.1	8.82	-3.07	18.8	19.12	+1.7			
U	12.04	0.33	2.74	2.73	25.3	-7.33	23.3	23.46	+0.87	54	53.21	-1.46			
Au	315	8.85	2.81										310	315+1.64	
Ag	0.403	14.2	3.52										0.42	0.403-4.05	

Table 2a. Analytical results in ppm (ICP-MS) of stream(s), soil(T), rock(R) and chip(c) samples.

sample	northing	easting	Au	Ag	As	Sb	Tl	Cu	Pb	Zn	Te	Co	Mn	Mo	Ba	Be	W	U	Bi	Th
T22	8.38529	39.1944	0.016	0.16	11.1	0.32	0.27	21.8	12.2	225	n.d	13.1	1685	2.71	664	4.11	1.32	1.3	0.1	9.57
T19	8.38793	39.1769	0.014	0.14	13	0.38	0.3	20.5	15.1	217	0.19	11.8	1595	2.84	591	5.21	1.57	1.38	0.1	11.2
T4	8.37969	39.1673	0.015	0.14	14.5	0.3	0.35	21	16.1	247	n.d	10.9	1500	3.08	544	5.49	1.48	1.6	0.13	12.5
T20	8.38708	39.1849	0.015	0.17	9.42	0.37	0.29	17.1	15	213	n.d	8.9	1475	3.35	427	5.52	1.55	1.74	0.09	11
T16	8.38657	39.1545	0.024	0.15	9.52	0.3	0.3	14.1	17.3	223	n.d	7.15	1575	3.92	399	5.85	1.71	1.95	0.1	12.8
T15	8.37674	39.142	0.016	0.21	9.74	0.38	0.33	22.8	15.3	288	n.d	12.5	1650	4.53	448	5.93	1.74	1.8	0.12	12.3
T14	8.37178	39.144	0.017	0.28	9.04	0.41	0.32	15.2	18.5	307	n.d	8.33	1645	3.84	364	5.76	1.83	2.19	0.1	14.4
T21	8.37538	39.1662	0.015	0.14	11.1	0.37	0.3	30.6	14	202	n.d	13.7	1505	2.77	559	5.15	1.19	1.06	0.09	10.7
T11	8.36634	39.1968	0.014	0.15	13	0.4	0.35	22.6	17.7	985	0.17	14	1530	1.86	564	5.18	1.63	1.08	0.13	12.9
T18	8.36869	39.1815	0.016	0.15	8.5	0.38	0.29	17.7	14.9	207	n.d	10.3	1605	2.4	611	5.06	1.33	1.32	0.1	10.7
T5	8.36391	39.1401	0.016	0.28	12.7	0.31	0.29	15.8	16.2	256	0.16	8.33	1575	4.81	417	5.86	1.54	2.09	0.13	12.2
T8	8.3567	39.1302	0.015	0.16	12.8	0.39	0.32	18.3	14	258	0.13	8.33	1465	2	612	4.84	1.39	1.32	0.11	11
T7	8.35805	39.1473	0.014	0.21	8.04	0.31	0.29	18.3	16	278	n.d	10.3	1550	3.23	484	5.38	1.54	1.5	0.1	11.6
T9	8.34689	39.201	0.017	0.25	14	1.49	0.26	17.2	13.8	357	n.d	10	1355	2.17	922	5.25	1.62	1.08	0.34	10.5
T1	8.35045	39.1734	0.016	0.36	11.3	0.29	0.29	10.7	18.1	259	n.d	4.41	1500	4.66	208	7.21	1.38	2.48	0.26	15.8
T2	8.3499	39.1627	0.017	0.51	10.4	0.41	0.72	11.6	21.8	287	n.d	6.79	1630	5.99	216	8.28	1.79	2.05	0.39	17.1
T3	8.34591	39.1612	0.016	0.38	10.5	0.24	0.29	11.9	17.6	212	0.14	6.51	1320	4.84	544	5.6	1.37	2	0.1	13
T10	8.33057	39.1822	0.017	0.21	15.1	0.49	0.36	26.6	15.1	521	n.d	16	1520	1.84	505	5.04	1.74	1.13	0.14	11.9
S10	8.36847	39.1634	0.02	0.56	4.42	0.2	0.027	8.11	16.4	106	0.14	4.72	1480	2.25	611	5.48	1.1	1.87	0.09	11.2
S2	8.36267	39.1768	0.02	0.65	6.3	0.2	0.28	5.46	16.3	243	n.d	2.57	1376	5.18	467	6.62	2.88	1.97	0.07	11.6
S1	8.36074	39.1795	0.017	0.29	4.79	0.13	0.28	6.37	13.2	227	n.d	3.05	1615	3.4	689	5.35	1.05	1.67	0.07	9.86
S9	8.36214	39.1641	0.023	1.6	8.54	0.39	0.54	7.48	27.1	381	0.13	7.48	1995	2.25	303	11.3	2.24	4.95	0.12	27.4
S7	8.35759	39.1725	0.018	0.51	5.19	0.12	0.24	9.01	14.9	214	n.d	3.28	1390	3.67	600	6.63	1.15	2.34	0.07	12.3
S8	8.35854	39.1712	0.023	0.89	7.04	2.29	0.34	5.06	19.1	249	n.d	2.21	1490	3.03	415	8.47	1.24	2.98	0.08	17.9
S6	8.34679	39.1696	0.019	0.67	7.23	0.2	0.27	9.33	15.5	203	n.d	4.76	1240	3.91	482	6.6	2.1	2.34	0.09	14.5
S4	8.34548	39.1681	0.017	0.04	8.81	0.36	0.37	32.7	8.75	205	0.74	27.1	1425	3.84	499	4.19	2.51	1.67	0.22	8.29
S11	8.35716	39.1484	0.22	0.52	7.68	0.2	0.23	11.5	13.2	320	n.d	5.62	3650	4.15	288	5.45	1.63	2	0.08	10.9
S3	8.34418	39.163	0.022	0.6	9.17	0.32	0.28	8.69	13.7	245	n.d	4.65	1955	3.45	431	5.59	1.76	1.83	0.07	9.98
S14	8.36844	39.1346	0.016	0.3	4.12	0.17	0.2	7.81	16.4	210	0.37	4.66	1250	3.14	561	5.79	1.11	2.02	0.06	10.7
S12	8.36496	39.1408	0.022	0.79	7.93	0.27	0.27	7.58	20.9	345	n.d	3.84	2600	4.32	253	7.72	1.7	2.76	0.1	16.9
S13	8.35824	39.1288	0.025	0.49	6.17	0.36	0.2	10.7	10.7	245	n.d	4	3500	3.2	330	3.74	1.91	1.35	0.05	7.76
C8	8.38574	39.1551	n.d	0.77	23.6	0.11	0.07	5.47	6.14	210	n.d	4.35		0.44	79.1	2.01	1.23	2.58	0.02	3.01
C10	8.36735	39.1327	n.d	0.2	1.37	0.33	0.09	4.89	3.21	77.4	n.d	1.39		7.18	57.2	1.6	3.26	1.55	0.02	3.18
C7	8.36261	39.1418	0.017	0.17	2.92	0.17	0.22	3.82	14.2	231	0.1	0.9		2.09	286	2.01	1.17	3.05	0.03	15.3
C9	8.37535	39.1759	n.d	0.1	0.37	0.19	0.03	3.1	3.09	65.1	n.d	3.1		1.24	649	0.32	0.13	4.01	0.02	1.34
C1	8.35818	39.179	n.d	0.28	1.69	0.56	0.09	7.45	8.85	285	n.d	1.19		11.1	147	1.22	5.84	3.66	0.02	3.62
C4	8.35638	39.1774	0.03	3.73	2.98	0.28	0.22	4.16	17.18	200	n.d	0.64		1.84	58.9	5.1	1.17	1.35	0.1	12.9
C3	8.35307	39.1762	n.d	3.19	5.79	0.81	0.27	4.16	27.7	283	n.d	1.49		4.54	122	8.59	2.35	1.74	0.1	45.7
C2	8.35276	39.1827	0.012	3.02	4.82	0.3	0.49	4.89	32.3	361	n.d	0.39		5	126	11.9	2.63	7.43	0.11	29.9
C5	8.34531	39.1621	0.015	2.75	4.69	0.15	0.14	4.16	25.1	385	0.1	1.1		2.02	82.6	9.76	1.28	1.64	0.03	23.3
C6	8.35823	39.1625	n.d	1.88	3.43	0.2	0.3	3.63	26.5	434	0.13	0.39		1.58	123	9.76	0.76	2.11	0.06	23.5
R7b	8.36778	39.1324	n.d	0.9	6.62	0.25	0.28	4.51	15.8	266	n.d	0.72		0.66	90.3	7.67	0.78	1.67	0.07	13.7
R7a	8.36356	39.1299																		
R8	8.38578	39.1558	n.d	1.63	2.59	0.21	0.25	4.08	19.1	300	0.1	0.89		1.66	278	6.62	0.88	1.09	0.02	18.4
R6b,c	8.33276	39.1906																		
R2	8.35722	39.1792																		
R4	8.35526	39.1717																		
R1	8.36165	39.1657	n.d	0.48	6.15	0.09	0.14	8.28	6.48	171	n.d	0.48		2.58	1058	2.91	1.33	1.05	n.d	6.87
R5	8.36383	39.1559																		
R6a	8.34961	39.1892																		
R9	8.39143	39.1757	n.d	0.23	8.24	0.52	0.16	8.8	8.66	177	0.21	2.57		6.21	2485	4.59	2.26	2.73	0.02	9.44

Table 2b. Analytical results (ICP-MS) of drill cutting samples of 17 elements from two drill boreholes.

Depth(m)	Au(ppm)	Ag(ppm)	As(ppm)	Sb(ppm)	Cu(ppm)	Pb(ppm)	Zn(ppm)	W(ppm)	Mo(ppm)	Be(ppm)	Co(ppm)	Te(ppm)	Bi(ppm)	Tl(ppm)	Ba(ppm)	Th(ppm)	U(ppm)
DH1-6	0.178	0	0	0	0	0	0	0	0	0	0	0	0	0	0	0	0
DH1-9	0.061	0.44	8.49	0.46	12.9	17.6	535	1.86	4.56	6.16	7.33		0.22	0.28	312	15.5	3.34
DH1-21	0.272	0	0	0	0	0	0	0	0	0	0	0	0	0	0	0	0
DH1-28	0.143	0	0	0	0	0	0	0	0	0	0	0	0	0	0	0	0
DH1-31	0.099	0	0	0	0	0	0	0	0	0	0	0	0	0	0	0	0
DH1-34	0.046	1.67	4.16	0.11	9.99	20.9	458	196	2.06	7.96	78.6	0.13	0.32	0.2	63.2	17.9	2.79
DH1-40	0.028	1.63	3.67	0.23	4.63	21.3	568	150	1.71	7.56	31.2	nd	0.05	0.2	47.3	18	2.58
DH1-49	0.21	0	0	0	0	0	0	0	0	0	0	0	0	0	0	0	0
DH1-55	0.056	0	0	0	0	0	0	0	0	0	0	0	0	0	0	0	0
DH1-58	0.101	0	0	0	0	0	0	0	0	0	0	0	0	0	0	0	0
DH1-67	0.056	0.1	7.17	0.1	4.63	9.52	649	2.03	1.44	1.42	50.9		0.16	0.27	375	3.62	0.8
DH1-73	0.161	0	0	0	0	0	0	0	0	0	0	0	0	0	0	0	0
DH1-82	0.099	0	0	0	0	0	0	0	0	0	0	0	0	0	0	0	0
DH1-88	0.045	0	0	0	0	0	0	0	0	0	0	0	0	0	0	0	0
DH1-97	0.232	0	0	0	0	0	0	0	0	0	0	0	0	0	0	0	0
DH1-100	0.13	0	0	0	0	0	0	0	0	0	0	0	0	0	0	0	0
DH1-121	0.11	0.55	13.2	1.2	77.6	18.2	475	3.03	2.27	8.94	1.24	0.23	0.11	0.41	406	18.7	3.61
DH1-130	0.045	0.57	5.66	0.36	45	16.4	281	3.35	2.22	9.25	1	0.29	0.09	0.58	474	18.2	3.16
DH1-139	0.232	0.71	5.92	0.33	5.5	17.3	311	2.52	1.99	8.28	0.85	nd	0.39	0.35	318	17.5	3.29
DH1-145	0.13	0	0	0	0	0	0	0	0	0	0	0	0	0	0	0	0
DH1-154	0.11	0	0	0	0	0	0	0	0	0	0	0	0	0	0	0	0
DH1-157	0.106	0	0	0	0	0	0	0	0	0	0	0	0	0	0	0	0
DH1-163	0.142	0.27	4.98	0.27	4.58	25.2	256	1.96	2.69	6.4	1.81	nd	0.07	0.26	261	14.9	2.95
DH1-172	0.131	0	0	0	0	0	0	0	0	0	0	0	0	0	0	0	0
DH1-181	0.057	0.25	5.02	0.27	8.11	17.7	264	1.93	4.14	6.67	2.96	nd	0.08	0.25	221	14.8	3.16
DH1-184	0.098	0.43	5.52	0.23	3.99	12.6	232	2.31	2.41	7.44	1.24	nd	0.06	0.32	322	14.8	2.1
DH2-6	0.056	0.37	9.2	0.38	15.5	23.4	304	1.95	3.71	8.99	8.36	0.25	0.12	0.36	389	18	3.15
DH2-9	0.266	0	0	0	0	0	0	0	0	0	0	0	0	0	0	0	0
DH2-30	0.312	0	0	0	0	0	0	0	0	0	0	0	0	0	0	0	0
DH2-36	0.165	0	0	0	0	0	0	0	0	0	0	0	0	0	0	0	0
DH2-39	0.215	0	0	0	0	0	0	0	0	0	0	0	0	0	0	0	0
DH2-45	0.195	0	0	0	0	0	0	0	0	0	0	0	0	0	0	0	0
DH2-51	0.177	0	0	0	0	0	0	0	0	0	0	0	0	0	0	0	0
DH2-60	0.077	0.35	5.41	0.27	9.53	22.9	357	5.62	4.33	8.96	5.45	0.12	0.08	0.33	263	18.1	3.51
DH2-63	0.116	0	0	0	0	0	0	0	0	0	0	0	0	0	0	0	0
DH2-69	0.097	0	0	0	0	0	0	0	0	0	0	0	0	0	0	0	0
DH2-72	0.155	0	0	0	0	0	0	0	0	0	0	0	0	0	0	0	0
DH2-75	0.11	0.52	6.5	0.24	4.64	27.5	324	2.34	1.89	9.04	0.88	0.1	0.08	0.38	453	20.4	4.42
DH2-87	0.095	0	0	0	0	0	0	0	0	0	0	0	0	0	0	0	0
DH2-90	0.097	0	0	0	0	0	0	0	0	0	0	0	0	0	0	0	0
DH2-96	0.09	0.2	9.53	0.27	13.8	29.4	309	2.37	1.84	7.91	11.6	nd	0.07	0.26	732	14.5	2.96
DH2-102	0.109	0	0	0	0	0	0	0	0	0	0	0	0	0	0	0	0
DH2-108	0.056	0.05	8.79	0.18	33.1	16.8	228	1.49	1.05	3.29	33.1	0.37	0.03	0.1	1238	5.93	1.4
DH2-111	0.095	0.06	8.18	0.12	30.2	12.2	194	1.06	1.21	3.19	31.5	nd	0.02	0.08	1243	6.02	1.36
DH2-114	0.056	0.08	8.13	0.14	28.9	10.4	179	0.95	1.37	2.67	30.2	0.47	0.02	0.08	1274	6.04	1.15
DH2-120	0.235	0	0	0	0	0	0	0	0	0	0	0	0	0	0	0	0
DH2-123	0.214	0	0	0	0	0	0	0	0	0	0	0	0	0	0	0	0
DH2-129	0.075	0	0	0	0	0	0	0	0	0	0	0	0	0	0	0	0
DH2-138	0.045	0.57	8.45	0.43	5.37	22.3	264	1.62	2.12	8.56	5.37	nd	0.07	0.31	444	16.7	3.2
DH2-141	0.182	0	0	0	0	0	0	0	0	0	0	0	0	0	0	0	0
DH2-144	0.131	0	0	0	0	0	0	0	0	0	0	0	0	0	0	0	0
DH2-147	0.187	0	0	0	0	0	0	0	0	0	0	0	0	0	0	0	0
DH2-150	0.145	0	0	0	0	0	0	0	0	0	0	0	0	0	0	0	0
DH2-152	0.046	0.2	4.78	0.38	1.47	19.6	274	1.2	1.91	10.7	1.47	0.22	0.04	0.31	300	16.1	2.09
DH2-156	0.051	0	0	0	0	0	0	0	0	0	0	0	0	0	0	0	0
DH2-159	0.012	0	0	0	0	0	0	0	0	0	0	0	0	0	0	0	0
DH2-162	0.302	0	0	0	0	0	0	0	0	0	0	0	0	0	0	0	0
DH2-165	0.25	0	0	0	0	0	0	0	0	0	0	0	0	0	0	0	0
DH2-168	0.141	0	0	0	0	0	0	0	0	0	0	0	0	0	0	0	0
DH2-171	0.83	0.26	5.13	0.48	5.7	21.5	232	26.2	2.01	9.97	5.7	nd	0.05	0.35	372	16.1	2.38
DH2-177	0.105	0	0	0	0	0	0	0	0	0	0	0	0	0	0	0	0
DH2-180	0.103	0	0	0	0	0	0	0	0	0	0	0	0	0	0	0	0

3.2. METHODS OF DATA HANDLING & MAP PREPARATION

3.2.1. Data Handling

The data comprises analytical result of stream sediment, soil, rock/chip and drill cutting samples for trace element concentration: Au, Ag, As, Sb, Tl, Te Cu, Pb, Zn, Mn, Co, Be, Ba, Mo, etc. These data sets and their field observations (rock type, co-ordinates, etc.) were stored in a floppy disc using GEOSOFT and MapInfo software. Result of each element was plotted with respect to sample location on the same base map.

Furthermore, statistical analysis was carried out and the spatial distribution of the elements is studied in order to see certain relationships of higher values with geology.

3.2.1.1. Stream Sediment & Soil Samples

To determine background, threshold and elemental association (correlation), statistical manipulations were carried out using PROBPLOT program. The work was conducted in sequential stages.

To characterize the type of distribution, a histogram and cummulative curve were drawn on probablity scale for normal distribution, or on log-normal probablity scale for log-normal distribution. Those plots with the best straight line were taken as an indication as to the type distribution for that element. Erratic values and outlier were avoided.

For those elements that showed a normal distribution, the background was taken as the range between the mean (x) plus or minus two times standard

deviation (s), i.e. (x +/- 2s). The threshold (T) was taken as the mean plus two standard deviation, i.e. (x + 2s).

For those elements that showed a log-normal distribution, the background was taken as the range between the geometric mean plus or minus two times the natural logarithm of the standard deviation (s), i.e. [geom. (x) + 2 ln (s)].

3.2.1.2. Rock/chip Sample and Drill core samples

These data were used to determine the type of elemental association (chemical and mineralogical zonation) and the normal trace metals content of the rocks in the studied area.

3.2.2. Map Preparation

The geological and geochemical maps were compiled at the same scale (1:50000), except the grid contour maps. The geochemical map includes grid contour, maps of high background zones, assay plots, and anomaly maps for selected element. Also a sample location map (fig.3) was compiled at a scale 1:50,000. All these maps were digitised using Mapinfo software. The grid contour maps for selected element were compiled using GEOSOFT software, which facilitates to see the anomalous areas.

Fig.3_ Sample location map (Gedemsa Caldera)

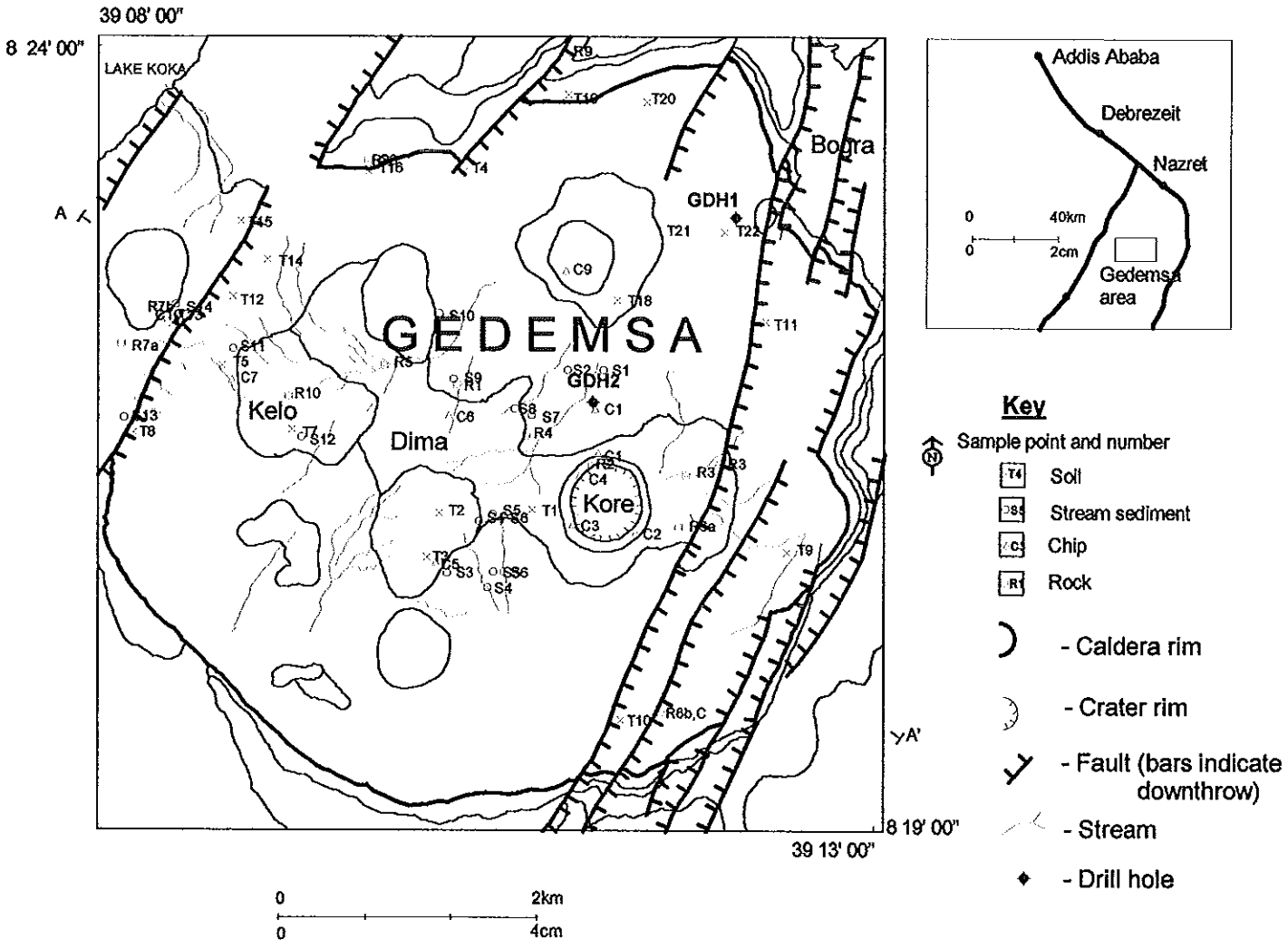

3.3. DESCRIPTION OF RESULTS

3.3.1. Stream sediment and soil sample

The Geochemical data of each element have been studied in terms of whole population and also of sample type (i.e. soil, stream sediment, etc). The latter one is in order to have an unbiased impression in the variation of distribution patterns of background populations, which can possibly be due to mixing of data from different groups. With this regard, the various statistical parameters were computed and studied by considering the distribution patterns of elements in each sample type. But due to the limited number of data, the result lacks representativness. Moreover, in an area where the distribution of element is normal, it is not necessary to study various statistical parameters for that element in smaller geological or morphological groups. Thus, for these reasons whole population data were considered in computing statistical parameters. Based on these results anomalous areas for selected elements were delineated.

Apart from the above ones, a regional trend surface map for each element (Au, Ag, As, Sb Cu, Pb, Zn, Mn,) was prepared by computing trend surfaces using techniques (griding/moving average and contouring) which assume that the geochemical surface (i.e. the distribution of background trace metal values in the space of the field work area), can be described by a homogeneous random function. As a result, estimation of the function parameters suffered from differences in sampling spacing along streams or profiles and between profiles or streams. The analysis of these trend surface maps for each element give certain pictures in respect of their abundance relationship in the high background area (Rose et al., 1972).

3.31.1. Gold

A histogram was prepared using a computer program (Probplot) for the whole population data set. The distribution of gold is near normal ranging in values from 0.014 to 0.0255 ppm with a mean (x) value of 0.0179 ppm. The standard deviation (s) is 0.0033 ppm and the threshold (T), which was defined at the mean plus two standard deviations (i.e., x+ 2s), is 0.024ppm.

Table 4a. Results of statistical parameters for gold.

Element	Range(ppm)	N	Mean(x) ppm	s(ppm)	T=x+2s(ppm)	Transfor.
Au	0.014-0.025	34	0.0179	0.0033	0.024	Arithmetic

Accordingly, five values were found to be anomalous and are located (fig. 7a) in the central,western and northwestern part. From the grid contour map (fig. 4a and 5a), the high background zones, which are bounded by 0.0212 ppm contour, are located in the central and northwestern part of the study area.

3.3.1.2. Silver

A histogram was prepared with the aid of a computer program (probplot) for the whole population data set. The distribution is near normal with a range of values from 0.1- 1.6 ppm and a mean value of 0.381ppm. The standard deviation is 0.297.

Table 4b. The statistical parameters computed for silver.

Element	N	Range(ppm)	x(ppm)	s(ppm)	T(x +2s)	Transformation
Ag	36	0.1- 1.6	0.382	0.297	0.971	Arithmetic

From the grid contour map (fig. 4b), the higher background zone is located in the central part bounded by 0.6ppm. Three values were found to be anomalous and are located (fig. 7a) in the central hills of post caldera volcanics.

3.3.1.3. Arsenic

The distribution of Arsenic from the histogram is near normal with a range of values from 1.3 - 15.1 ppm and a mean value (x) of 9.243 ppm. The standard deviation is 3.188 ppm.

Table 4c. The statistical parameters computed for As.

Element	N	Range (ppm)	X (ppm)	s (ppm)	T(x+2s)	Transformation
As	36	1.3 - 15.1	9.243	3.188	15.619	Arithmetic

The anomalous arsenic values, are shown on the Arsenic anomaly map (fig.7b) to be located in the southeastern part of the area under study.

From the raw data, a grid contour map was produced. The highest value zone bounded by the contour 12 ppm is located (fig 4c.) in the central north, western and southeastern part, and the map shows a general trend in the NE-SW direction with undulating values of low magnitude.

3.3.1.4. Antimony

The histogram for antimony shows a slightly skewed distribution pattern so that its logarithmic transformation was considered in computing the various statistical parameters. It has a range of values from 0.12 - 1.49 ppm with a geometric mean (geom.x) of 0.325 ppm.

Table 4d. Results of statistical parameters for antimony.

Element	N	Range (ppm)	Geom. mean(x)	s(log)	T (Geom.x+2ln(s))	Transformation
Sb	35	0.12-1.49	0.325	0.238	0.972	logarithmic

Accordingly two values were found to be anomalous which are located in the central and southeast part of the area (fig.7c). The grid contour map (fig.4d) for antimony is largely dominated by low background values as compared to the average crustal content for common soil (about 5 ppm). There are, however, broad zones of relatively higher values at two areas, i.e. central and central-west. These higher value zones are bounded by a contour of 0.6 ppm. The central zone extends to the SE whereas the one at the central west is widening to the west.

3.3.1.5. Lead

Lead distribution in the area is near normal as shown by its histogram. Consequently a threshold level was defined at x + 2s.

Table 4e. The statistical parameter for Lead.

Element	N	Range (ppm)	x(ppm)	s	T=x + 2s	Transformation
Pb	36	6 -27.1	13.472	3.493	20.458	Arithmetic

According to the above analysis two values were found to be well above the threshold and are therefore anomalous (fig.7d).

From the grid contour map higher value zone (greater than 17 ppm) for lead generally trends in NW and SSW direction from the centre. The zone of highest

value, which is bounded by a contour of 19 ppm, is located in the central, northeastern and central eastern part of the area under study (fig.4e).

3.3.1.6. Zinc

As the zinc distribution is not normal, values were transformed into logarithms. The threshold (T) was defined at geometric mean plus two times the standard deviation (s), i.e. geom. x + 2ln(s), and all values above it were considered as anomalies.

Table 4f. Results of statistical parameters for Zinc.

Element	N	Range (ppm)	Geom.x (ppm)	s(log)	T	Transformation
Zn	36	106-985	360	149.42	558	Logarithmic

The anomalous values were categorised and shown on the anomaly map for zinc (fig.7e). About four samples were found to be anomalous.

Grid contour map for zinc show a trend in an east - west direction, along the central chains of post-caldera volcanic hills, with undulating higher values bounded by 409 ppm (fig.4f). Two highs (peaks) were located in the central part of the area near Kore crater, both coinciding with the chain of Ittisa hills, with broad extension to the south and Southwest.

3.3.1.7. Copper

According to the normal histogram and cummulative frequency curve, the copper values show two populations. The lower one ranging from 1.7 to 15.5 ppm with a mean of 9.176 ppm and a standard deviation of 2.789 ppm. In the second population the values range from 15.5 to 29.3 ppm.

Table 4g. Results of statistical analysis for copper.

Element	N	Range(ppm)	Mean(x)	s	T=x+2s	Transformation
Cu	19	1.7 - 15.5	9.176	2.789	14.755	Arithmetic
	17	15.5 - 29.3	19.364	3.836	27.037	Arithmetic

The second population is, therefore, the background population considering the average crustal abundance and only two values are well above the threshold (fig.7g).

The trend surface map of background values shows no specific pattern of variations. Highest values bounded by the 18 ppm contour are located in the southeast, south west and north eastern part of the study area (fig.4g).

3.3.1.7. Manganese

The distribution of manganese is fairly uniform as revealed by the cumulative frequency curve. The threshold is defined at the mean plus two standard deviations, i.e. x +2s, as it shows a normal distribution.

Table 4h. The parameter summary statistics for Manganese.

Element	N	Range	Mean (x) (ppm)	S	T(x+2s)	Transformation
Mn	36		1086.444	227.931	1682.307	Arithmetic

All values above the threshold are considered as anomalous, which are then categorised into two groups visually on the basis of their abundance in a particular range (fig.7g). These are values between x + 2s and x + 4s, and those greater than x + 4s. Accordingly, nine values were found to be anomalous.

Fig4.1a_ Geochemical contour map of

Gold in stream sediment

GEDEMSA AREA

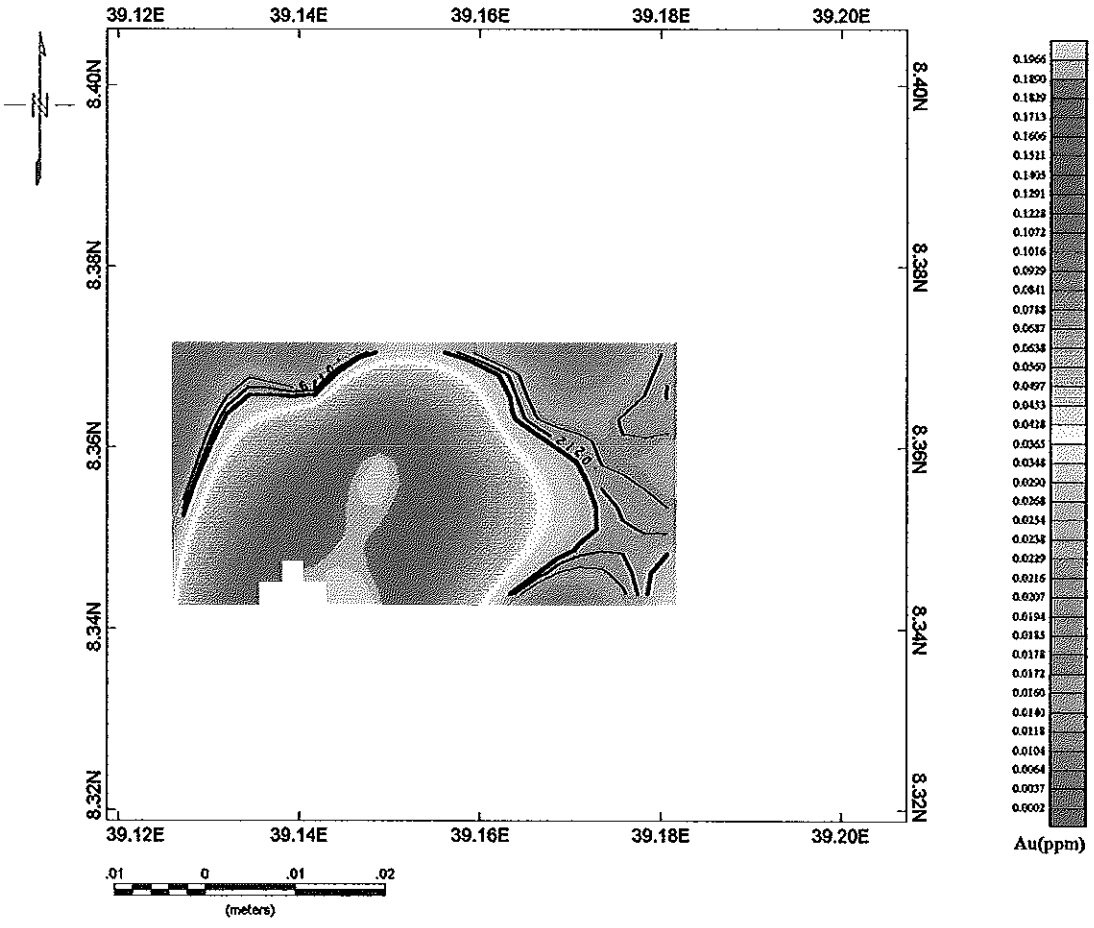

Fig. 4.2a_ Geochemical countour map of

Gold in soil samples

GEDEMSA AREA

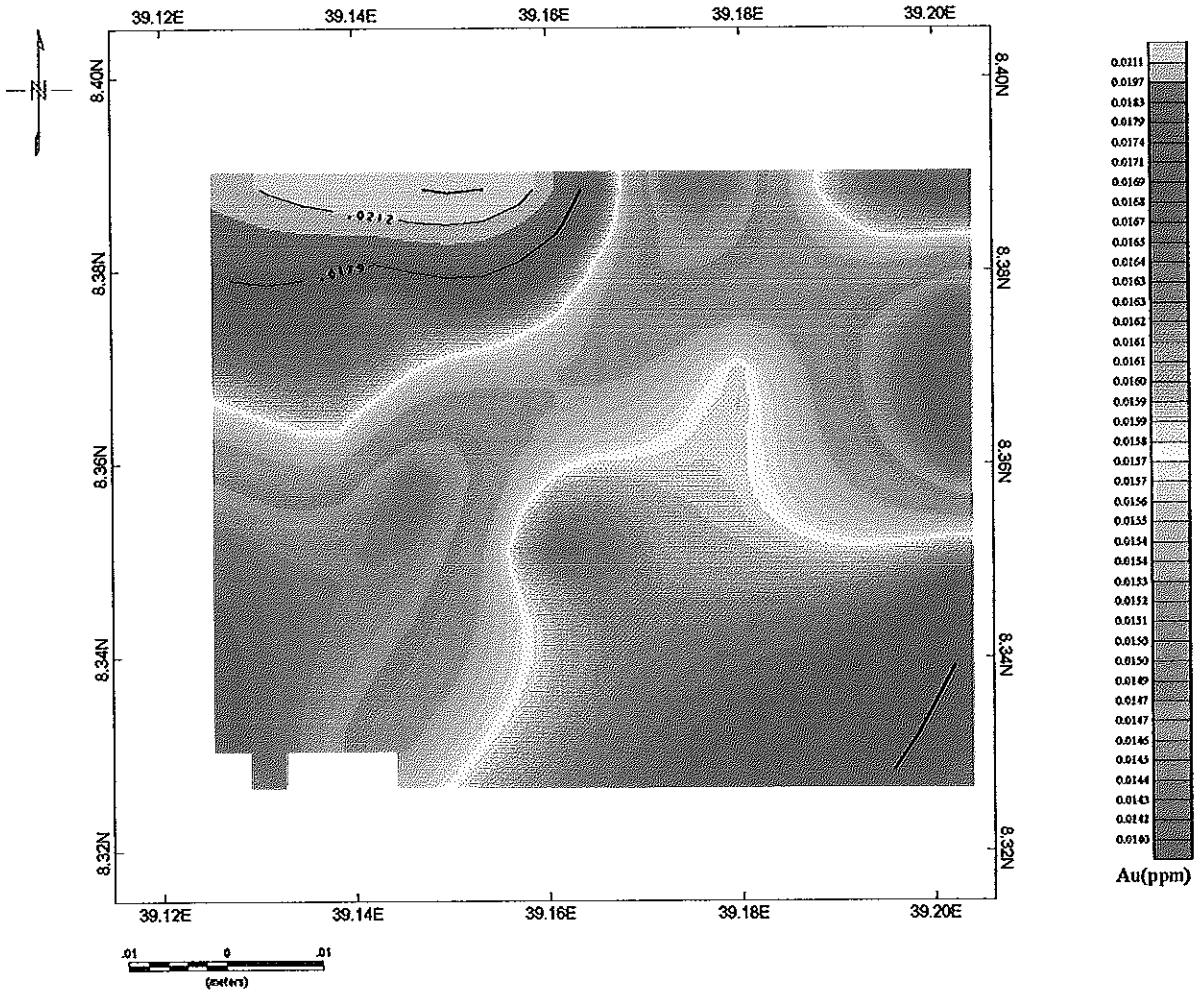

Fig4.1b_Geochemical contour map of

Silver in stream sediment

GEDEMSA AREA

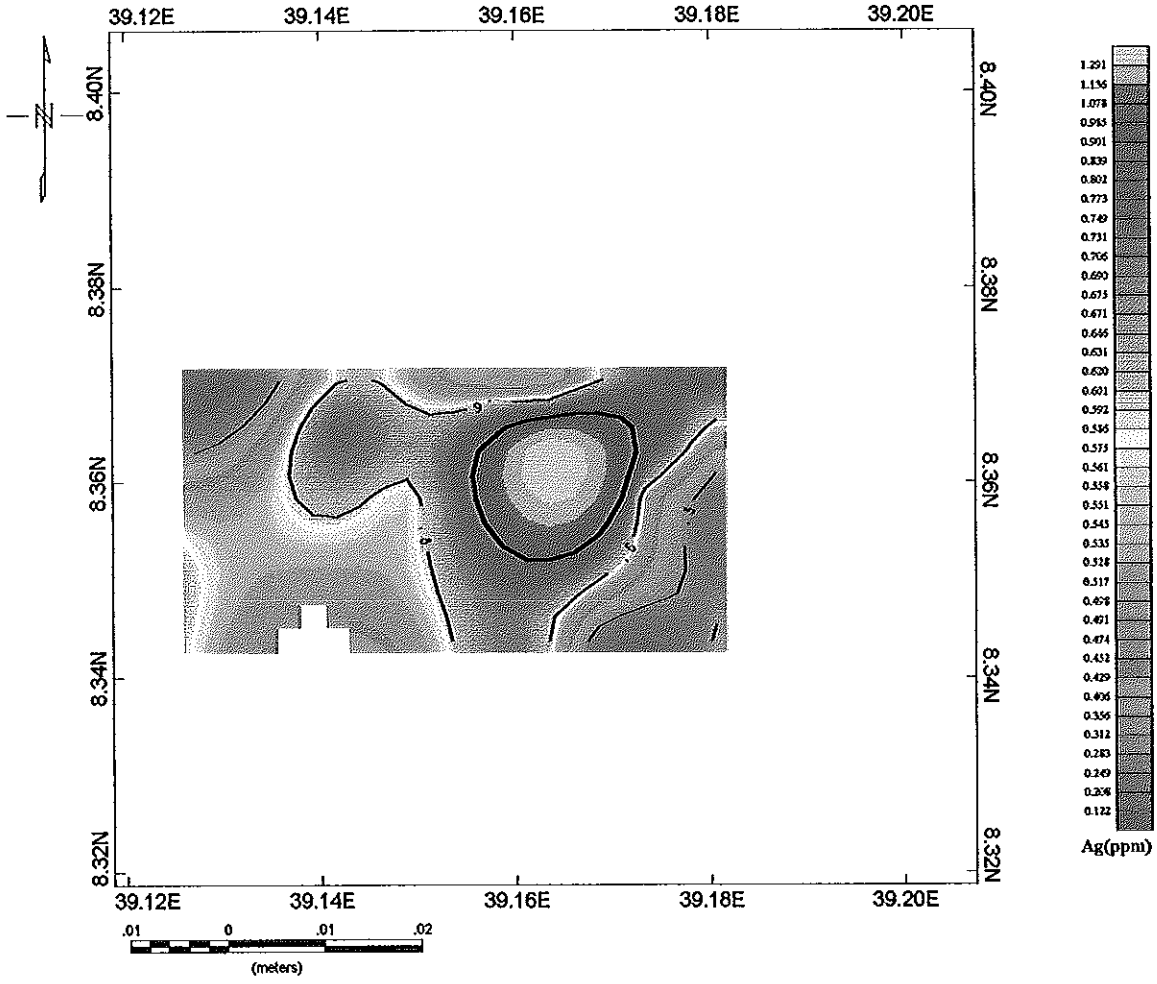

Fig. 4.2b_ Geochemical countour map of

Silver in soil samples

GEDEMSA AREA

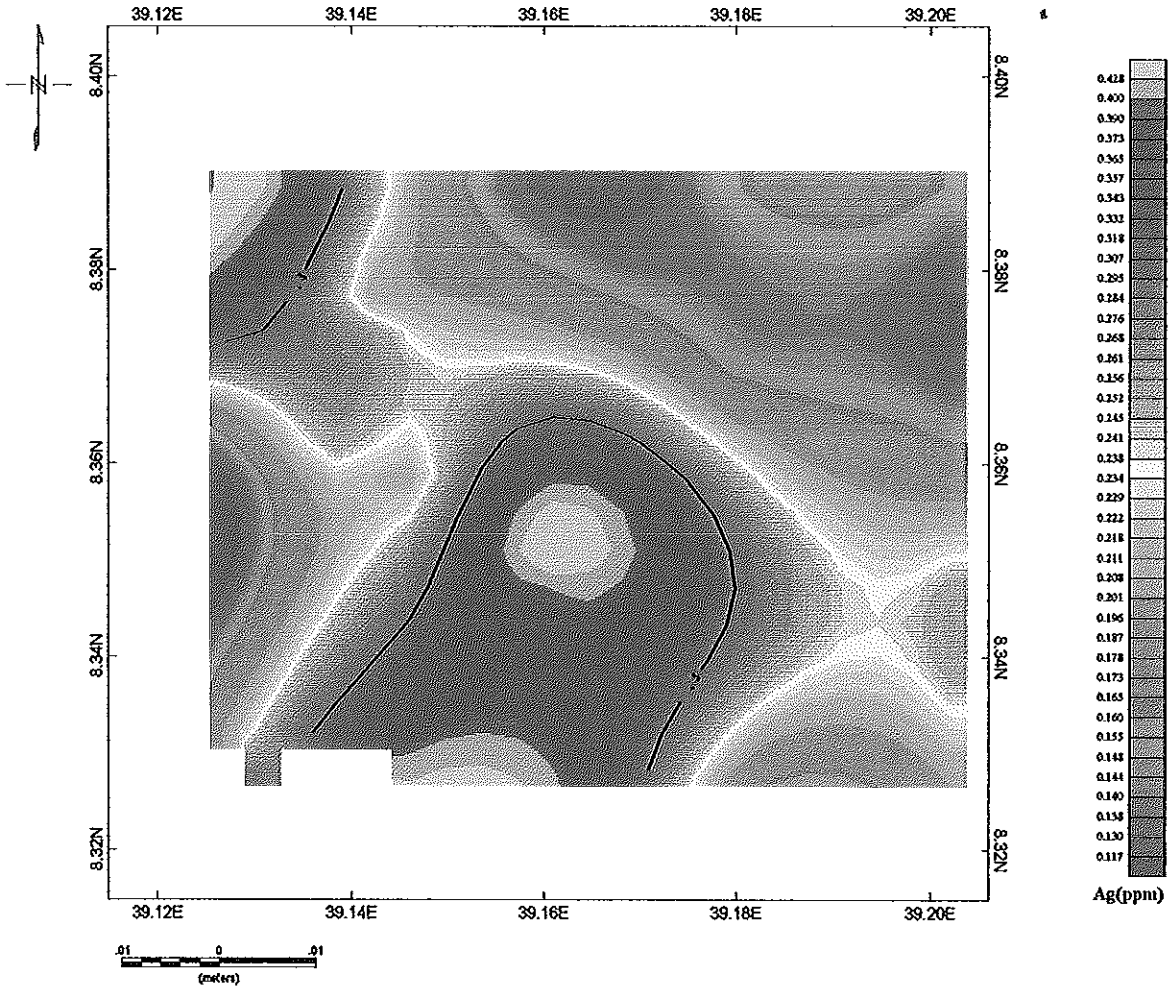

Fig4.1c_Geochemical contour map of

Arsenic in stream sediment

GEDEMSA AREA

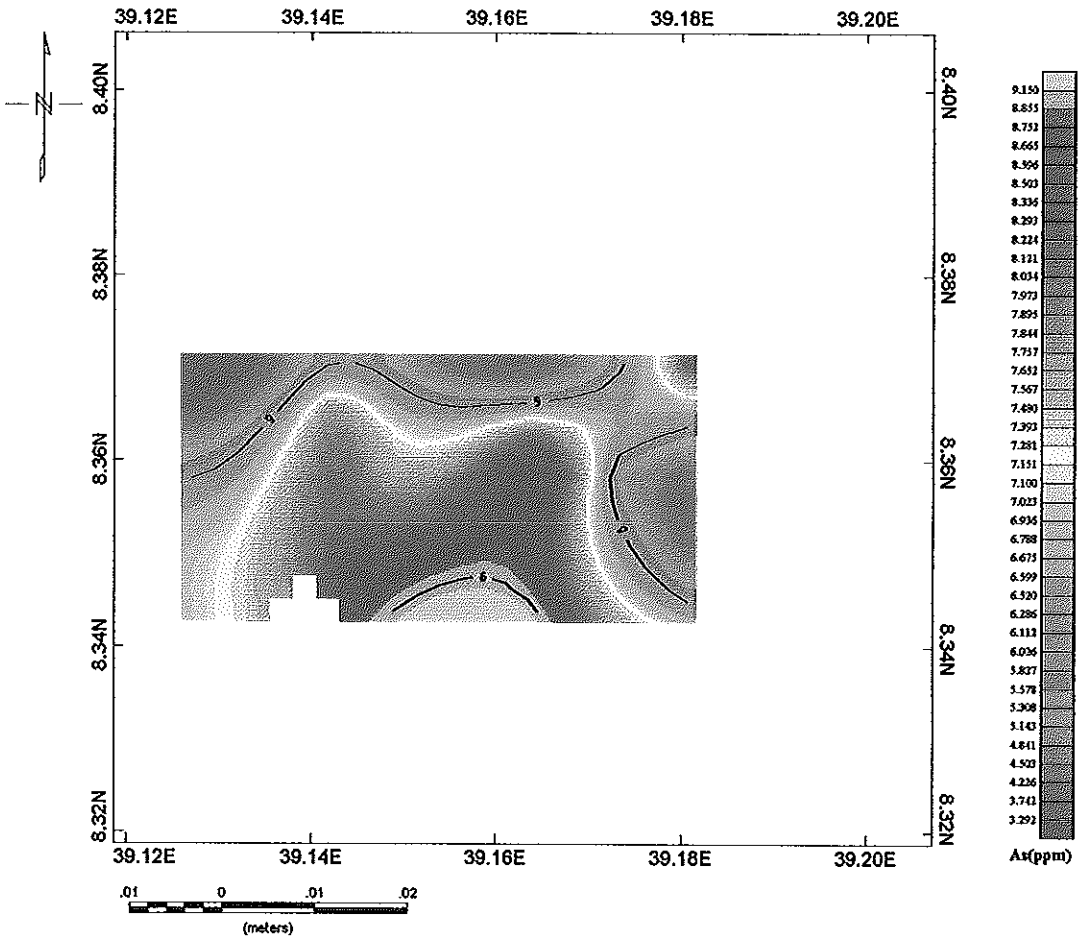

Fig. 4.2c_ Geochemical countour map of

Arsenic in soil samples

GEDEMSA AREA

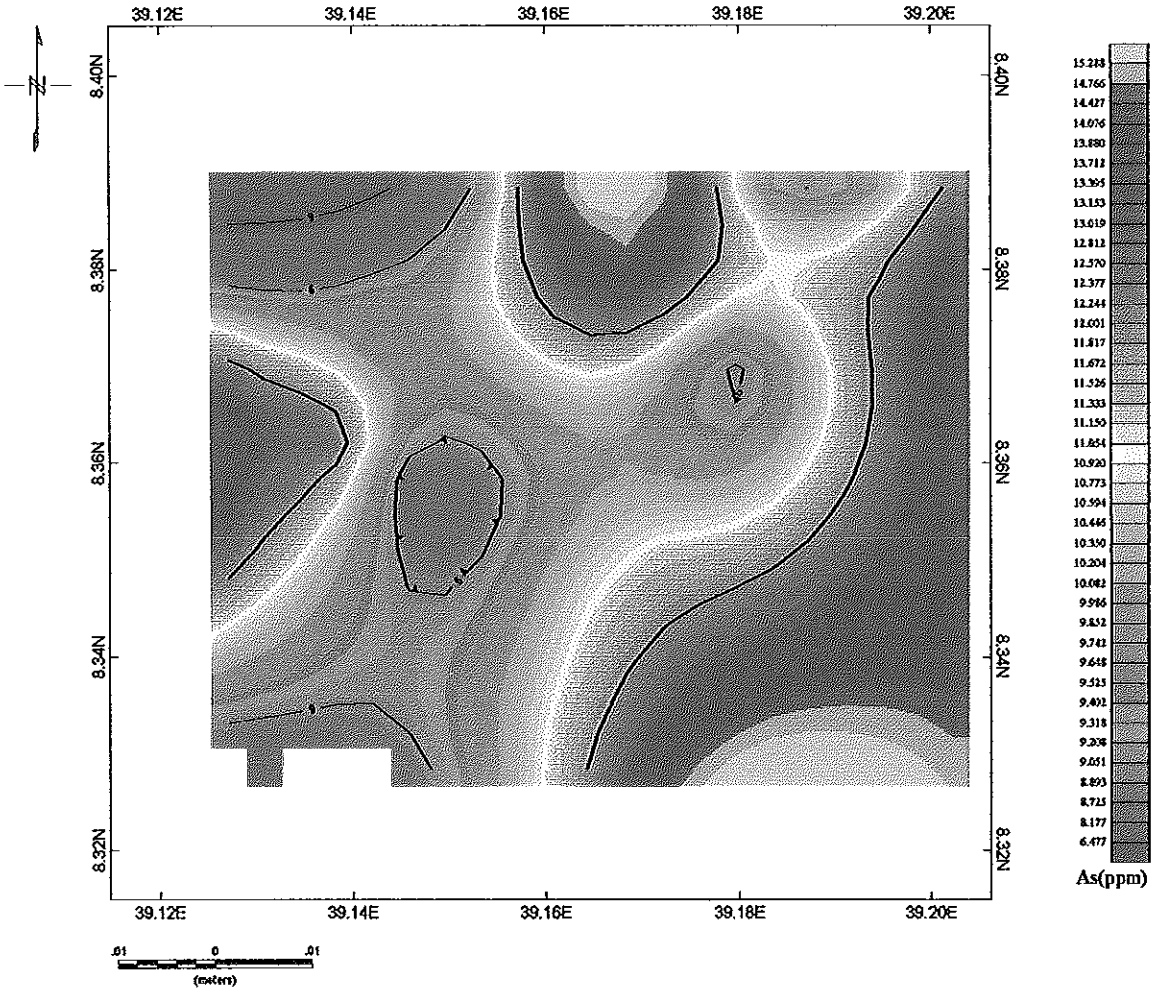

Fig4.1d_Geochemical contour map of

Antimony in stream sediment

GEDEMSA AREA

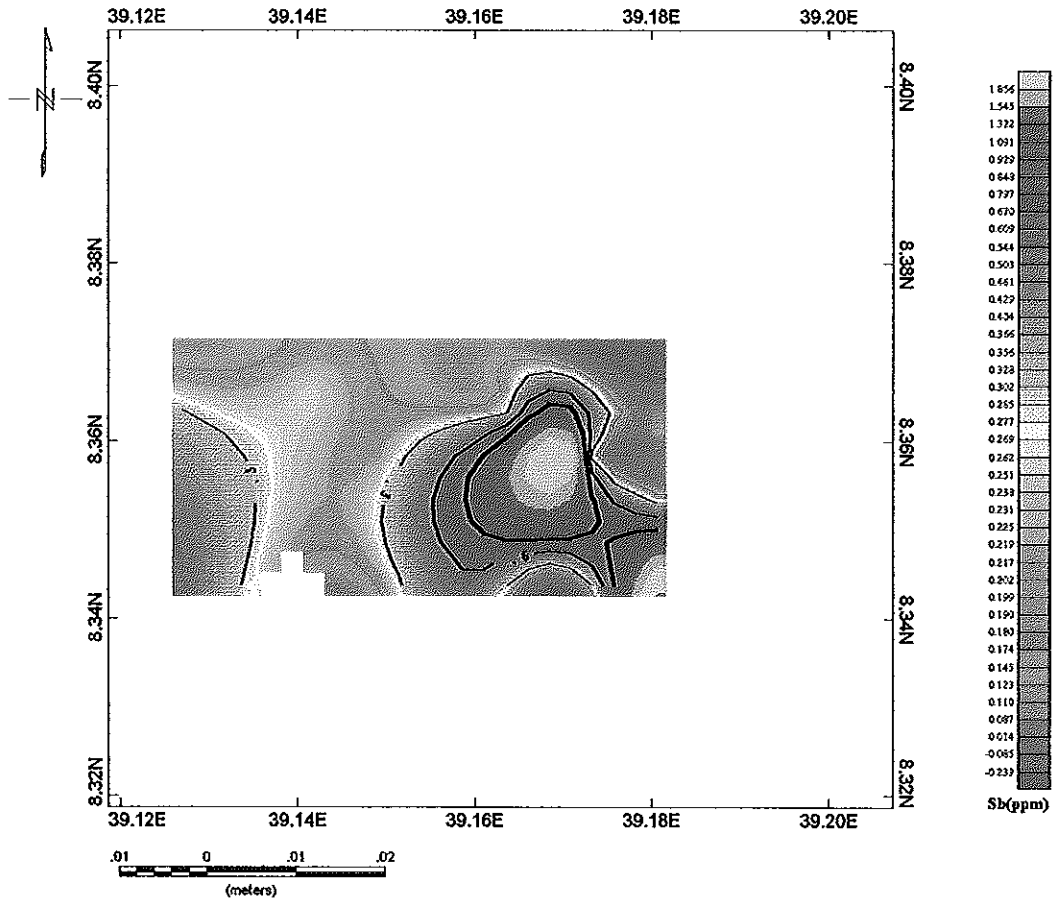

Fig. 4.2d_ Geochemical countour map of

Antimony in soil samples

GEDEMSA AREA

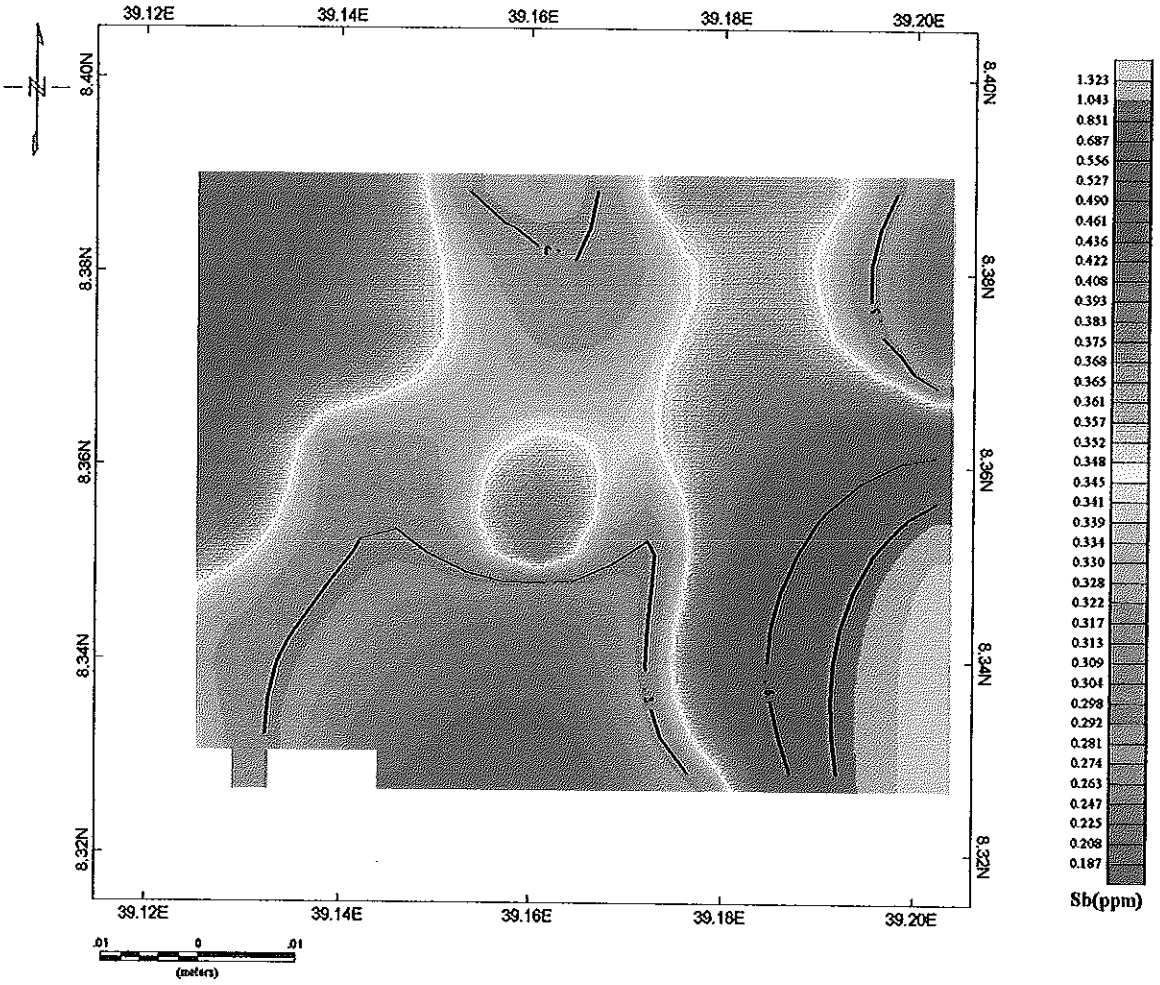

Fig4.1f_Geochemical contour map of

Zinc in stream sediment

GEDEMSA AREA

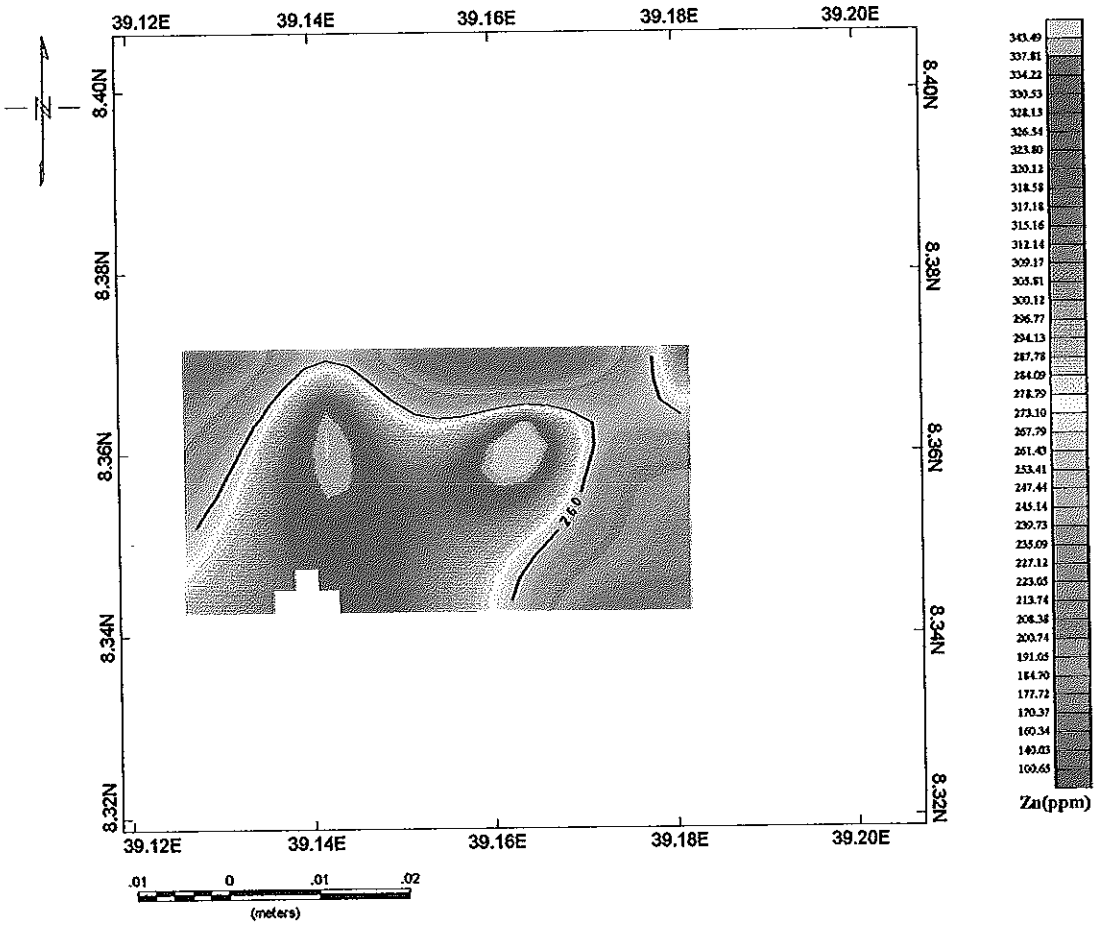

Fig. 4.2f_ Geochemical countour map of

Zinc in soil samples

GEDEMSA AREA

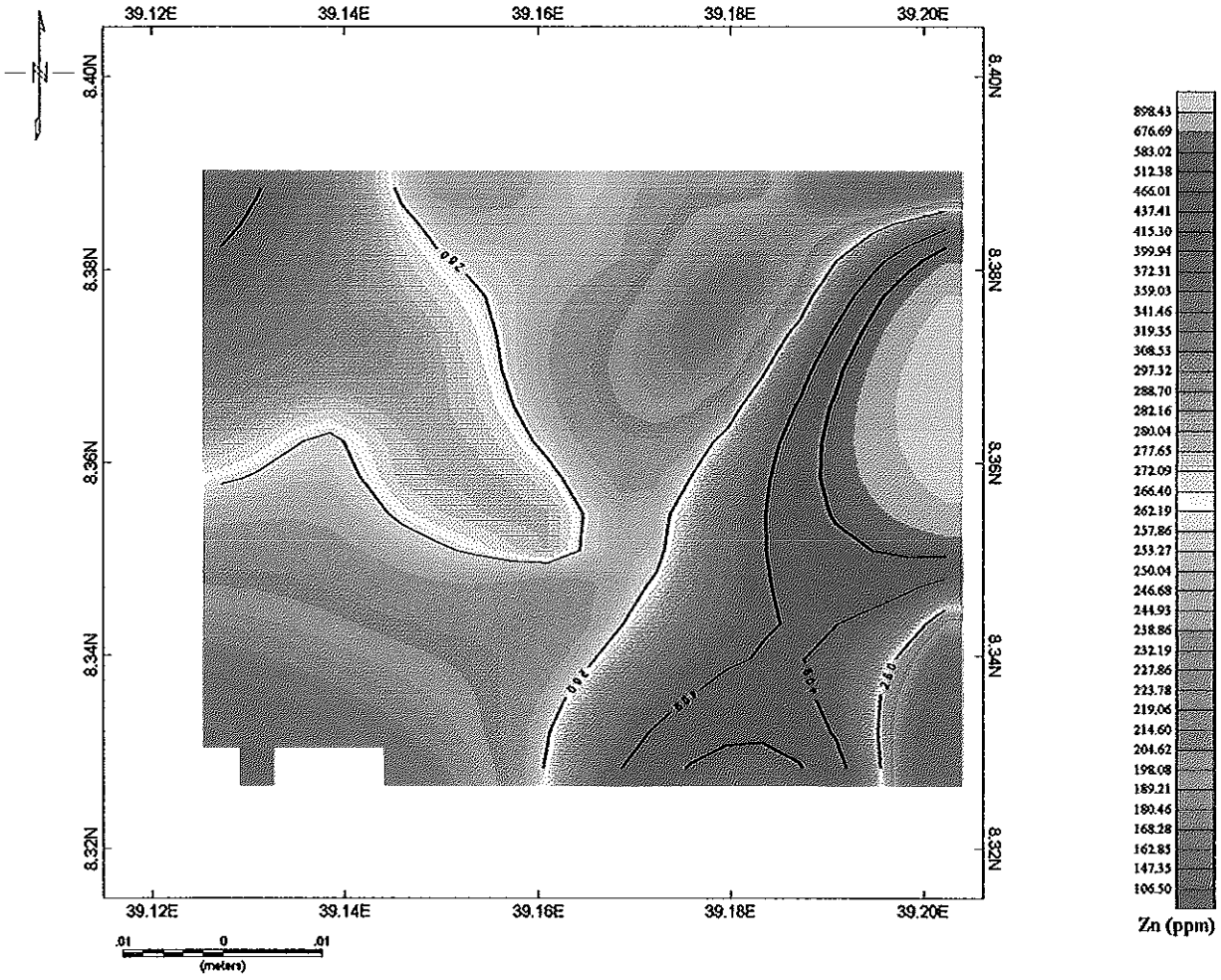

Fig4.1g_Geochemical contour map of

Copper in stream sediment

GEDEMSA AREA

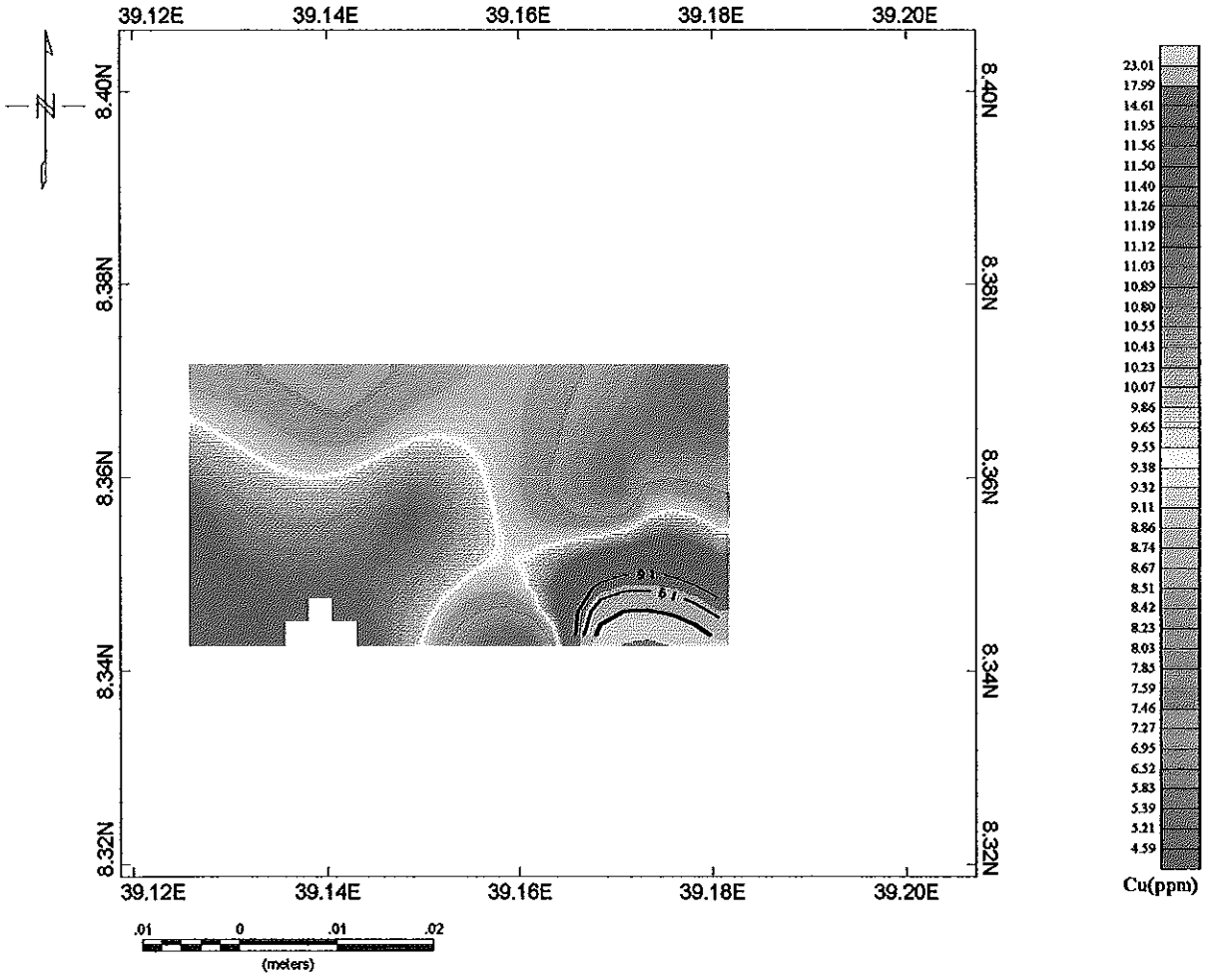

Fig. 4.2g_ Geochemical countour map of
Copper in soil samples
GEDEMSA AREA

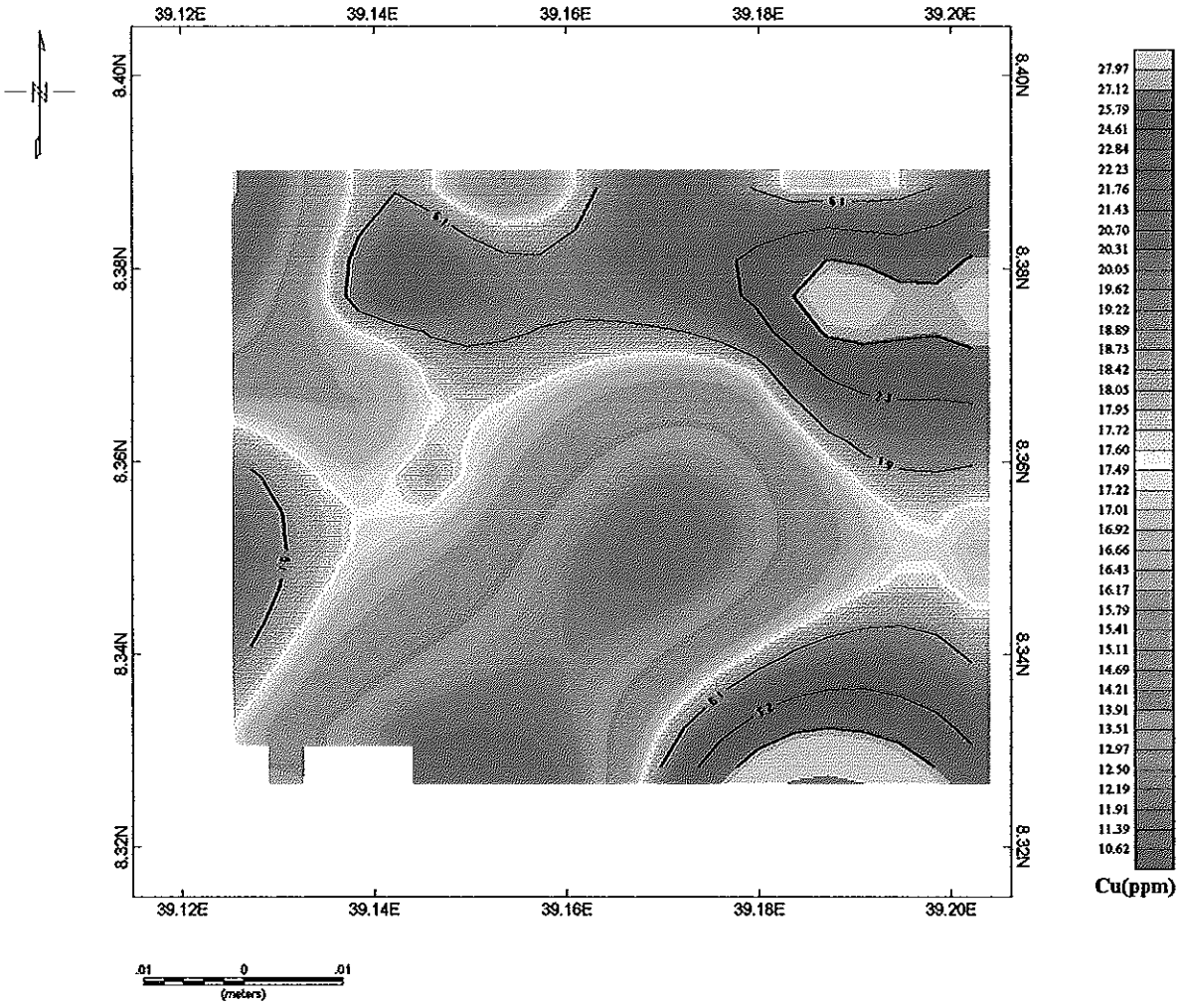

Fig. 4.2h_ Geochemical countour map of
Manganese in soil samples
GEDEMSA AREA

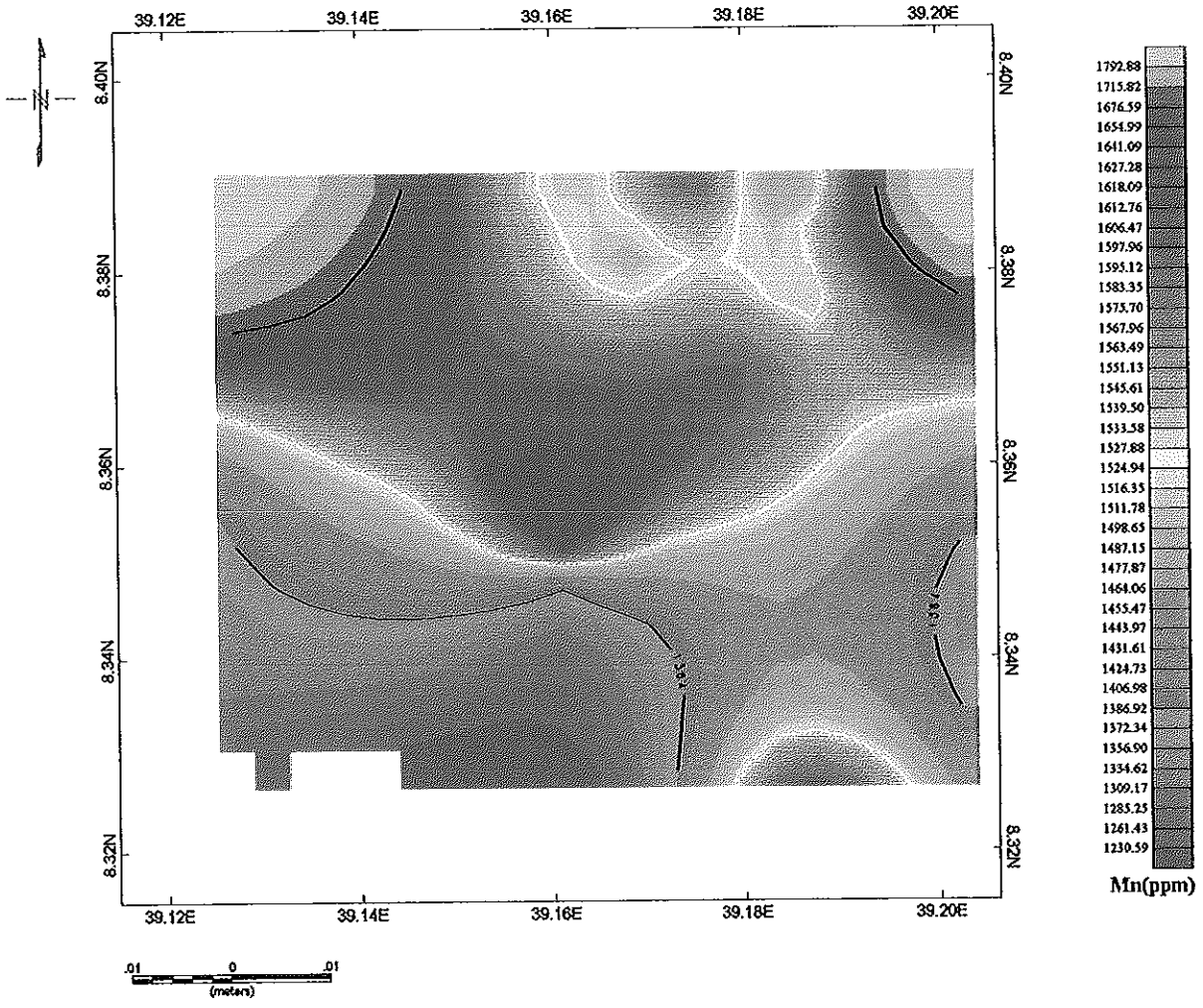

Fig4.1h_Geochemical contour map of

Manganese in stream sediment

GEDEMSA AREA

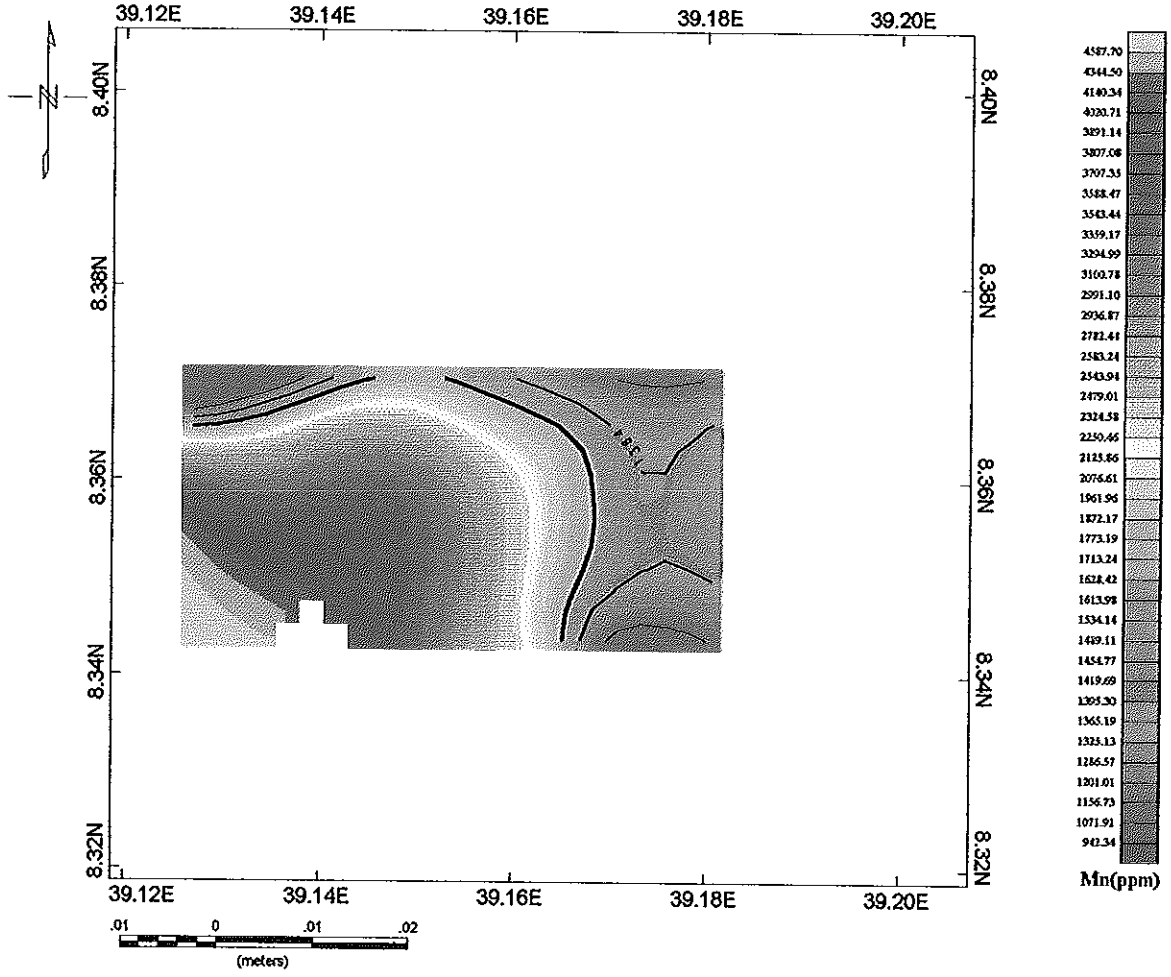

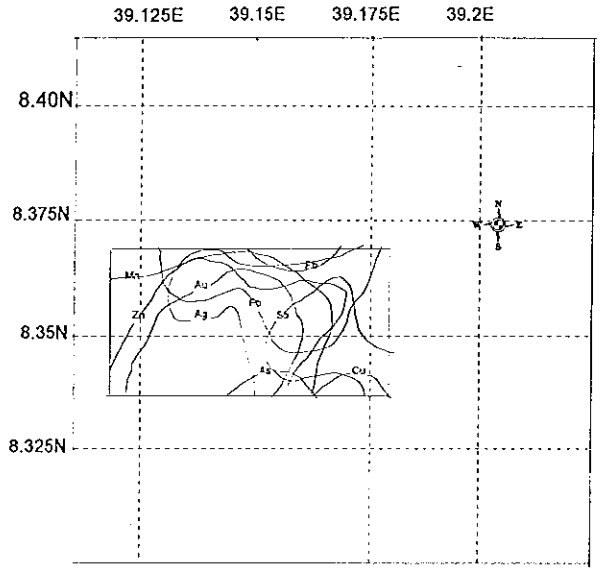

Fig.5a Spatial distribution of high background values: STREAM SED.

KEY

Au - gold
Ag - silver
As - arsenic
Sb - antimony
Pb - lead
Zn - zinc
Cu - copper
Mn - manganese

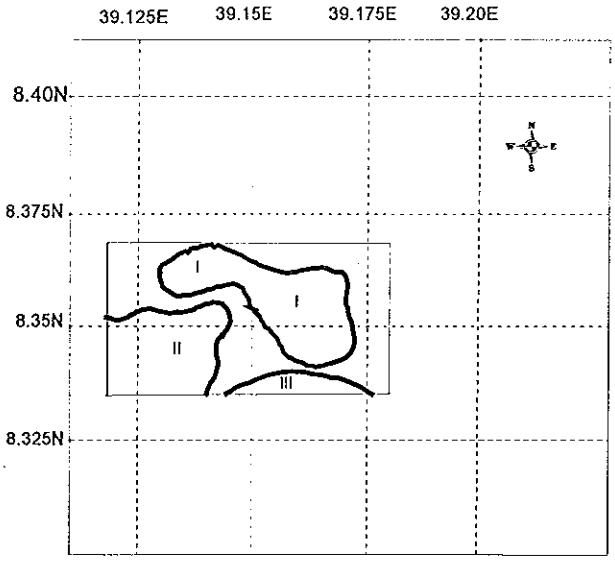

Fig.5b Simplified summary map of high background zones: STREAM SED.

KEY

Zone I : Au - Ag - Pb - Sb high
II : Au - Mn - (Zn) high
III : Cu - As high

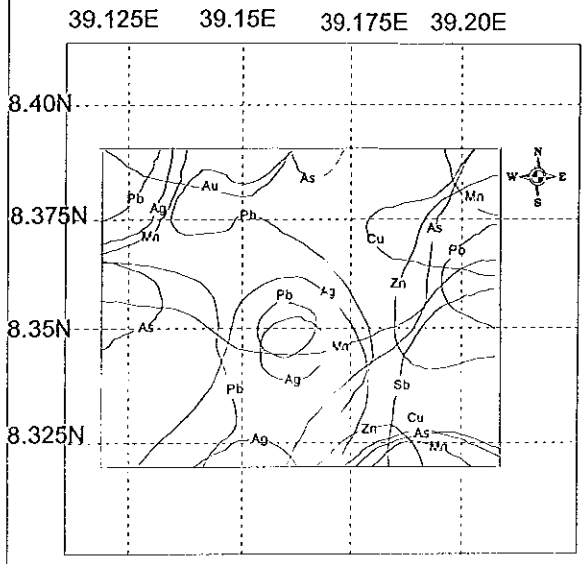

Fig.6a Spatial distribution of high background values of elements in Soil. GEDEMSA

KEY

Au - Gold
Ag - Silver
As - Arsenic
Sb - Antimony
Pb - Lead
Zn - Zinc
Cu - Copper
Mn - Manganese

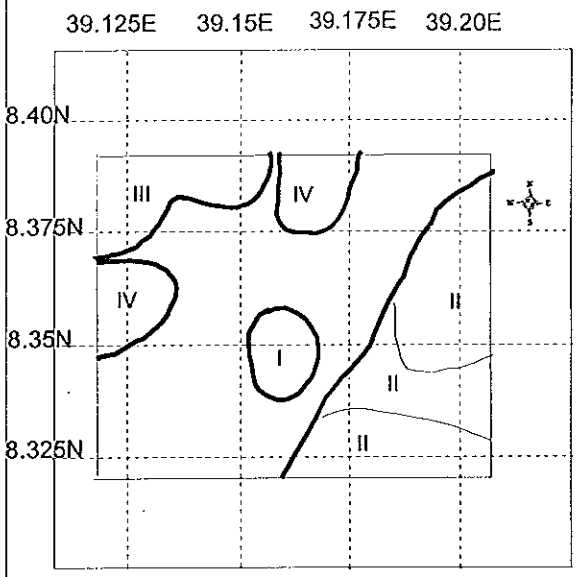

Fig.6b Simplified summary map of high background zones from soil.

KEY

Zone I: Ag-Pb high
II: As-Sb-Cu-(Zn)-(Mn)-(Pb) high
III: (Au)-Ag-Pb-Mn high
IV: As high

From the grid contour map (fig.4h), the higher background zone, which is bounded by contour 1400 ppm and is situated in the central west, NW and NE.

Generally, the analyses of geochemical contour map for each element give certain pictures with respect to their abundance relationship in the high background area. These analyses were made in an attempt to recognise associations between elements based on the presence or absence of common features in the grid - contour maps of individual elements, as well as based on the fact that the association had to make a geochemical sense. This approach made it possible to make a reasonably fair choice between the various alternatives and to present a number of associations as follows: ***[Ag - Pb -- (Sb)- (Zn)]; [Au - Mn – Zn]; [As-Cu]; [As - Sb- Cu- Zn -Mn]; [As].***

The geochemical landscape (fig.5 & 6) of the area, thus, can be summarised into various zones based on the association of certain elements.

Zone I : Ag – Pb; Ag- Pb - Zn - Sb in central and central west.

Zone II : As - Cu ; As - Cu - Sb - Zn - Mn in the NE and SE side of the area.

Zone III : Ag -Pb - Mn - northwest (soil).

Zone IV : As - north and west (soil).

Zone V: Au- Zn - Mn south west (stream)

On the other hand, regional threshold values computed by statistical treatment of the whole background population of these geochemical data were used to produce a local anomaly map from the assay plots (fig.7).

Anomalous values for each element demarcated on the map lead to delineation of certain zones (fig.8) of anomalous values for one or more elements in each zone. These zones were further regrouped on the basis of inter-element association. The

Fig 7a . Au analytical results (ICP-MS) in stream & soil samples (circles).

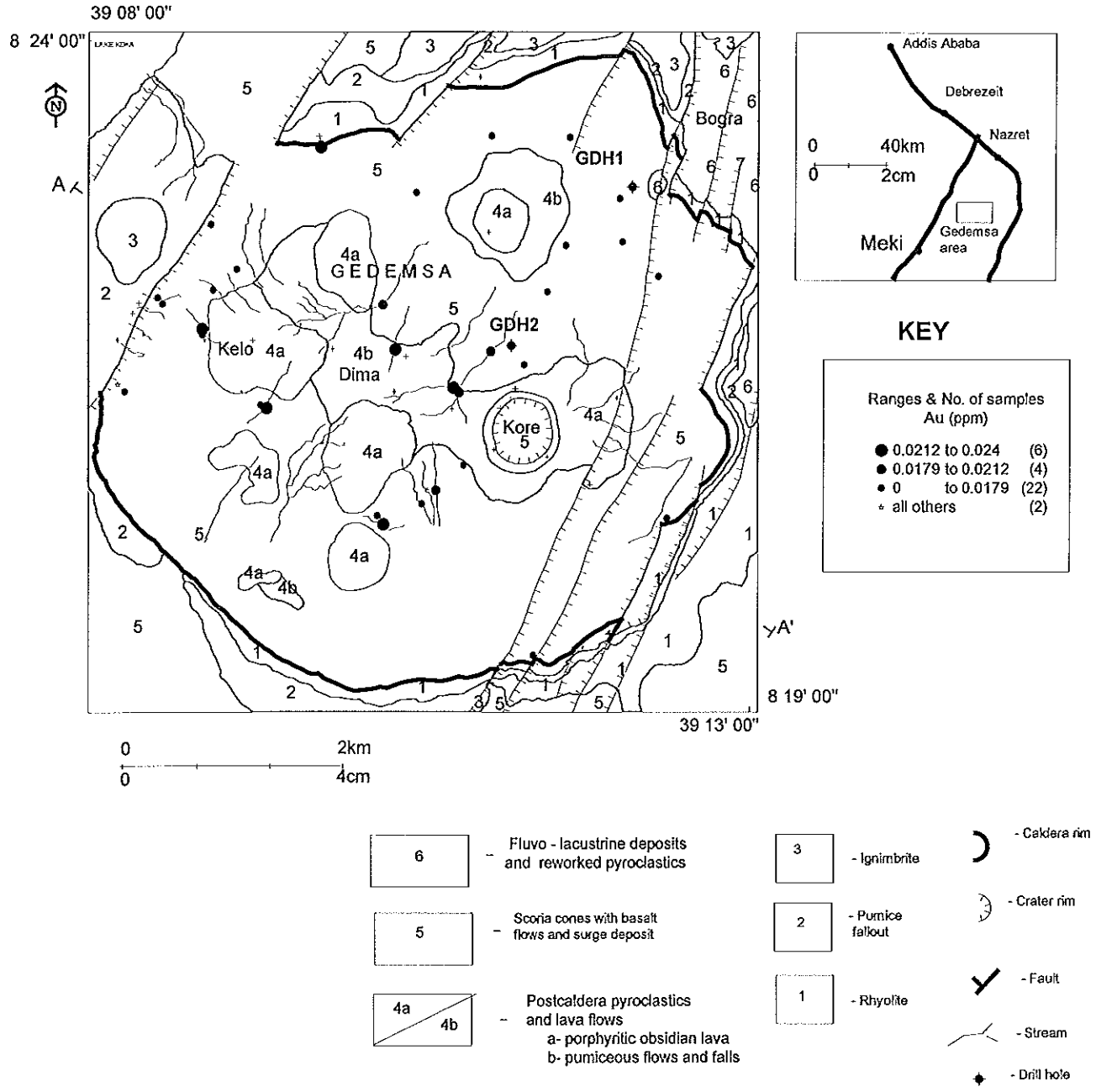

Fig 7c . Arsenic analytical results (ICP-MS) in stream & soil (circles) and rock/chip samples.

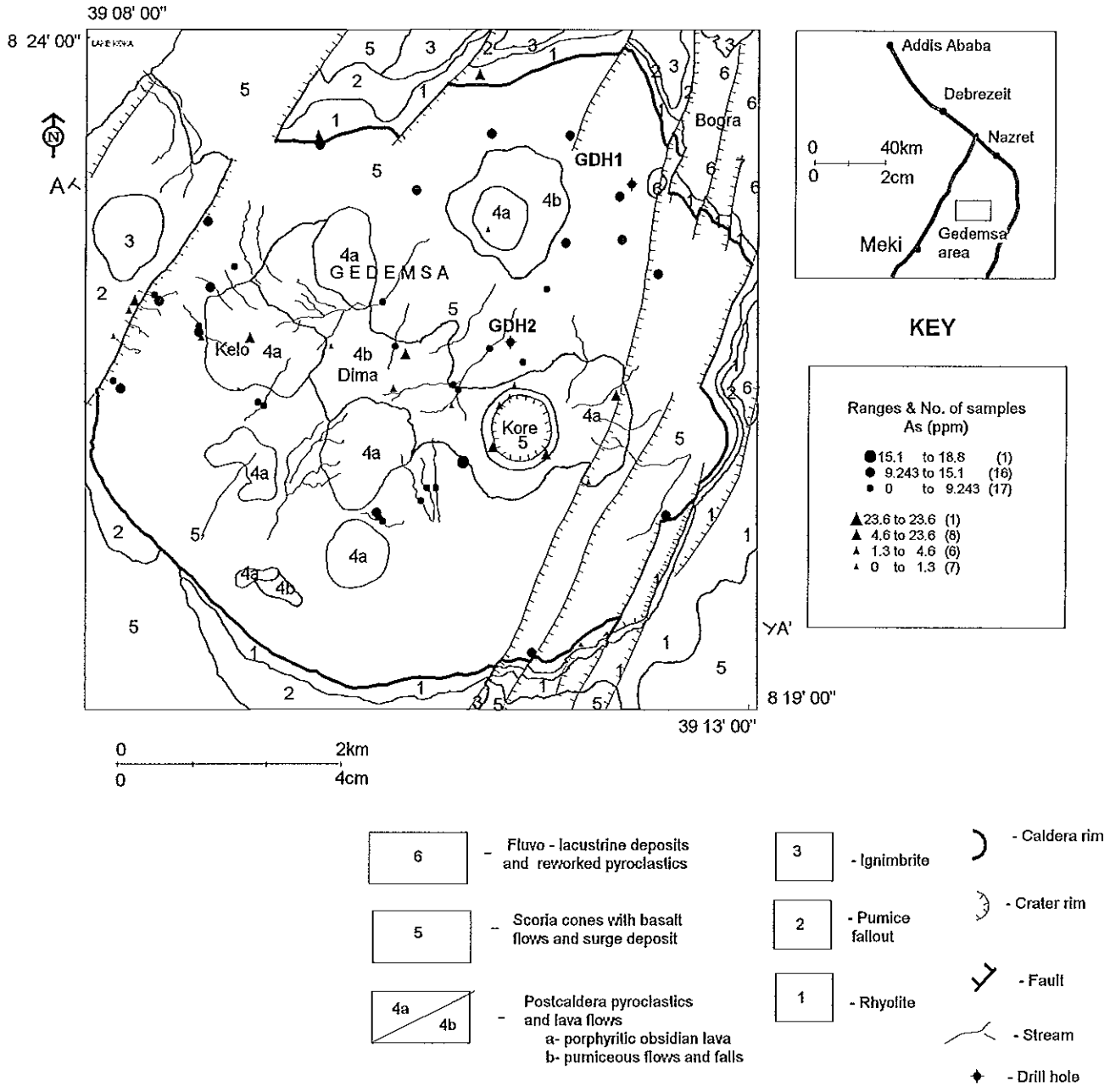

Fig 7d . Antimony analytical results (ICP-MS) in stream & soil (circles) and rock/chip samples.

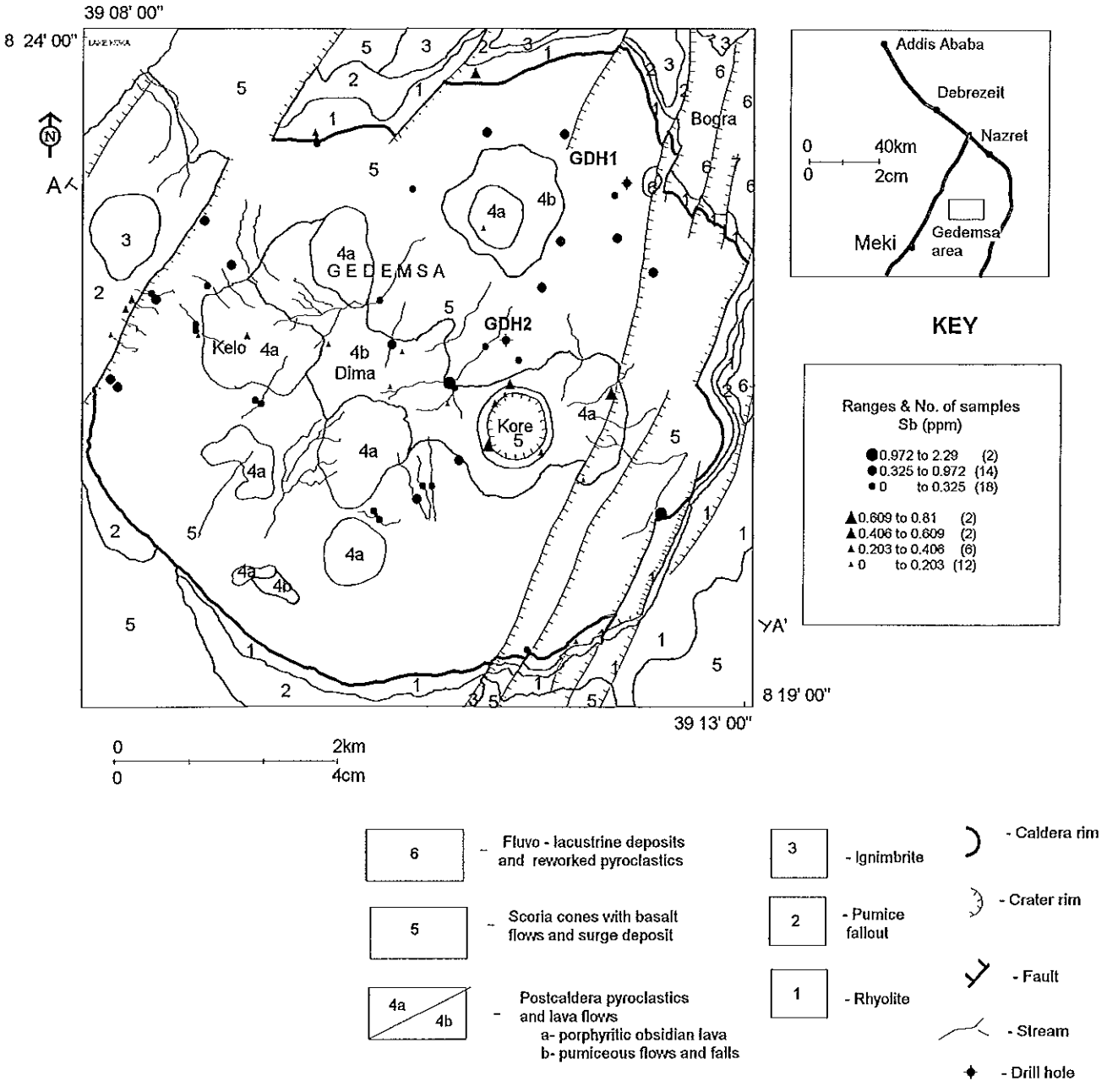

Fig 7e . Lead analytical results (ICP-MS) in stream & soil (circles) and rock/chip samples.

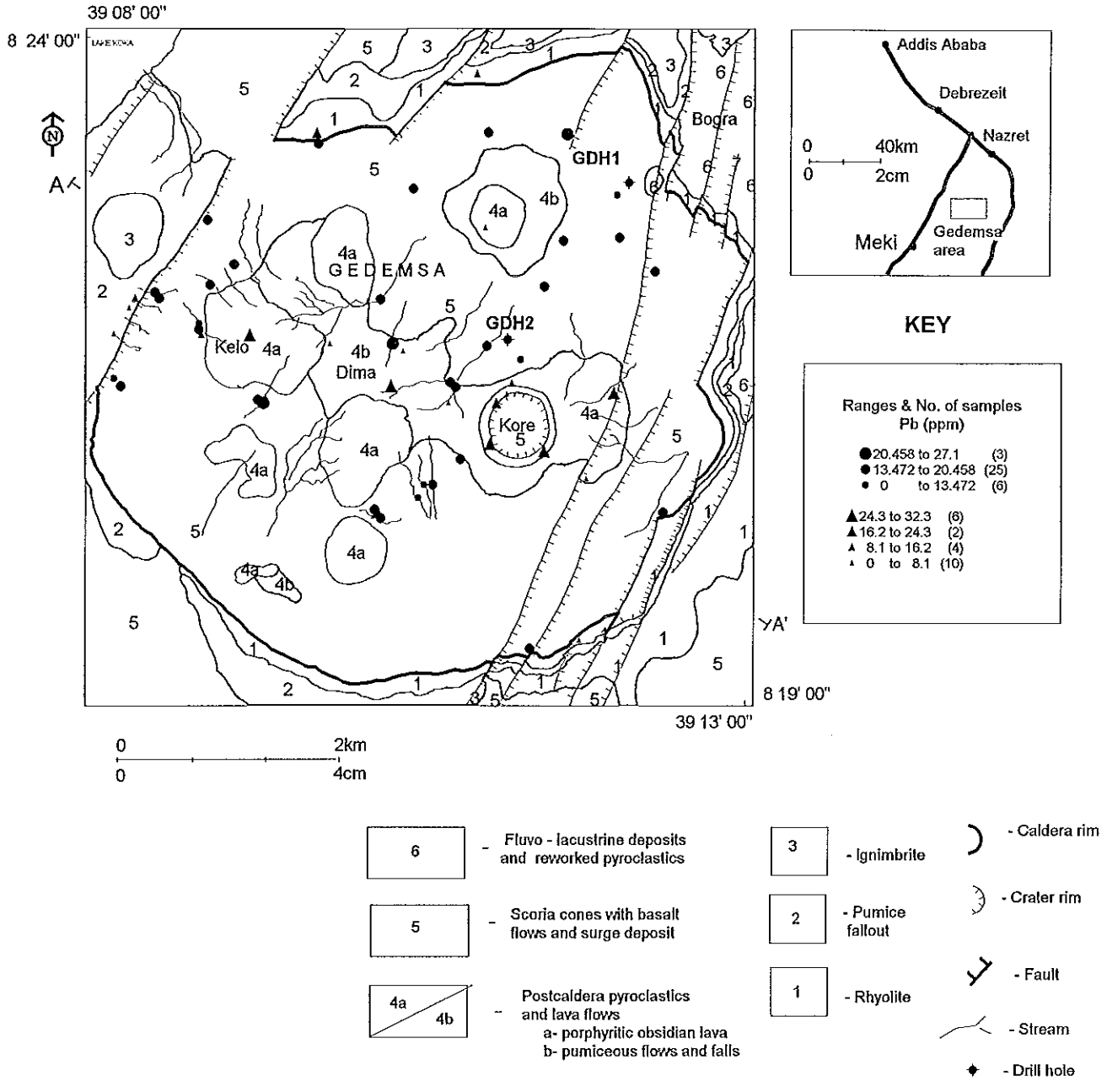

Fig 7f . Zinc analytical results (ICP-MS) in stream & soil (circles) and rock/chip samples.

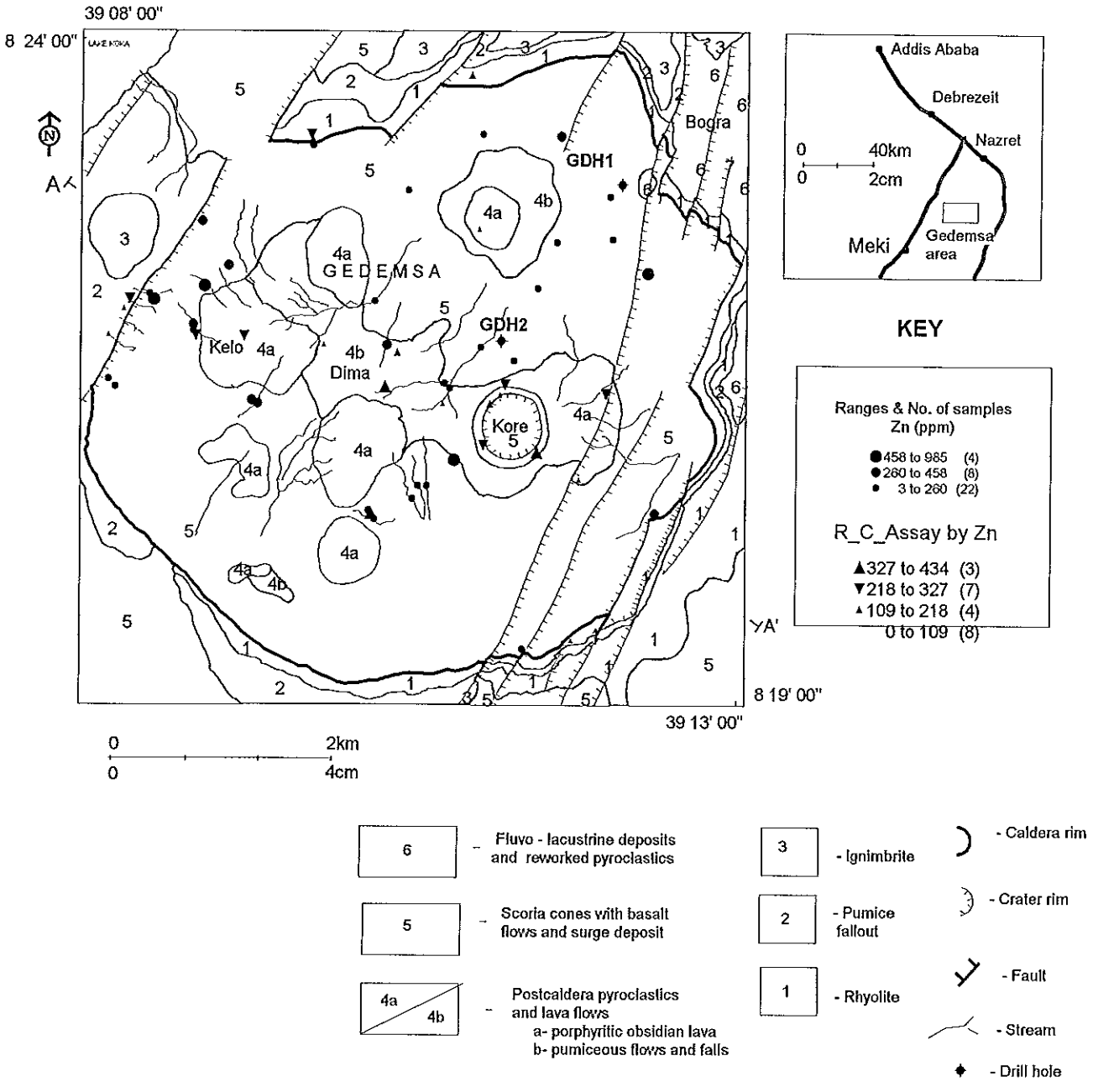

Fig 7g . Zinc analytical results (ICP-MS) in stream & soil (circles) and rock/chip samples.

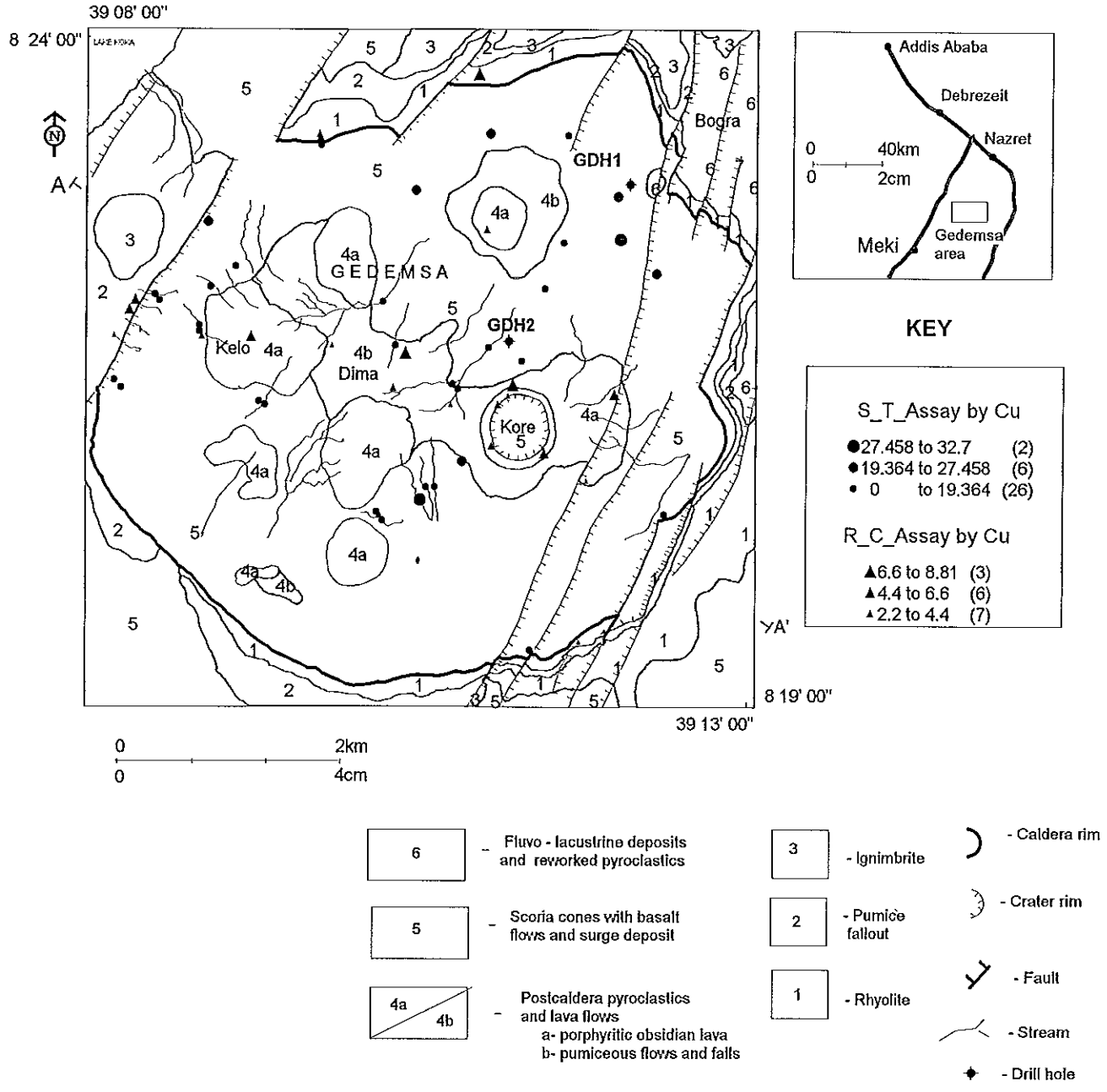

Fig 7h . Manganese analytical results (ICP-MS) in stream & soil samples (circles).

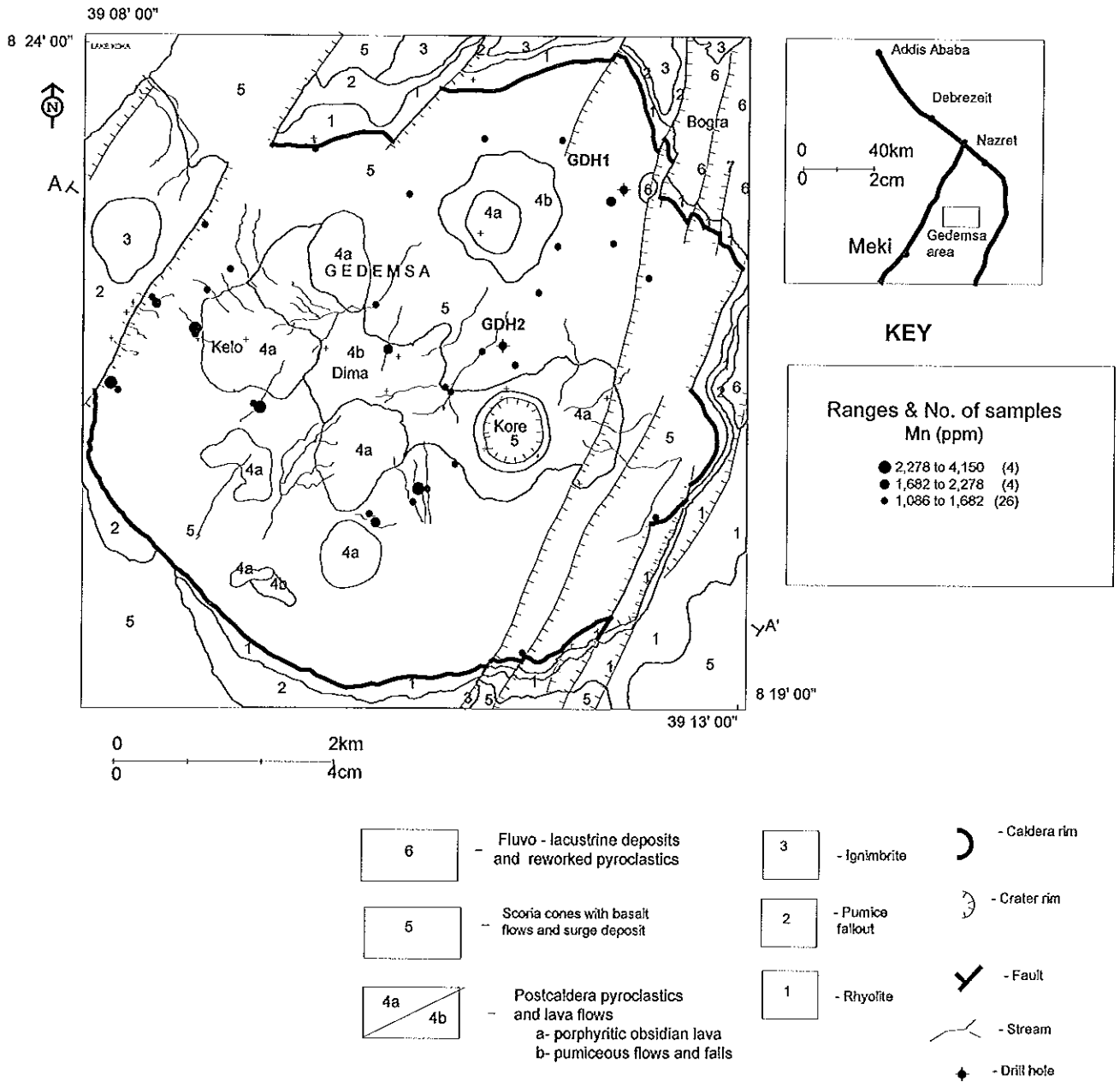

Fig 8. Geochemical summary map of anomalies for stream and soil data

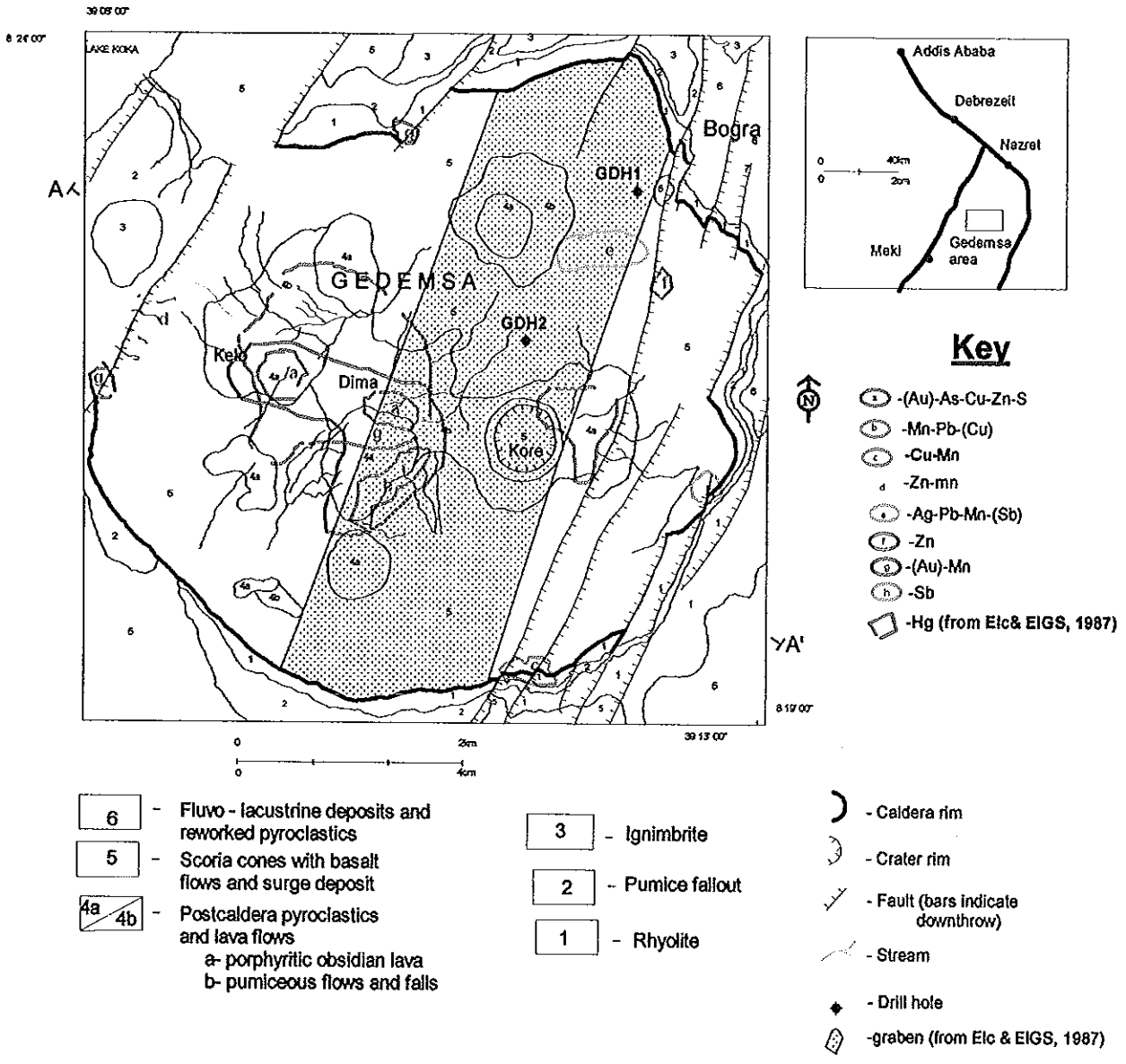

following categories of anomalies, based on elemental associations, have been demarcated: -

a) Ag-Pb-Mn- (Sb) : Central and central west along the chain
b) As - Cu - Zn : Southern part along fault
c) Zn - Mn : West along fault
d) Cu - Mn - Zn : NNE along fault
e) Others : Zn - north, Sb : south east both along fault

When compared to the average abundance of the earth's crust and / or abundance in average soil the area is generally higher by factor of considerable amount for Au, Ag, Mn, Zn and relatively As.

3.3.2. Rock/chip Samples

These include chips from quartz veins (mostly chalcedonic: GCH-001, 004 006, 007, 009, 010) and altered rocks (silicified, chloritized, and mostly ferruginized: GCH-002, 003, 005, 008), and rock samples (GRS-001, GRS-003, etc).

The geochemical data from these samples were used in order to analyse and study the geochemical distribution pattern of trace elements and their relative abundance in the veins, alteration zones and enclosing rocks of the study area using different methods. Statistical parameters (mean, standard deviation, maximum, minimum) were calculated for selected elements (Table 4). Background values for each element were necessary to be computed, however, this was not so due to the inhomogenity and small number of data, of data and non systematic or random sampling, as treatment of such data leads to wrong conclusion. Instead, assay returns were simply compared with the crustal average abundance of the trace elements in these or similar rocks. This helps to envisage the enrichment - depletion pattern of the rocks of the area with respect to the trace element. For the purpose of comparison values given by Rose et al. (1979) was used as a reference

(Table 5). Simple variation diagrams as content vs. sample type (rock/chip) were used to compare and study type of elemental association and their distribution pattern (fig. 11).

Table 4. Statistical parameter calculated for whole population data of rock and chip samples (for 17 samples).

Element	Average content in *(granite.; crust)*	Mean (ppm)	Max (ppm)	Min (ppm)	standard deviation (ppm)
Au	0.004 ; 0007	0.0185	0.03	0.012	0.008
Ag	0.04 ; 0.07	0.1521	4.78	0.10	1.304
AS	1.5 ; 1.8	5.694	23.6	0.37	5.376
Sb	0.2 ; 0.2	0.298	0.81	0.09	0.202
Cu	10 ; 55	5.1	8.8	3.1	1.78
Pb	20 ; 12.5	15.31	32.3	3.09	9.71
Zn	40 ; 70	246.12	434	65.1	107.1
Mo	2 ; 1.5	3.44	11.1	0.44	3.03
Ba	600 ; 425	403.01	2485	57.2	150
W	2 ; 1.5	1.79	5.84	0.13	1.44
Be	5 ; 1.5	5.29	11.9	0.32	3.17
Bi	0.1; 0.17	0.05	0.11	0.02	0.036
Co	1; 25	1.4	4.35	0.39	1.162
U	4.8; 2.7	2.55	7.43	1.05	1.681
Th	17, 10	15.01	45.7	1.34	12.46
Tl	0.75; 0.45	0.196	0.49	0.03	0.12

The general pattern of variations in trace element distribution are well illustrated by the graphs in fig 11a-c. Gold is detectable only in four samples collected from chalcedonic-qtz veins and altered wall rocks with a range of concentrations of 12 to 30 ppb, which still is 5 - 10 times higher than the average crustal gold value for granitic rocks. Silver generally shows considerably higher values, compared to the

level of crustal average for granite with values ranging from 0.1ppm to 4.16 ppm. Samples collected from the veins and altered wall rocks (at kore crater and surrounding hills) maintain a consistently higher content (average 3ppm) than the rock samples where it tends to be relatively lower (0.23-1ppm). Arsenic is at higher level, in all the samples, than the crustal average content for granite ranging from 1.69 to 23.16 ppm. It tends to be relatively higher in the rock samples and some altered wall rocks than the vein materials. In the former, it shows relatively, consistent level of concentration with only two peak values 23.6 ppm and 18.5 ppm for two samples collected from chloritized and brecciated rocks along the western and eastern faults, respectively. Antimony is generally at or near the level f crustal average for granitic rocks with some high values for samples from vein and silicified materials. The highest (0.81ppm) is for chip samples from a silicified and oxidized wall rock. Copper is consistently present, in all the samples, at lower level of concentration than the crustal average for granite with its single highest concentration (82.9ppm) coinciding with sample from vesicular olivine basalt (GRS-009A-table1). The same single peak (49.3 ppm) was shown by cobalt related to this sample. It is at about the level of granitic crustal average for the other samples with the exception of two higher values (4.35 ppm and 4.22) for samples from a brecciated and silicified and/or chloritized rocks along faults trending NNE both in the eastern and western part, respectively. The base metals lead and Zinc tend to be higher in chip samples of veins and altered wall rocks than the enclosing rock samples. The highest values for Zn and Pb, 434 and 32.3 ppm, respectively, are from a silicified and chloritized chip sample, which are limonitized along fractures. One rock sample (GRS-010-90) from epidotized tuff shows appreciably higher values of Ag (4.16ppm), Zn (305 ppm) and Pb (26.4 ppm). Similarly, Pb, Be, Tl, and to some extent Th essentially have higher values in this same sample. Barium is generally present below the levels for granitic crustal average with two exceptionally higher concentrations, 1058 and 2485 ppm, from rhyolite (GRS-001-90) at Kelo hill and lithic tuff (GRS-009C) at the northern

Table 6 . Average abundance (or range) of selected minor and trace elements in the Earth's crust, various rocks, soil and river water (All values in ppm, except those for river water which are ppb)

Element	Earth's crust	Ultra mafic	Basalt	Granodiorite	Granite	Shale	Limestone	Soil	River water
Ag	0.07	0.06	0.1	0.07	0.04	0.05	1	0.1	0.3
As	1.8	1	2	2	1.5	15	2.5	1-50	2
Au	0.004	0.005	0.004	0.004	0.004	0.004	0.005	—	0.002
B	10	5	5	20	15	100	10	2-100	10
Ba	425	2	250	500	600	700	100	100-3000	10
Be	2.8	—	0.5	2	5	3	1	6	—
Bi	0.17	0.02	0.15	—	0.1	0.18	—	—	—
Br	2.5	1	3.6	—	2.9	4	6.2	—	20
Cd	0.2	—	0.2	0.2	0.2	0.2	0.1	1	—
Ce	60	8	35	40	46	50	10	—	0.06
Cl	130	85	60	—	165	180	150	—	7800
Co	25	150	50	10	1	20	4	1-40	0.2
Cr	100	2000	200	20	4	100	10	5-1000	1
Cs	3	—	1	2	5	5	—	6	0.02
Cu	55	10	100	30	10	50	15	2-100	7
Dy	3	0.59	3	3.2	0.5	5	0.4	—	0.05
Er	2.8	0.36	1.69	4.8	0.2	2	0.5	—	0.05
Eu	1.2	0.16	1.27	1.2	—	1	—	—	0.07
F	625	100	400	—	735	740	330	—	100
Ga	15	1	12	18	18	20	0.06	15	0.09
Gd	5.4	0.65	4.7	7.4	2	6	0.6	—	0.04
Ge	1.5	1	1.5	1	1.5	1.5	0.1	1	—
Hf	3	0.5	2	2	4	3	0.5	—	—
Hg	0.08	—	0.08	0.08	0.08	0.5	0.05	0.03	0.007
Ho	1.2	0.14	0.64	1.6	0.07	1	0.1	—	0.01
I	0.5	0.5	0.5	—	0.5	2.2	1.2	—	7
In	0.1	0.01	0.1	0.1	0.1	0.1	0.02	—	—
Ir	0.0004	—	—	—	—	—	—	—	—
La	30	3.3	10.5	36	25	20	6	—	0.2
Li	20	—	10	25	30	60	20	5-200	3
Lu	0.50	0.064	0.20	—	0.01	0.5	—	—	0.008
Mn	950	1300	2200	1200	500	850	1100	850	7
Mo	1.5	0.3	1	1	2	3	1	2	1
Nb	20	15	20	20	20	20	—	—	—
Nd	28	3.4	17.8	26	18	24	3	—	0.2
Ni	75	2000	150	20	0.5	70	12	5-500	0.3
Os	0.0004	—	—	—	—	—	—	—	—
Pb	12.5	0.1	5	15	20	20	8	2-200	3
Pd	0.004	0.02	0.02	—	0.002	—	—	—	—
Pr	8.2	1.02	3.9	8.5	4.6	6	1	—	0.03
Pt	0.002	0.02	0.02	—	0.008	—	—	—	—
Rb	90	—	30	120	150	140	5	20-500	1
Re	0.0005	—	0.0005	—	0.0005	—	—	—	—
Rh	0.0001	—	—	—	—	—	—	—	—
Ru	0.0004	—	—	—	—	—	—	—	—
Sb	0.2	0.1	0.2	0.2	0.2	1	—	5	1
Sc	16	10	38	10	5	15	5	—	0.004
Se	0.05	—	0.05	—	0.05	0.6	0.08	0.2	0.2
Sm	6	0.57	4.2	6.8	3	6	0.8	—	0.03
Sn	2	0.5	1	2	3	4	4	10	—
Sr	375	1	465	450	285	300	500	50-1000	50
Ta	2	1	0.5	2	3.5	2	—	—	—
Tb	0.9	0.088	0.63	1.3	0.05	1	—	—	0.008
Te	0.001	0.001	0.001	0.001	0.001	0.01	—	—	—
Th	10	0.003	2.2	10	17	12	2	13	0.1
Ti	5700	3000	9000	8000	2300	4600	400	5000	3
Tl	0.45	0.05	0.1	0.5	0.75	0.3	—	0.1	—
Tm	0.48	0.053	0.21	0.5	—	0.2	0.1	—	0.009
U	2.7	0.001	0.6	3	4.8	4	2	1	0.4
V	135	50	250	100	20	130	15	20-500	0.9
W	1.5	0.5	1	2	2	2	0.5	—	0.03
Y	30	—	25	30	40	25	15	—	0.7
Yb	3	0.43	1.11	3.6	0.06	3	0.1	—	0.05
Zn	70	50	100	60	40	100	25	10-300	20
Zr	165	50	150	140	180	160	20	300	—

Notes:
Dashes (—) indicate no data are available.

Figure 11. Trace element pattern for selected elementsin rock/chip samples.

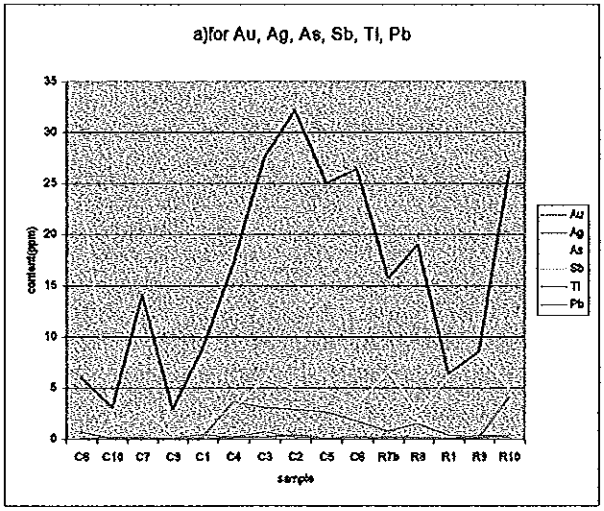

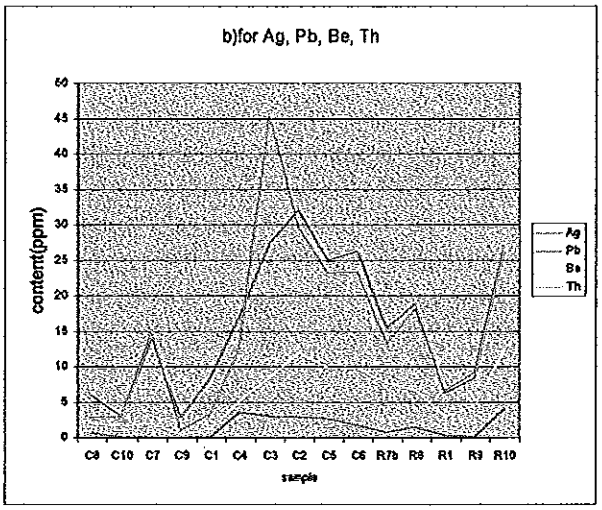

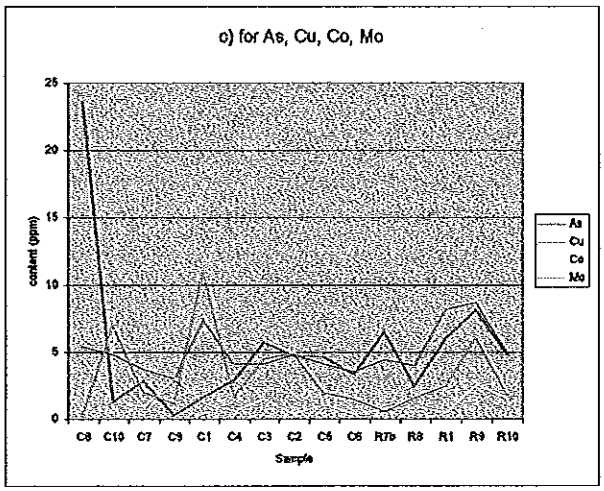

Fig 10. Geochemical summary map of anomalies for data from rock/chip samples.

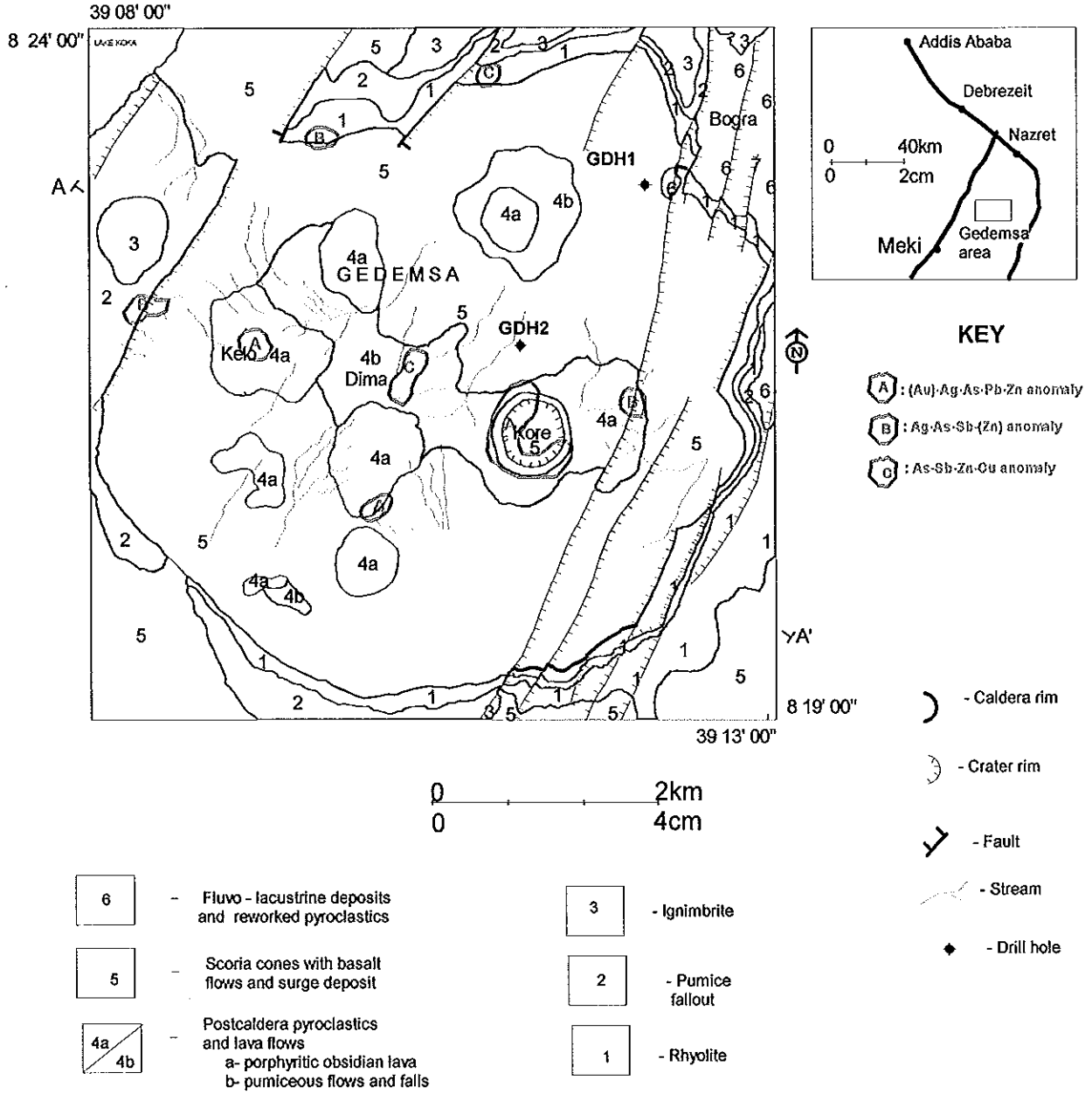

rim of the caldera. Tellurium was not detectable in enough samples for patterns to be established (the same was true for gold). Its highest value (0.21 ppm) was from sample GRS-009 (an altered lithic tuff). The highest values for Co and Cu are related to the epidotized basalt sample. Au is detected only in few samples of veins and silicified rock samples being associated with the first group described earlier. A close association was observed among Ag- Pb-Be-Th-Tl in one sample from an altered tuff (GRS-010-90) where most of them have maximum values. This can not yet simply be explained by lithologic factors.

In addition a separate map for selected element was also produced by presenting the value (range of values) of these elements at individual sample point to see their spatial distribution pattern (fig.7a-h) and overlaps between anomalous values were studied, so that anomalous zones consisting of two or more elements could be delineated (fig.10). Accordingly three categories of anomalies, based on metal associations, were recognised.

a) (Au) - Ag - As - Sb - Pb - Zn : around Kore crater in the chain of postcaldera products
b) Ag - As - Sb - Zn : along western and eastern faults
c) As - Cu - Sb - Zn : northern with in rock samples

From the figure, most of the anomalies are spatially distributed along the E-W running chains of post-caldera pyroclastic falls and flows, and lava domes, while the rest are located along the fault systems at the eastern and western part within the caldera. This might indicate that the anomalies are related to mineralizations by hydrothermal processes associated with irregular fracture system along those chains and along major faults. It should also be mentioned that most of the trace elements are highly concentrated in the altered rocks and/or veins than the unaltered ones, reflecting the importance of hydrothermal processes as the cause for mineralization.

As compared to the average crustal abundance for granite/rhyolite there is enrichment of Au, Ag (average 1.55g/t), Zn and relatively As in most samples. Antimony and relatively Pb are at about or a little below their average crustal abundance. Most of the samples are depleted in Tl, Cu, Co, and Ba. Though detected in few samples only, Au and Te considerably exceed their mean crustal content for granite/rhyolite.

3-3-3 Drill Cuttings /core samples

Elc & EIGS have drilled two exploratory wells (GDH-1& GDH-2) with an average depth 180m, for the purpose of investigating the subsurface geothermal resource in the Gedemsa Caldera. The stratigraphies of the two wells are reported in Figures 12 and 13, and consist of volcanic and volcano sedimentary sequences. Drill cutting and core samples were collected from the wells at a depth interval of three meters.

The drill wells were collared in alluvium consisting of pumiceous materials and passed into pumiceous breccias with minor rhyolite and basalt lava to some depths, below which were encountered pumiceous ignimbrites and rhyolite lavas, which remained in the rocks to total depths. The rocks beneath the pumiceous breccias occurred repeatedly in the geologic column of the second well (GDH-2), alternating with one another.

As an x-ray petrographic determination for alteration mineral assemblages of the drill cuttings is not yet done, the drill-hole logs were the only generalized data for the determination of alteration assemblage. Accordingly, the alluvium and volcanic breccias relatively show little or no alterations. The basalt lava generally contain sparse oxidized zones with minor secondary calcite of open space fillings and microcrystalline feldspars. Some ferrous oxides (haematitization) and minor clayey alteration products were observed in pumiceous ignimbrites. The rhyolite

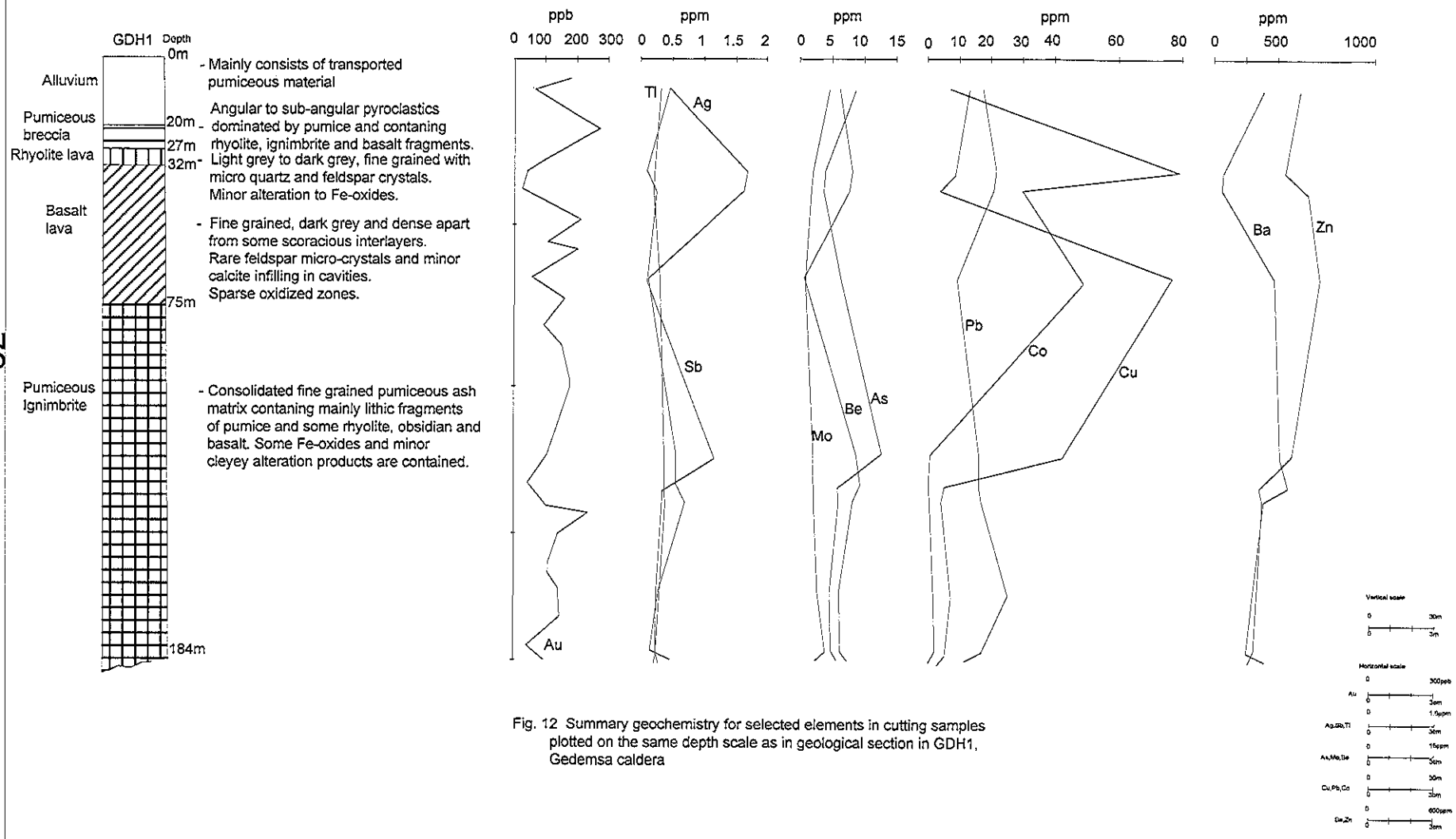

Fig. 12 Summary geochemistry for selected elements in cutting samples plotted on the same depth scale as in geological section in GDH1, Gedemsa caldera

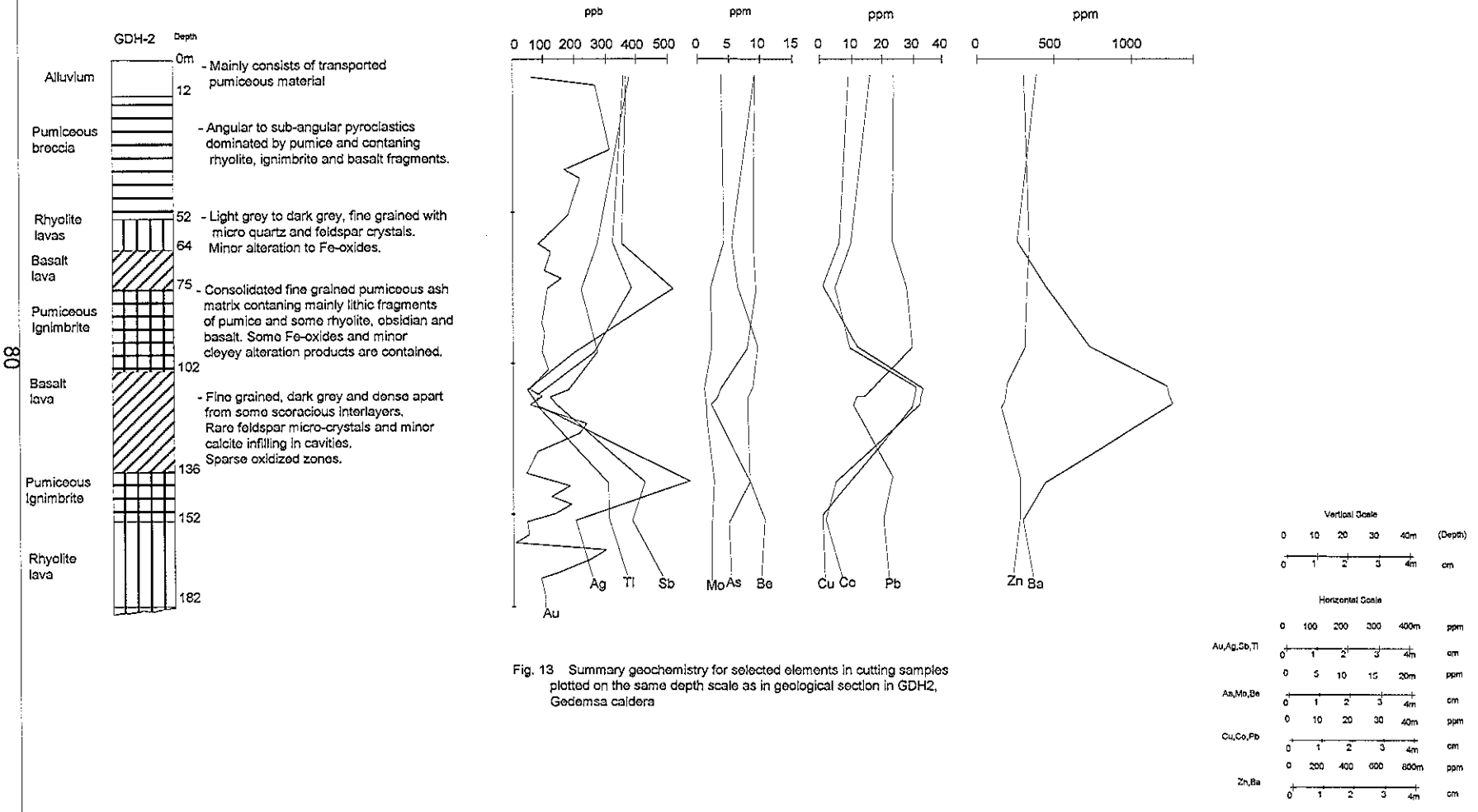

Fig. 13 Summary geochemistry for selected elements in cutting samples plotted on the same depth scale as in geological section in GDH2, Gedemsa caldera

lavas were altered to an assemblage containing microquartz (hydrothermal quartz) and k-feldspar (adularia?) crystals with minor alteration to ferrous oxides.

Samples of drill cuttings from both wells have been analyzed for gold and other related trace elements for the possibility of epithermal precious metal (gold) mineralization. Figures 12 and 13 show selected geochemical data plotted as a function of depth for drill holes GDH-1 and GDH-2, respectively from Gedemsa, as described earlier.

From the data, gold is present in all samples where its content is consistently above 0.1ppm (more than ten times its crustal average in granite/rhyolite) with a maximum value of about 0.4 ppm. Although the distribution pattern of gold contents is relatively irregular, there are some consistent intervals of significant gold concentration which could possibly be related to important occurrences of Au - mineralization.

In the first drill hole GDH-1 (fig.12) the pattern of vertical variation in elemental concentration of the rock are relatively irregular and trends are more difficult to identify. In this drill hole, gold is relatively higher (0.178ppm) near the surface in the alluvium and it sharply drops off to 0.06 ppm at a depth of 9m. It then appears to increase consistently with depth forming a 10m interval of mineralization, within the pumiceous breccia (and rhyolite lava) with an average content of 0.171 ppm and a maximum value of 0.272 ppm. This highest value coincides with the contact between the alluvium and pumiceous breccias. Below this depth is the basalt where the Au value is lower, with only two irregular highs, 0.21 ppm & 0.1ppm at a depth of 49m and 58m, respectively. This lower value of Au is accompanied by higher values of Ag, Sb, As, Cu and Co. Then, two intervals of consistently higher values occur within the pumiceous ignimbrite beginning at a depth of 73m, and near the interface between the basalt and the pumiceous ignimbrite. The first one, a 25m interval with average Au content of 0.15ppm and

the second a 33m interval with average Au value of 0.144ppm. In the second case there is a decrease in Ag, sb, As content and an increase in Cu, Pb and Zn.

Silver is generally high near the surface in this drill hole to a depth of 40 m with an average value of 1.25ppm and highest content of 1.67 ppm. It suddenly drops to the lowest value (0.09 ppm) with in the basalt at a depth of 67m. Below this depth, the value increases with Ag values greater than 0.55 ppm, within the pumiceous ignimbrite, for an interval of 18m (from depth of 121m to 139m). This interval coincides with that of high Au interval. The Ag content, then decreases to total depth with slight increase at the bottom of the well, as in the case of Au, As and Sb. The reverse is true at the bottom of the well for Pb-Zn-Cu.

Arsenic, antimony and Thallium are distributed in a similar manner. They are generally higher near surface and tend to decrease with depth to the zone of high Au interval (121m) where they all again attain their highest levels of concentrations 13.2ppm and 0.5ppm, respectively. Below this depth they decrease consistently to total depth with a slight increase, again near the bottom of the hole. An exception for arsenic is that below a depth of 120m, it keeps consistent value of 5 ppm to nearly total depth.

Beryllium and barium both show consistently constant values throughout the hole, with a slightly higher values, at the middle of hole 121-136m whose averages are 8.75ppm and 375ppm respectively. This higher value zone coincides with the high Au interval within the pumiceous ignimbrite.

Lead and bismuth concentrations show relatively similar distribution pattern. Both are higher near the surface with average concentration of 20.9ppm and 0.3 ppm, respectively, and decrease irregularly to about 130m of depth. Then, they both tend to increase to a sharp peak of 25.2 ppm and 0.4 ppm, respectively, in the interval with the highest Au interval below which they both drop to total depth.

relatively Zn beginning at a level a little above the gold. The second one on the other hand is only for gold.

Ag, Sb, Tl, Be, Pb and also Zn have relatively similar distribution pattern. There is a great consistency in their concentration (slightly increasing with depth) throughout the hole, with a sharp drop to their lowest levels at depths between 108–114 meters, which coincide with basaltic lava. Conversely As, Ba, Cu and Co are highest in this interval, keeping a consistent concentration in the rest of the hole (but slightly decreasing with depth).

Tellurium was detectable only in few samples where its concentrations are generally high varying from 0.1 to 0.47 ppm.

4. DISCUSSION OF RESULTS

The results obtained so far represents a preliminary phase of studies on epithermal gold occurrences in the Gedemsa caldera, within the MER. Even if much work has to be done in order to give a reasonably well documented synthesis, a workable hypothesis for future detailed studies can be forwarded from the obtained observations and results.

The geochemical raw data of each element showed that distribution of the background population is not homogeneous and that there are variations in patterns and relative abundance of elements in the geological samples of the area under study. These variations in background trace metal contents may reflect changes in lithology (lithological control), or they might be due to subsequent addition or removal of metals (e.g. restricted zones of mineralization can be surrounded by wide pervasive zones where trace elements are added or leached, or faulting and emplacement of igneous bodies (e.g. domes/dykes, veins,) may produce a redistribution of trace elements in geochemical landscape; or else, surficial processes may have their own effects on the distribution of background trace metal contents, or they might have leached and concentrated trace metals from an ore. To verify the various possibilities, the main features of the geochemical data analysis (i.e. trace element distribution pattern, spatial distribution pattern of anomalies, relative abundance (higher) of trace metals, etc) will be discussed in relation to the various controlling geological factors (e.g. litholgy, structure, alteration, etc).

From geochemical data, for soil and stream sediments it is obvious that the surficial processes have been important phenomena in forming significant anomalies of Mn, Ag and relatively Zn in soils and streams. Supergene oxidation by percolating meteoric water, for instance, might convert sulphides into sulphates and oxides of various metals, which would be reconcentrated in the secondary environments. The

same phenomena may result in precipitation of the less mobile trace elements from their solutions. The wider dispersion pattern of Mn and Zn regardless of lithologies may suggest that they are primarily localized along closely spaced numerous weak zones and further mobilized and redistributed by secondary processes. Ag and relatively Pb are rather localized to certain zones probably because of their lesser mobility in surface (secondary) conditions.

On the other hand, geochemical data from rock/chip and cutting samples are of great importance in direct interpretation of data in terms of both trace metal content and their distribution pattern within the rock and/or vein materials.

The interesting aspects about rock/chip sample data are the higher content of Ag (up to 4.16 g/t), As and to some extent of Pb. Thus, although none of the rock/chip samples contains sufficient base metals (Pb, Cu, Zn) to be of ore grade, the Ag content is sufficiently high to constitute ore (significant mineralization), at least locally, in a shallow non thermal environment. The same can also be said of gold in drill cuttings. Ag is strongly associated to Zn and Pb in veins and silicified samples, which may suggest that it may be precipitated as native Ag in veins or is hosted in sulphides of Zn and Pb during the controlling hydrothermal processes. However, no such minerals were observed to support this suggestion. Highest values for arsenic, on the other hand are for samples along the major faults characterized by alteration and brecciation of the host rock. Analyses of drill cutting samples have also confirmed that there is close association among Ag - Pb - Zn and that they are higher at the surface decreasing with depth, where as Asarsenic on the contrary increases with depth. Ag and As are generally closely associated in rock/chip samples (e.g. surface precipitates) but are not so close in drill cuttings.

Generally, the most important feature of the geochemical data from Gedemsa samples is that they are enriched in Au, Ag, Mn, and relatively Zn and As.

Anomalous values for Ag and Pb are consistently confined within the central post-caldera chain, whereas that of Zn and Mn are sporadically distributed in the caldera. Anomalies of As, Sb, Zn, and (Cu) particularly characterize the closely spaced faults in the east.

The fact that anomalies are rather spatially concentrated along the E-W running chains of post-caldera pyroclastic products and lava domes, (Kore and surrounding hills) or at the viscinity of major faults, signifies that mineralization is related to some sort of hydrothermal processes along the mentioned geological features. A 3km wide NNE trending graben, with a downthrow of several hundred meters and which is bounded to the east and west by major faults was identified from high gravity and geoelectric anomaly (Elc & EIGS, 1987). This structural system therefore seems to be a locus of particularly high permeability for hydrothermal activities, because of its tectonic history. Anomalies of Radon, CO2 and Hg (Elc & EIGS), that are restricted in the graben system are related to this effect. This suggestion supports the fact that the relatively mobile epithermal and associated elements (i.e. As, Sb, Zn, and (Cu)), that are anomalous around faults (fig.8) are probably due to processes along this system.

Fossil hydrothermal system which is presently dying off due to self-sealing is presumed (Elc & EIGS, 1987) to have occurred along the E-W running chains and might have caused the Hg anomaly. The numerous irregular fractures filled by silica (? chalcedony) are supportive evidence for this assumption. These phenomena could also be the cause for local anomalies around Kore crater and surrounding hills. The wide geochemical halo of both Mn and Hg around those local anomalies (fig.8) of other elements would be indicative of important mineralization related to this phenomena (self sealing, brecciation & boiling), similar to that described by Silberman and Berger (1985) for Round Mountain, Nevada.

The main goals in studying the trace-element pattern of samples (rock/chip & drill cutting) from Gedemsa were to provide insights into the origin of ore-bearing system (which needs more data than available) and to provide data and interpretation useful for future exploration studies. The trace element pattern from rock/chip and drill cutting sample at Gedemsa is complex and can not be simplified into distinct and separate system.

Nevertheless, a general pattern of zoning appears to be present such that a scheme of qualitative evaluation could be set up. Good signals for the approach to the zone of important mineralization would be, higher content of Ag, As and relatively Sb and Pb from rock/chip data (fig. 10 and 11) and the alternating high gold intervals from drill cutting data. These include intervals associated with higher values for Ag, As, Sb and Pb within the pumiceous ignimbrite, high Au interval within pumiceous breccia and those at the interface between pumiceous ignimbrite and basalt lava (fig.12 and 13). The latter case is accompanied by a slight decrease in Cu and Co.

Evidence that might point to a concealed system could be the anomalous quantities of silica as open space filling and the relative abundance of the epithermal elements that are mobile than Au and Ag. Tl, As, and Hg may be useful in identifying such escape channels, probably not in separate minerals of these minor elements but as concentrations in clays and in hydrothermal silica minerals.

Thus, even if the geochemical zoning pattern (from the complex nature of pattern and the shallow depth of drilling data) does not conform, in total, to those predicted by the epithermal models or the geothermal analogy, they do have some regularity, and could with future refinement be tested as predictive tools.

The relatively higher content of precious metals (i.e. Au & Ag) in rock/chip and cutting samples being associated with potassic alteration and the types of alteration in the area in general, together with the limited surface manifestation of epithermal

activities within the caldera favour a suggestion that mineralization is related to low sulphidation type of epithermal system. Moreover, the Ag/Au ratio (table.6) of the geochemical data from the Gedemsa samples (i.e.10 – 100 ppm) shows that chloride complexing was dominant. These ratios are important in determining the type of dominant complexing and the expected nature of the epithermal system (Cole and Drummond, 1986). Thus, systems with Ag/Au ratios less or equal to one tend to be dominated by native Au and electrum, sulphide complexing of Au is dominant, and temperatures are less than 250^{0}C. Systems where Ag/Au ratios are greater than one is characterized by argentite, base metal sulphides, sulphosalts, and electrum, with only minor gold. In this case chloride complexing is dominant and the temperatures are greater than 250^{0}C. It is possible that the same type of complexing is further especially important for Ag and base metals (Pb, Cu, and Zn) in higher temperature. However, this needs a support from further detailed investigation (Pirajno, 1992).

Gedemsa is among the best studied for their geothermal resources and results of these studies (Elc & EIGS, 1987) have shown that potential heat source is hosted by geothermal systems (fluid).

In addition to sources of heat and fluids (as in geothermal systems), the epithermal precious-metal deposits need a source of metal, a mechanism of metal transportation to a place of deposition, a mechanism of precipitation and deposition to operate, so that economic concentrations of the metals can occur (Silberman & Berger, 1992).

In the case of Gedemsa, gold (possibly also other metals) is likely to originate from Precambrian basement, which is presumed to extend northward under the rift floor. Although a source of metal is available, an enrichment of gold mineralization by epithermal processes should occur. The geothermal fluids (hot) are the ones

Table 6. Ag/Au ratios from Gedemsa geochemical data.

Sample	Au(ppm)	Ag(ppm)	Ag/Au
T22	0.016	0.16	10
T19	0.014	0.14	14.7
T4	0.015	0.14	9.3
T20	0.015	0.17	11.33
T16	0.024	0.15	6.25
T15	0.016	0.21	13.12
T14	0.017	0.28	16.25
T21	0.015	0.14	9.33
T11	0.014	0.15	10.7
T18	0.016	0.15	9.37
T5	0.016	0.28	15.55
T8	0.015	0.16	10.7
T7	0.014	0.21	15
T9	0.017	0.25	14.7
T1	0.016	0.36	22.5
T2	0.017	0.51	23.75
T3	0.016	0.38	12.35
T10	0.017	0.21	12.35
S10	0.02	0.56	28
S2	0.02	0.65	32.5
S1	0.017	0.29	17
S9	0.023	1.6	69.57
S7	0.018	0.51	28.33
S8	0.023	0.89	38.69
S6	0.019	0.67	35.26
S4	0.017	0.04	2.35
S11	0.22	0.52	23.6
S3	0.022	0.6	45.45
S14	0.016	0.3	18.75
S12	0.022	0.79	35.9
S13	0.025	0.49	19.6
C2	0.012	3.02	251.67
C5	0.015	2.75	183.3
C7	0.017	0.17	10
C4	0.03	3.73	125
R10	0.017	4.16	244.7

Sample	Au	Ag	Ag/Au
DH1-9	0.055	0.44	8
DH1-34	0.047	1.67	35.53
DH1-40	0.029	1.63	56.2
DH1-67	0.046	1.42	1.95
DH1-121	0.077	0.55	7.75
DH1-130	0.044	0.57	13.33
DH1-36	0.12	0.71	5.92
DH1-163	0.06	0.27	4.5
DH1-181	0.049	0.25	5.1
DH1-184	0.067	0.43	6.42
DH2-6	0.041	0.37	9.02
DH2-60	0.046	0.09	7.6
DH2-75	0.05	0.52	10.4
DH2-96	0.051	0.2	3.92
DH2-108	0.033	0.05	1.51
DH2-111	0.043	0.06	2.5
DH2-114	0.032	0.08	2.5
DH2-138	0.028	0.57	20.36
DH2-152	0.03	0.2	6.67
DH2-171	0.056	0.26	4.64

responsible to leach metals and rise up through major fractures to shallow depth where they deposit their metals.

Recent research at Broadlands, New Zealand, for example, has shown that the geothermal fluids are near saturation with respect to gold and electum, which are actively being precipitated at the well head. This implies that alkaline-Chloride thermal waters in general may be saturated with gold and that the source of gold is of less importance than the precipitation mechanism (Silberman & Berger, 1992). Thus, proposing a framework for these mechanisms is so important, as it is a basis for the exploration work.

Generally, precipitation of metals from the hydrothermal solution takes place whenever the transporting complex is destabilized and as a result the solubility of the metal in question is greatly reduced. In summary, precipitation of Au (also of other metals) takes place in response to changes in temperature, pressure, pH, Eh and the activity of reduced S. Hydrothermal breccias and fluid inclusion studies have also shown that boiling and also fluid mixing are very important processes for ore deposition in epithermal systems (Pirajno, 1992).

The geological setting of the study area (caldera structure) together with favourable structural features (closely spaced penetrative fault systems) and the nature of host-rock permeability at the surface (shallow depth) facilitate the above-considered mechanism. The two prominent ones for precipitation are boiling and mixing. The drilling data from Gedemsa samples represent only limited depth where gold is concentrated in permeable and/or porous units at the surface, at the interface between porous and hard (impermeable) units, and relatively within the impermeable units at depth. These fact indicate that mineralization at various levels is favoured dominantly by mixing of surface (meteoric) water (that feeds the unconfined ground water body) with heated shallow aquifers at the surface, or

directly with deep seated chloride-rich water which laterally flow under impermeable beds. Deposition could be by buffering effect (resulting in change of physicochemical conditions, i.e., pH, temperature, pressure, etc.) of the meteoric water and alkali-silicates on the shallow aquifer dominated by volatile (gas rich) phase condense and the deep seated hydrothermal fluid, there by facilitating metal precipitation. Apart from these, sporadic occurrences of alterations and mineralizations may be related to the irregular fracture systems within the partly impermeable units, which could potentially localize sites of mineral enrichment or to local deposition by brecciation and self-sealing (after boiling). The co_2 anomalies encountered in the system in the east conform that these phenomena are likely to occur, because upon boiling volatile compounds like co_2 separate and escape to the surface along fractures. The release of co_2 causes a rise of the pH in the remaining solutions, while their salinity increment by itself causes precipitation of calcite and also other minerals (e.g. adularia) together with the precious metals and sulphides (Silberman & Berger, 1992). The precipitation results in decreasing permeability and hence the system will be self sealed.

Although all these considerations need further careful investigation, the existing volcanic structure (caldera), the high annual precipitation characterizing the area, the high permeability of the surface and the much lesser permeability of the underlying rocks all favour this model.

From analysis of drill cutting samples the mean gold content of the Gedemsa samples is much greater than the maximum gold value reported in literatures, i.e. 3ppb for rhyolite, 5 ppb for the upper lithosphere (Boyle, 1979, 1987).

From exploration point of view though it is not yet possible to give any economic evaluation at this level, the field and analytical data appear encouraging for the development of exploration and a preliminary reserve estimate for gold. Considering the thickness and spatial coverage of layers with high gold intervals,

5. CONCLUSION AND RECOMMENDATIONS

5.1. CONCLUSIONS

As it was the main objective of this work to, firstly, confirm mineral occurrences in the area of study with respect to epithermal Au and Ag and associated base metals and secondly to possibly delineate anomalous zones of these occurrences, it has well achieved its goals. Furthermore, being the first in its kind, the results of this study has also shaded light to the prospecting and exploration sectors concerned in search for similar economically important mineral resources.

All geological features at Gedemsa, i.e. the type of surficially exposed rocks, the structural setting (caldera), and its active faulting (tectonics) and volcanism with the results of previous studies for its geothermal potential made the Gedemsa a possible target area of epithermal precious-metal deposit. This is, furthermore, supported by features such as sinters, brecciation and sealing, etc. as indicative of fossil hydrothermal activities.

A total of 76 samples of various types have been assayed for suits of elements (related to epithermal type deposits) and a study were made on the geochemical data, in order to confirm the occurrence and possibly delineate anomaly related to ore.

From geochemical data of surface samples (stream sediment, soil and chip/rocks), it is possible for most elements to realistically define a threshold value and separate the background from the anomalous ones. With reference to the spatial distribution of anomalous values of the various elements, localities with anomalous values for one or more elements were broadly classified into various types according to the observed anomalous metal associations.

In regards to the background distribution the following is concluded:

1. In terms of crustal global abundance (Clarks) the surveyed region,
   a) Is enriched in Au, Ag, Mn, and Zn, and relatively As.
   b) Have normal values of Sb, Pb, (W, U, Be)
   c) Is somewhat depleted in Cu, Te, Co
2. Interms of inter-element association from correlation of geochemical distribution pattern and similarities in trend surfaces, it is possible to combine the various elements into the following groups: Ag-Pb; Ag-Pb-Sb-Zn- (Mn); As-Cu-(Zn)-(Sb) and Au-Mn-Zn in soil and stream sediment, Rock/chip, whereas, Au-Ag-As-Sb-Pb in both rock/chip and drill cuttings,

The controls of elemental spatial distribution are as yet unclear, but in all likelihood are due to the interaction of several physical and chemical processes taking place in the area. Further detail investigations will unravel these problems.

3. From the exploration point of view the following localities are important to be considered,
   a) An area in the central part of the E-W trending post-caldera pyroclastic products that show a wide sub-circular halo of Mn and Hg (Elc and EIGS, 1987) surrounding smaller anomalous zones of Ag, As, Sb, Pb. This deserve further attention.
   b) Anomalous zones along the faults both in the east (SE) and the western part within the caldera.
   c) From the drilling data, high gold values (av. 0.2g/t) were found in various rock types at different level of mineralization. Considering the economic

aspect as discussed earlier, the upper pumice layer could be a starting material for prospecting and development of exploration for future.

On the basis of geochemical data observation from the drill cuttings, it has been well tried to establish a geochemical pattern, though it seems so complex at the moment to give any genetic conclusion. Both the stratigraphy as well as the structure, together with the hydrological and nature of hydrothermal systems seem to constitute an important control on the trace - element distribution pattern.

Zones of high gold intervals that are related to permeable (porous) units (pumiceous breccia and pumiceous ignimbrites) and, at the interface between porous and impermeable units (hard rocks), need further attention by considering the thickness of the zone and spatial coverage (surficial area) of the unit.

Apart from these, the preliminary results were encouraging and deserve follow-up work. It is also well expected that optimum results will be obtained by integrated geochemical and geophysical techniques

However, since this is a preliminary one, there is always a need for further follow-up works and investigations in order to substantiate and strengthen the already achieved results. This will focus in pinpointing the cause of anomalies and possible ores and appraisal of economic potential of the mineral occurrences. Thus, in regards to these facts, the following exploration and research works are recommended.

5.2. RECOMMENDATION

a. Detail geochemical works on the proposed anomalous zones, i.e. grid soil sampling, channel sampling (on trenches) in areas related to the fossil hydrothermal zones in the central E-W trending post caldera pyroclastic products, and those confined with the graben structure crossing the central-eastern part of the caldera encompassing the Kore core crater (Elc & EIGS, 1987).

b. Detailed structural mapping is necessary in order to workout the complicated fracture systems with their various vein composition, to confirm the existence of the proposed graben system, and to distinguish between anomalies and alteration related to the various fracture or fault systems in time and space.

c. Geophysical works of follow-up scale including gravity, electrical and magnetic at the proposed promising area.

d. Additional exploratory bore holes at the viscinity of known fluid-driving structural features and in relation to promising areas at greater depth than the previous ones.

e. Detailed petrological and magmatologic studies involving isotope studies to relate mineralization to these geological features (alteration zones, veins, breccia zones, etc.).

Furthermore, the modelling and understanding of the features of the mineralization is also important to properly prospect, explore and develop other mineral occurrences of the same nature in the country. Thus, together with exploration program researches should be conducted so that geological

information are organized. These data are of great importance in the interpretation and unravelling of the genetic features of the mineral deposit. In order to achieve those conclusions about the genesis of the ore deposits or mineralization, and outline a possible genetic model, the following studies should be carried out: -

1) Fluid inclusions and stable isotope studies as a continuation of geothermal studies. The results of these studies help in identifying the physicochemical conditions of precipitation (i.e. formation temperature and pressure of ore forming solutions) and overall mechanisms or processes (mixing of fluids and/or boiling) responsible for mineralization.

2) Study on mineralogy (both ore and alteration), parageneses and geochemistry of both surface and deepest horizons in order to define the parageneses at depth and hence to correctly identify the different generation of ore metals (e.g. gold) with their respective physico-chemical conditions. Detail microscopic and diffraction study on ore minerals is an important guide as to identify or classify the genesis of mineralization or ore deposit.

6. REFERENCES

Ayalew, D., 1994. **Volcanology, Petrology and Geochemistry of the Gedemsa Volcano.** M. Sc. Thesis, AAU, Addis Ababa.

Baker, B.H., Mohr, P.A. and William, L.A. (1972). **Geology of the Eastern Rift System of Africa.** Geol. Soc. Am., Spec. Pap., 136, p. 67.

Berger, B.R., and Bethke, P.M., 1985. **Geology and Geochemistry of Epithermal Systems**: Society of Economic Geologists, Reviews in Economic Geology, V.2.

Boyle, R.W., 1979. **The Geochemistry of Gold and its Deposits.** Geological Survey Canada Bulletin 280, 584 P.

Davis (1973). **Statistics and Data Analysis in Geology.** Wiley New York.

Di Paola, G.M., (1972). **The Ethiopian Rift Valley (Between $7^0$00' and $8^0$40' lat. North).** Bull. Volcan. 36:317-560.

de Wit, M.J., and Senbeto Chewaka, 1981. **Plate Tectonic and Metallogenesis: Some Guidelines to Ethiopian Mineral Deposit.** EIGS.

EIGS and Elc (1987). **Geothermal Reconnaissance Study of Selected Sites of the Ethiopian Rift System.** Geothermal Report, pp. 5-1 and 5-34.

Franco Pirajno, 1992. **Hydrothermal Mineral deposits. Principles and Fundamental concepts for the Exploration Geologist.** Springer - Verlag, Berlin, Germany.

Hayba, D.O., Bethke, P.M., Heald, P., and Foley, N.K., 1985, **Geologic, Mineralogical, and Geochemical Characteristics of Volcanic-hosted Epithermal Precious-metal deposit**; in **Berger, B.R., and Bethke, P.M.** (eds), Geology and Geochemistry of Epithermal Systems: Society of Economic Geologists, Reviews in Economic Geology, V.2.

Jelenc, D.A., 1966. **Mineral Occurrences of Ethiopia.** Min. of Mines, Addis Ababa.

Kazmin, V., Seife-Michael Berhe, Nicoletti, M. and Petrucciani, C. (1980). **Evolution of the Northern part of the Ethiopian Rift.** Rome, Italy. Academia Nazionale dei Lincei 47: 275 – 292.

Kebede, S., 1988. **Results of Shallow Wells Drilling at Gedemsa.** Geothermal Prospect, Tech. Report, EIGS.

Merla, G., Abatte, E., Azzroli, A., Burni, P., Fazzouli, M., Sagari, M., and Tacconi, P., 1979. **Comments on the geological map of Ethiopia and Somalia, Scale 1: 2,000,000**: Frienze, Italy, Consiglio Nazionale delle Ricerche, p.1–89.

Mohr, P.A (1967). **The Ethiopian Rift System.** Bull. Geophys. Obs., 11:1-65.

Mohr, P. A., and Potter,E. C., 1976. **The Sagatu Ridge dike swarms. Ethiopian rift margins**: Journal of Volcanology and Geothermal Reaserch, V. I, p. 27-37.

Peccerillo A., Yirgu G., and Ayalew D., 1995. **Genesis of acid Volcanics along the Main Ethiopian Rift. A Case History of the Gedemsa Volcano.** SINET: Ethiopia. J. Sci., Vol. 18, pp. 23-50.

Rose, A.W., Hawks, H.E., and Webbs, J.S., 1979. **Geochemistry in Mineral Exploration.** Academic Press, London.

Silberman, M.L., and Berger, B.R., 1985, **Relationship of Trace element patterns to Alteration and Morphology in Epithermal Precious-Metal Deposits**; in Berger, B.R., and Bethke, P.M. (eds), **Geology and Geochemistry of Epithermal Systems: Society of Economic Geologists**, Reviews in Economic Geology, V.2.

Thrall, R., 1973. **Gedemsa Caldera, Ethiopia. Centre for Astrophysics**, USA. Reprint Ser. N. 280, pp. 71 – 80.

White, D.E., 1981.**Active Geothermal Systems and Hydrothermal Ore Deposits.** Econ. Geol. 75th Anniversary Volume, pp. 392-423

Zanettin, B., Justin – Visentin, E.,Nicoletti, M., and Piccerillo, E.M., 1980, **correlation among Ethiopian Volcanic formation with special references to the Chronological and Stratigraphic problems of the Trap Series**: Rome, Italy, Academia Nazionale dei Lincei, 47, p.231 – 252.